EVALUATION OF THE REQUIREMENT OF COMPLEX FUNCTIONAL FORMS IN GROUND-MOTION PREDICTION EQUATIONS IN TERMS OF DISTANCE METRICS: REGIONAL AND GLOBAL APPLICATIONS

YER HAREKETİ TAHMİN DENKLEMLERİNDE KOMPLEKS FONKSİYON YAPISININ GEREKLİLİĞİNİN MESAFE TÜRLERİ CİNSİNDEN DEĞERLENDİRİLMESİ: BÖLGESEL VE GLOBAL UYGULAMALAR

OĞUZ SALİH OKÇU

ASSOC. PROF. DR. M. ABDULLAH SANDIKKAYA

Supervisor

ASSOC. PROF. DR. ÖZKAN KALE

Co-Supervisor

Submitted to

Graduate School of Science and Engineering of Hacettepe University

as a Partial Fulfillment to the Requirements

for the Award of Degree of Master of Science

in Civil Engineering.

2020

to the “complex functional forms” in my life…

ÖZET

YER HAREKETİ TAHMİN DENKLEMLERİNDE KOMPLEKS FONKSİYON YAPISININ GEREKLİLİĞİNİN MESAFE TÜRLERİ CİNSİNDEN DEĞERLENDİRİLMESİ: BÖLGESEL VE GLOBAL UYGULAMALAR

Oğuz Salih OKÇU

Yüksek Lisans, İnşaat Mühendisliği Bölümü

Tez Danışmanı: Doç. Dr. M. Abdullah SANDIKKAYA

Eş Danışman: Doç. Dr. Özkan KALE

Eylül 2020, 91 sayfa

Çalışma kapsamında ilk olarak Türkiye ve global ölçekli iki deprem yer hareketi veri tabanı derlenmiştir. Türkiye deprem veri tabanından Joyner-Boore (R_{JB}) ve fay kırığına en yakın mesafe (R_{RUP}) tabanlı yer hareketi tahmin denklemleri (YHTD) türetilerek farklı deprem senaryoları altında karşılaştırmaları yapılmıştır. Türkiye ve Avrupa'da yapılan YHTD uygulamalarında R_{JB} mesafe türü daha basit hesaplama aşamalarına sahip olduğu için araştırmacıların büyük bir kısmı tarafından tercih edilmektedir. Yapılan karşılaştırmalar ışığında, Türkiye ve Avrupa tabanlı YHTD'lerde çok tercih edilmeyen mesafe türü olan R_{RUP} parametresinin de Türkiye için uygunluğu değerlendirilmiştir. Ayrıca R_{JB} ve R_{RUP} denklemlerinin odak merkez (hiposantr) derinliğine bağımlılıkları da artık analizleri yardımıyla yapılmıştır. Çalışmanın diğer etabında ise global deprem veri tabanı kullanılarak basit ve kompleks fonksiyon yapılarındaki denklemlerin

değerlendirmeleri yapılmıştır. Bu aşamada, basit fonksiyon yapısına ilk olarak hiposantr derinliği ve dalma açısı terimleri ve sonrasında da tavan blok terimleri eklenerek kompleks fonksiyon yapısındaki YHTD'ler geliştirilmiştir. Böylelikle kompleks fonksiyon yapısının artıları ve eksileri, R_{JB} ve R_{RUP} tanımlarına bağlı olarak denklemlere bir belirsizlik katılıp katılmadığı ve mesafe türü kaynaklı olası bir epistemik belirsizliğin varlığı da irdelenmiştir. Sonuç olarak kompleks fonksiyon yapısındaki R_{RUP} tabanlı denklemler yerine daha basit yapıdaki R_{JB} tabanlı denklemlerin geliştirilmesinin daha makul bir seçenek olduğu gözlemlenmiştir. Ayrıca denklemlerin medyan tahminlerinde ve standart sapmalarında mesafe türüne bağlı olarak epistemik belirsizliğin varlığı da gözlemlenmiştir.

Anahtar Kelimeler: Yer hereketi tahmin denklemi, Joyner-Boore mesafesi, Fay kırığına en yakın mesafe, Kompleks fonksiyon yapısı, Epistemik belirsizlik

ABSTRACT

EVALUATION OF THE REQUIREMENT OF COMPLEX FUNCTIONAL FORMS IN GROUND-MOTION PREDICTION EQUATIONS IN TERMS OF DISTANCE METRICS: REGIONAL AND GLOBAL APPLICATIONS

Oğuz Salih OKÇU

Master of Science, Department of Civil Engineering

Supervisor: Assoc. Prof. Dr. M. Abdullah SANDIKKAYA

Co- Supervisor: Assoc. Prof. Dr. Özkan KALE

September 2020, 91 pages

The Turkish and global scale ground-motion databases are firstly compiled in the scope of the study. Joyner-Boore (R_{JB}) and closest distance to the fault rupture (R_{RUP}) ground-motion prediction equations (GMPEs) are developed from the Turkish ground-motion database and their comparisons are performed under different earthquake scenarios. In the GMPEs application conducted in Turkey and Europe, the R_{JB} distance metric is preferred by a significant part of the researchers because of its simple calculation steps. In the light of comparisons conducted in this study, suitability of the R_{RUP} distance metric that is not preferred in Turkey and Europe is evaluated for its potential use for Turkey. In addition, statistical dependence of the selected R_{JB} and developed R_{RUP} GMPEs to the hypocentral depth term are examined by the help of residual analysis. In the next stage of the study, the evaluations of the basic and complex functional form

GMPEs are conducted by employing global ground-motion database. In this stage, the GMPEs in complex functional form are developed by firstly adding the hypocentral depth term and dip terms, and then the hanging wall terms to the basic functional form. In this vein, advantages and disadvantages of complex functional form, the existence of any difference related the definition of R_{JB} and R_{RUP} distances, and the existence of epistemic uncertainty depending on the distance types are evaluated. As a result, development of the R_{JB} based models can be considered as more sufficient with respect to the R_{RUP} based GMPEs. In addition, it is observed that the median predictions and standard deviations of GMPEs include epistemic uncertainty depending on the selected distance metric.

Keywords: Ground-motion prediction equation, Joyner-Boore distance, Rupture distance, Complex functional form, Epistemic uncertainty.

TEŞEKKÜR

Lisansüstü eğitimim boyunca engin bilgi ve tecrübelerinden yararlandığım, sadece bilimsel anlamda değil sahip olduğu eşsiz bilgisiyle hayatıma yön veren, desteğini esirgemeyerek her zaman yanımda olduğunu hissettiren değerli hocalarım Doç. Dr. Özkan KALE'ye ve Doç. Dr. M. Abdullah SANDIKKAYA'ya,

Yardımları, yapıcı yorumları ve önerileriyle tezimi tamamlamamda bana yardımcı olan sayın jüri üyelerim Prof. Dr. Zeynep GÜLERCE, Prof. Dr. Berna UNUTMAZ, Doç. Dr. Alper ALDEMİR ve Dr. Öğr. Üyesi Bekir Özer AY'a,

Bu tezin tamamlanmasında 118M720 numaralı proje ile maddi destek sağlayan TUBİTAK'a,

Hayatım boyunca her koşulda bana destek veren ve sabır gösteren, önceliklerini her zaman benim önceliklerime göre değiştiren ve bunun karşılığını hiçbir zaman tam olarak ödeyemeyeceğim, bugünlere gelmemde en büyük katkıları olan, bu hayatta hiçbir şeye asla değişmeyeceğim canım aileme,

Sonsuz teşekkürler…

Oğuz Salih OKÇU

Eylül 2020, Ankara

TABLE OF CONTENTS

LIST OF FIGURES

LIST OF TABLES

SYMBOLS AND ABBREVIATIONS

Symbols

T	Period
R_{EPI}	Epicentral distance
R_{HYP}	Hypocentral distance
Z_{HYP}	Hypocentral depth
R_{RUP}	Rupture distance
R_{JB}	Joyner-Boore distance
R_X	Horizontal distance between site and upper edge of the fault rupture
M_W	Moment magnitude
Z_{TOR}	Depth of upper edge of the fault rupture
RW	Rupture width
V_{S30}	Average shear wave velocity of upper 30m layer of soil
V_{REF}	750 m/s
V_{CON}	1000 m/s
PSA_{1130}	Spectral Value of reference rock site of Chiou and Youngs (2008) study
PGA_{REF}	Maximum ground acceleration value for reference rock that calculated for V_{S30} = 750 m/s
Dip	Dipping angle of the fractured fault
f_{mag}	Magnitude scaling function
f_{dis}	Distance scaling function
f_{sof}	Style-of-faulting scaling function
f_{aat}	Anelastic distance attenuation function

f_{site}	Site amplification function
f_{lin}	Linear site effects function
f_{nl}	Nonlinear site effects function
f_{hyp}	Hypocentral depth effects function
$f_{hyp,H}$	Hypocentral depth model
$f_{hyp,M}$	Magnitude dependent hypocentral depth model
f_{hng}	Hanging wall effects function
$f_{hng,RX}$	R_X dependent hanging wall effects function
$f_{hng,RRUP}$	R_{RUP} dependent hanging wall effects function
$f_{hng,RJB}$	R_{JB} dependent hanging wall effects function
$f_{hng,MW}$	M_W dependent hanging wall effects function
$f_{hng,ZTOR}$	Z_{TOR} dependent hanging wall effects function
$f_{hng,\delta}$	Dipping angle dependent hanging wall effects function
σ	Total standard deviation
τ	Between-event standard deviation
Φ	Within-event standard deviation
Φ_{S2S}	Site-to-site standard deviation

Abbreviations

GMPE	Ground-Motion Prediction Equation
NGA	Next Generation Attenuation Project
NGA-West2	Next Generation Attenuation Project West 2 Database
PGA	Peak Ground Acceleration
PSA	Pseudo-Spectral Acceleration
HW	Hanging Wall

1. INTRODUCTION

This section has separated into subtopics. Those subtopics are about strong ground-motion databases which form the main scope of this study, details of the distance-metrics, general functional forms of ground-motion prediction equations (GMPEs) and information about current GMPEs.

1.1. Strong Ground-Motion Databases

Strong ground-motion databases are considered as the fundamental resources for earthquake researches. In this context, it is very important to have reliable parameters of these databases and to keep them updated with the newest information. In the last decade, strong ground-motion databases reached a certain reliability level with the studies that have been done in Turkey and Europe (e.g., Akkar et al., 2010; Akkar et al. 2014a). It is also possible to show Ancheta et al. (2014) as a global scale database, which is a part of NGA-West2 project and the most up-to-date data of global databases. All the catalogue parameters that are going to use for developing the GMPEs (moment magnitude, distance metrics, fault types, site classes, fault geometries, etc.) and ground-motion intensity measures such as peak ground acceleration (PGA), peak ground velocity (PGV) and pseudo-spectral acceleration (PSA) are included in these databases.

1.2. Distance Metrics

From past to present, usage of distance metrics in functional forms of GMPEs has been passed through a certain evolution. Epicentral distance (R_{EPI}, the distance between site and the surface projection of the earthquake center) and hypocentral distance (R_{HYP}, the distance between site and the earthquake center) are the common distance metrics that are used in previous generation of predictive models. The truth of causing big problems, because of those distance

metrics are modelling the fault source as a point source, has been revealed with the researches after middle and high magnitude earthquakes that have measurable fault rupture dimensions (extended source).

Bommer and Akkar (2012) showed that, usage of point source distance metrics (R_{EPI} and R_{HYP}) can cause overprediction of spectral acceleration at a site that is exposed to a middle or high magnitude earthquake (biased ground-motion intensity measure estimates). Therefore, GMPE developers concentrated on alternative distance metrics that can consider extended sources, instead of point sources. The most common and the most used extended source distance metrics are closest distance to fault rupture (R_{RUP}) and Joyner-Boore distance (R_{JB}; Joyner and Boore, 1981). While R_{JB} is defined as the closest distance between site and surface projection of the fault rupture, R_{RUP} is the closest distance between site and fault rupture.

The relation between fault geometry of mentioned distance metrics and a considered site (or station) has been shown in Figure 1.1. As seen clearly in here, while R_{EPI} and R_{HYP} are calculated considering the starting point of the fault rupture, in R_{JB} and R_{RUP} calculation, dimensions of the fault rupture are also gaining importance. At this point, two important differences between R_{JB} and R_{RUP} can be mentioned: hanging wall and hypocentral depth concepts. While R_{JB} equals to 0 km value on all the points of surface projection of the fractured fault (namely, different site locations), R_{RUP} becomes ≥ 0 km because of the focal depth effect. This situation gives R_{JB} distance metric feature of considering hanging wall effects directly, by the definition. For R_{RUP} distance metric, this definition requires additional features. There will be explanations regarding to hanging wall in the following subsections. Another important difference that differs two distance metrics is the matter that hypocentral depth term is not given in definition of R_{JB} distance metric but it is considered directly in definition of R_{RUP} distance metric. These two differences bring out two separate ways of developing GMPEs with revealing two different interpretations between researchers.

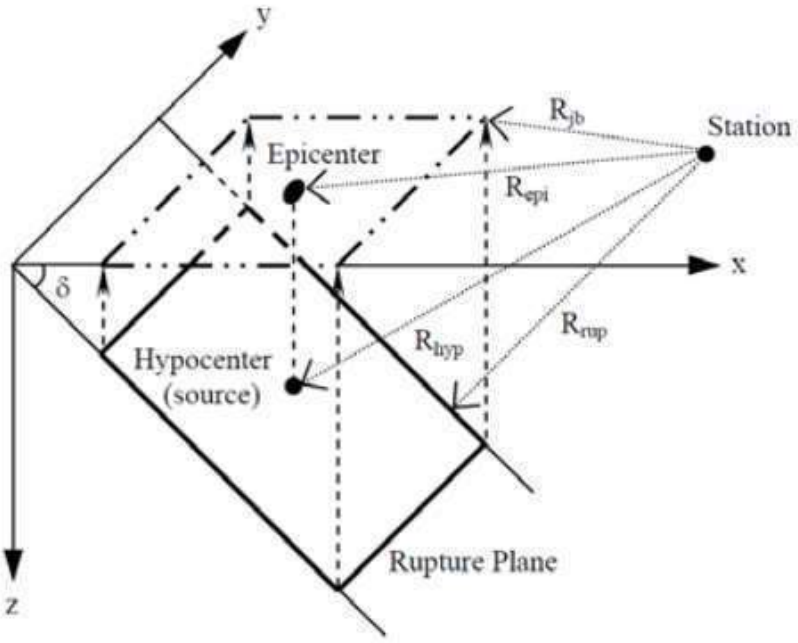

Figure 1.1. Schematically demonstration of point source (R_{EPI} and R_{HYP}) and extended source (R_{RUP} and R_{JB}) distance-metrics (Erdoğan, 2008).

1.3. General Functional Forms of GMPEs

A reliable GMPE must have a functional from that includes particular earthquake parameters that reflects source, path and site characteristics. In consideration of current developments, a basic functional form that is given between Equation 1.1 – 1.6 is required to look out for magnitude (f_{mag}), distance (f_{dis}), style of faulting (f_{sof}), anelastic distance attenuation (f_{aat}) and site classification (f_{site}) differences. By the help of this kind of equation, necessary ground-motion intensity measures (GMIM) can be obtained with using four earthquake parameters (moment magnitude, M_W; distance, R_{JB}; normal, F_{NM}, reverse, F_{RV}, or strike-slip style of faulting; time-based average of shear wave velocity of the uppermost 30 m of top soil, V_{S30}). This functional form may be named as “basic functional form” because of scarcity of parameters and general structure. This equation, which is formed mainly after Abrahamson and Silva (2008) study and later Sandıkkaya et al. (2013) site classification model has been added, is used as main functional form of prediction methods Akkar et al. (2014b) and Kale et al. (2015).

$$lnY = f_{mag} + f_{dis} + f_{sof} + f_{aat} + f_{site} \tag{1.1}$$

$$f_{mag} = \begin{cases} b_1 + b_2(M_W - 6.75) + b_3(8.5 - M_W)^2, & M_W \leq 6.75 \\ b_1 + b_7(M_W - 6.75) + b_3(8.5 - M_W)^2, & M_W > 6.75 \end{cases} \tag{1.2}$$

$$f_{dis} = [b_4 + b_5 (M_W - 6.75)] \ln \sqrt{R_{JB}^2 + b_6^2} \tag{1.3}$$

$$f_{sof} = b_8 F_{NM} + b_9 F_{RV} \tag{1.4}$$

$$f_{aat} = \begin{cases} 0, & R_{JB} \leq 80 \\ b_{10}(R_{JB} - 80), & R_{JB} > 80 \end{cases} \tag{1.5}$$

$$f_{site} = \begin{cases} sb_1 \ln\left(\frac{V_{S30}}{V_{REF}}\right) + sb_2 \ln\left[\frac{PGA_{REF} + c\,(V_{S30}/V_{REF})^n}{(PGA_{REF} + c)(V_{S30}/V_{REF})^n}\right], & V_{S30} < V_{REF} \\ sb_1 \ln\left(\frac{\min\,(V_{S30}, V_{CON})}{V_{REF}}\right), & V_{S30} \geq V_{REF} \end{cases} \tag{1.6}$$

It is possible that sub-terms of basic functional form, which has been shown in Equation 1.1, might show different features. The important matters that have to be included are:

- nonlinear magnitude dependency of function of equation as stated in Bommer et al. (2010),
- magnitude dependent distance attenuation,

- one or two-staged maximum likelihood method (Joyner and Boore, 1993) or derivation according to random-effects method (Abrahamson and Youngs, 1992),
- usage of prediction parameters like moment magnitude and extended-source distance metrics, considering site effects having regard to V_{S30}.

Equation 1.7 can be given as an alternative to consider linear (f_{lin}) and nonlinear (f_{nl}) site effects shown in Equation 1.6, which is given as an example. This form of equation considers reference rock site spectral value (PSA_{1130}) to define seismic demand for soil nonlinearity and used in CY08 (Chiou and Young, 2008) and CY14 (Chiou and Youngs, 2014).

$$f_{site} = f_{lin} + f_{nl} \tag{1.7}$$

$$f_{lin} = s_1 min\left\{\ln\left(\frac{V_{S30}}{1130}\right), 0\right\} \tag{1.7a}$$

$$f_{nl} = s_4\left[e^{s_5(\min(V_{S30},1130)-360)} - e^{s_5(1130-360)}\right]\ln\left(\frac{PSA_{1130} + s_3}{s_3}\right) \tag{1.7b}$$

Rather than basic functional form, especially GMPE developers who works with global databases add hanging wall model term to the function that defined in Equation 1.1 when R_{RUP} distance metric is employed as prediction parameter. According to fault geometry, earthquake effects on sites that are on moving block are higher and observed spectral values are greater. Parameters that are used for considering these effects are: horizontal distance between site and upper edge of the fault rupture (R_X), depth of upper edge of the fault rupture (Z_{TOR}), rupture width (RW) and dipping angle of the rupture (Dip). According to location of the site (footing wall or hanging wall), R_X may take negative (footing wall) or

positive (hanging wall) values. In addition to these parameters, R_{JB} and R_{RUP} distance metrics have been shown in Figure 1.2. for different fault orientations.

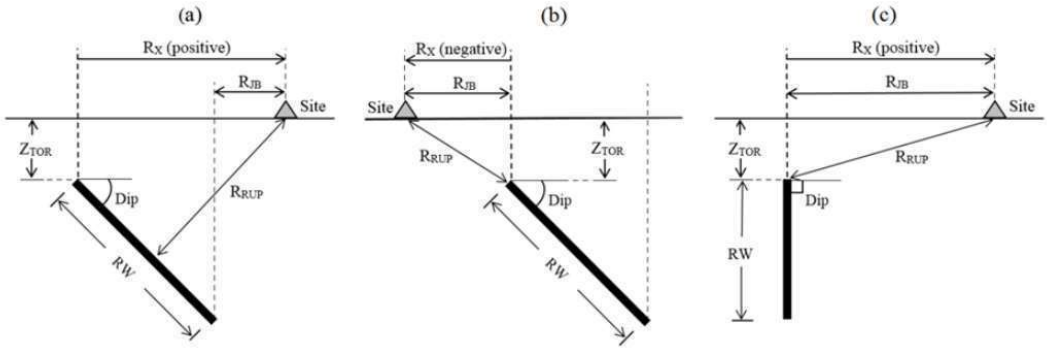

Figure 1.2. Demonstrations of distance metrics for different fault rupture geometries: a) a site on hanging wall side of a dipping fault, b) a site on footing wall side of a dipping fault, c) a site on a vertical fault (adopted from Campbell and Bozorgnia, 2014).

For considering hanging wall effects, one of the alternative models to add on Equation 1.1 is given in Equation 1.10 and sub-terms of this equation are also given between Equation 1.11 - 1.17. These equations are developed with records from NGA-West2 database (Ancheta et al., 2014) in Donahue and Abrahamson (2014) and then simplified to make it more practical to use in GMPEs by Abrahamson et al. (2014). Equation 1.10 has a complicated structure dependent on dipping angle of the fault ($f_{hng,\,dip}$), magnitude ($f_{hng,\,Mw}$), R_X ($f_{hng,\,Rx}$), Z_{TOR} ($f_{hng,\,ZTOR}$) and R_{JB} ($f_{hng,\,RJB}$) terms. This situation generates the need of four additional prediction parameters. To this end, when this function added in the main functional form, it is possible to name it as “complex functional form”.

$$f_{hng} = b_{12}\, f_{hng,dip}\, f_{hng,M_W}\, f_{hng,R_X}\, f_{hng,Z_{TOR}}\, f_{hng,R_{JB}} \qquad (1.10)$$

$$f_{hng,dip} = \begin{cases} (90 - dip)/45, & dip > 30 \\ 60/45, & dip \leq 30 \end{cases} \qquad (1.11)$$

$$f_{hng,M_W} = \begin{cases} 1 + a_{HW}(M_W - 6.5), & M_W \geq 6.5 \\ 1 + a_{HW}(M_W - 6.5) - (1 - a_{HW})(M_W - 6.5)^2, & 5.5 < M_W < 6.5 \\ 0, & M_W \leq 5.5 \end{cases} \quad (1.12)$$

$$f_{hng,R_X} = \begin{cases} h_1 + h_2\left(\frac{R_X}{R_1}\right) + h_3\left(\frac{R_X}{R_1}\right)^2, & R_X < R_1 \\ 1 - \left(\frac{R_X - R_1}{R_2 - R_1}\right)^2, & R_1 \leq R_X \leq R_2 \\ 0, & R_X > R_2 \end{cases} \quad (1.13)$$

$$R_1 = W \cos(dip) \quad (1.14)$$

$$R_2 = 3\,R_1 \quad (1.15)$$

$$f_{hng,Z_{TOR}} = \begin{cases} 1 - \frac{{Z_{TOR}}^2}{100}, & Z_{TOR} \leq 10 \\ 0, & Z_{TOR} > 10 \end{cases} \quad (1.16)$$

$$f_{hng,R_{JB}} = \begin{cases} 1, & R_{JB} = 0 \\ 1 - R_{JB}/30, & R_{JB} < 30 \\ 0, & R_{JB} \geq 30 \end{cases} \quad (1.17)$$

1.4. Information About Current GMPEs

Akkar and Cagnan (2010), Bindi et al. (2011), Akkar et al. (2014b), Bindi et al. (2014), Derras et al. (2014), Kale et al. (2015), Kuehn and Scherbaum (2016), Kotha et al. (2016) developed GMPEs for Europe and Middle East, and global models of Boore and Atkinson (2008) and Boore et al. (2014) GMPEs can be classified as basic functional form GMPEs and they've been developed using R_{JB} as a distance metric. On the other hand, from global NGA-West1 and NGA-West2 GMPEs Abrahamson and Silva (2008), Campbell and Bozorgnia (2008, 2014), Chiou and Youngs (2008, 2014), Abrahamson et al. (2014); Japanese based Zhao et al. (2006) and Cauzzi et al. (2015) use R_{RUP} as main prediction parameter. From these global equations, NGA based equations are classified as complex functional form, others (Japanese based) are classified as basic functional form GMPE. In addition to this, R_{JB} distance metric is also required for hanging wall modelling as secondary distance parameter in the R_{RUP} based NGA models.

In the light of these information, it can be said that, researchers who work with Europe and Middle-East data, prefer basic functional form and form their equations on R_{JB} distance-metric. Here, one of the most important reasons to choose R_{JB} is lower number of earthquake parameters to calculate R_{JB} than to calculate R_{RUP} distance-metric. While it is enough to know the dimensions of the fractured fault and the dipping angle for R_{JB} calculation, to calculate R_{RUP}, Z_{TOR} which can add an effective uncertainty to calculations depending on the quality of database and the focal depth information are needed in addition. Furthermore, in R_{RUP} based GMPEs, requirement of consideration of hanging wall effects in ground-motion predictions and putting the functional form into a complex structure can be shown as another reason.

Putting aside the choice of distance metric, complex functional form has its own deficits. Adding more terms to the functional form make it more complex. As this complexity grows, regression analyses are getting complicated either and making

it harder for models to converge, which is statistically lowering the reliability of models. Also, these additional terms require additional earthquake parameters and this situation brings forward the problem of inadequate number of earthquake parameters in strong-motion databases. Even though a more complex model will be presented, it will cause another problem in the user-side, such as the limitation of usage in probabilistic seismic hazard analyses because of the requirement of more earthquake parameters. Problems like these push GMPE developers to use simpler functional forms in their equations.

If there's another evaluation wanted to be done about current GMPEs, this can be investigating the answer of the question: Does distance metric (R_{JB} or R_{RUP}) which is selected as a main prediction parameter effect the predictions of ground-motion intensity measure? At this point, to make a fast evaluation, median predictions of Abrahamson et al. (2014) – ASK14, Boore et al. (2014) – BSSA14, Campbell and Bozorgnia (2014) – CB14 and Chiou and Youngs (2014) – CY14 from NGA-West2 equations are obtained under two different earthquake scenarios and compared in Figure 1.3. Different source to site distances are considered and equivalent R_{JB}, R_{RUP} and R_X distance values are specified for site locations. Figure 1.3 is plotted for spectral acceleration value of T = 0.2 s versus change of R_X distance value. Important differences between predictions of equations are observed here for close distances depending on magnitude. These differences are smaller between R_{RUP} equations but R_{JB} equation (BSSA14) apparently follows different path than others. All the equations here are developed under the same main database (Ancheta et al., 2014) but developed with different number of recordings according the special selection criteria of different studies. In addition to this, they all have different functional forms. In this context, it is hard to say that type of distance metric is the main reason for these differences. This subject can be understood by changing only the distance parameter and fixing all the other components.

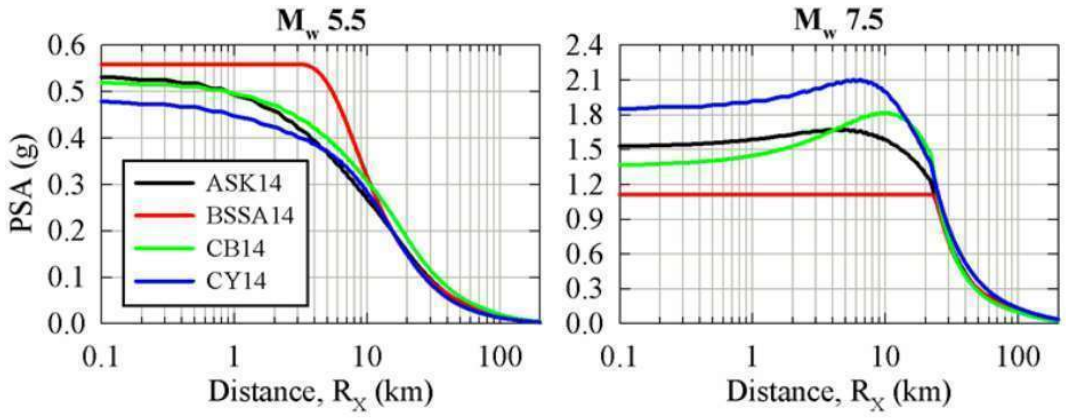

Figure 1.3. Change of spectral acceleration values of T = 0.2 s versus distance (V_{S30} = 760 m/s; fault type: reverse; sites are on the hanging wall side).

Another matter that come into light is considering hypocentral depth as a prediction parameter in R_{JB} GMPEs. Campbell (2016) discusses that this situation is causing some inconsistencies in GMPE predictions. However, this comment hasn't been done in the result of an extensive study about this matter. Campbell (2016) comprises residual analyses of several Europe GMPEs (Akkar et al., 2014; Bindi et al., 2014; etc.) using the database that have been used for Campbell and Bozorgnia (2014). Also, in the results of the evaluations have been done in Campbell (2016), trends have seen in hypocentral depth versus between-event distributions of Pan-European equations which are using R_{JB} distance metric. Although, the present R_{JB} equations don't use hypocentral depth term as a prediction parameter, in this study the necessity of hypocentral depth term in both R_{JB} and R_{RUP} equations will be shown.

Differences between median predictions of different equations given in Figure 1.3 brings forward the epistemic uncertainty concept that have to be considered during the calculations of probabilistic seismic hazard analyses. Budnitz et al. (1997) and Bommer (2012) emphasized that there have to be a specific dispersion in the median predictions of GMPEs that have chosen for seismic hazard analyses. If exactly the same ground-motion intensity measure

predictions cannot be obtained from R_{JB} and R_{RUP} models, then it is possible to talk about an epistemic uncertainty depends on modelling deficiency.

1.5. Content of This Study

In the light of the information that summarized above, using Turkish Strong-Motion database, a R_{RUP} GMPE which is equivalent to R_{JB} model in Kale et al. (2015), will be developed. Here, the most suitable function parameters will be compiled for R_{RUP} model with making an evaluation between necessary functional forms and earthquake database, then GMPE coefficients will be obtained with implementing nonlinear multi-staged regression. Thereafter, general evaluations will be held with comparisons between present Kale et al. (2015) equation and recently developed equation under different earthquake scenarios. In the scope of this stage, effects of focal depth to analyses that mentioned in the previous section will be discussed.

In the second and main part of the content of this study, earthquake recordings that are suitable to the extent of this study in main earthquake parameters (M_W, R_{JB}, R_{RUP}, style of faulting, V_{S30}, etc.) and record qualities (filter status, usable period values, wave structure quality, etc.) will be chosen and similar processes will be held as the previous stage. In this stage, different than previous stage, two different GMPEs that holds both distance-metrics (R_{JB} and R_{RUP}) as main prediction parameters will be derived. Derivation of these GMPEs will be from basic functional form to complex functional form and in the end of these steps, there will be many R_{JB} and R_{RUP} GMPEs in different functional forms that have been derived from the same database. Thus, it will get easier to evaluate the basic and complex functional forms. At this stage, the aim of this study is not to develop a new global GMPE but rather to investigate the resemblance of two GMPEs derived from different distance-metrics and examine the degree of which complex functional form is necessary, in an exhaustive way. Therefore, GMPEs are going to derive for significant critical period values. Comparisons of GMPEs will be held for spectral prediction values of GMPEs in critical earthquake

scenarios that will be generated for different magnitude (M_W), distance (R_{JB}, R_{RUP} and R_X) and style of faulting (reverse and strike-slip) in these period values.

1.6. Organization of This Study

In this study, epistemic uncertainties between two distance-metrics (R_{JB} and R_{RUP}) have been evaluated in the results of residual analyses, median and random variability comparisons which are obtained as a product of regression analyses have been made. Regressions analyses are conducted on two different databases. In the Second Chapter of this study, compilation of those two databases has been presented. In the Third Chapter, as regional applications, regression analyses are performed with using Turkish Strong-Motion database; residuals, median and standard deviations of those GMPEs are evaluated. In the Fourth Chapter, transformation from basic to complex functional form has been conducted with adding a new term to GMPEs in every step. Evaluations of residuals, median and standard deviations also have been made in this chapter for every GMPE that developed under the global database. Finally, the summary and the conclusions of this study are presented in Chapter 5.

2. COMPILATION OF STRONG GROUND-MOTION DATABASES

Database which has been used for the evaluation of R_{RUP} GMPE, which is developed with using Turkish data, is taken from Kale et al. (2015). The database which has been used here, contains R_{JB} distance metric. To make suitable to the purpose of this study R_{RUP} distance metrics have been added to the relevant database. The database which has been used in the second part of this study is adjusted with the record quality and the compatibility criteria of records to GMPEs from Campbell and Bozorgnia (2014) which is for this study, the most convenient set of NGA-West2 database, which contains nearly 21000 records.

2.1. Compilation of Turkish Strong-Motion Database

In the scope of this study, the strong motion database that uses Joyner-Boore distance metric (R_{JB}; the closest distance of record station to the fault surface projectile) and has been developed for Kale et al. (2015) is taken directly. Moment magnitude of the earthquake (M_W), distance between the source and the station (as R_{JB}), style of faulting of earthquake, average shear wave velocity of the record station (V_{S30}; average shear wave velocity of the upper 30m layer of the soil) and hypocentral depth (Z_{HYP}) have been used as the parameters for development of the GMPEs from this database. In addition to these, the closest distance to the fault source from record station (R_{RUP}) also has been added to the database as it's going to be the main parameter in this study. Despite the fact that there are fault plane solutions for 13 records in Kale et al. (2015) database, R_{RUP} information couldn't have been gathered for these records. R_{RUP} distance metrics of these records have been re-calculated considering their ruptured fault planes and added to the database.

The compiled database includes 670 strong ground-motion acceleration records of magnitude between 4.0 and 7.6 ($4.0 \leq M_W \leq 7.6$), R_{JB} and $R_{RUP} \leq 200$ km and hypocenter depth up to 35 km from 175 active shallow crustal earthquakes.

Number of records that belongs to strike-slip and normal fault earthquakes are more than reverse ones. This situation was evaluated consistent considering the general fault type of Turkey. In the database, according to Turkish Building Earthquake Code 2018 (TBEC18) site conditions, acceleration recordings are dominant in ZC (360 m/s ≤ V_{S30} < 760 m/s) and ZD (180 m/s ≤ V_{S30} < 360 m/s) site classes. Alongside with this, the database includes sufficient amount of rock type (ZA and ZB, V_{S30} > 760 m/s) of acceleration records. Therefore, consistent regression results can be obtained.

General seismological features of the database shown in Figure 2.1. R_{JB} and R_{RUP} distance metrics versus M_W distribution has been shown in Figure 2.1.a while the comparison of R_{JB} and R_{RUP} distance metrics between each other has been given in Figure 2.1.b. In these figures, to show on logarithmic axis, records with distance values lower than 0.1 km (3 for R_{RUP} and 9 for R_{JB}) are taken as 0.1 km. In this stage, when Figure 2.1.b has been analyzed, it can be seen that there's a serious discrepancy between R_{JB} and R_{RUP} but especially after 80 km this dispersion diminishes completely. This observation, which is completely coincides with the literature (Akkar et al., 2014), is connected to definition of distance metrics and projectile surface area of fractured fault.

To evaluate the possible effect of hypocentral depth, which is one of the most important topics of this study, to ground-motion prediction equations that use especially R_{JB} distance metric, Figure 2.2 has been illustrated. In this figure, change of hypocentral depth of earthquakes in the compiled ground-motion database versus magnitude has been shown. In addition to this change, distribution of fault types also has been shown on this figure using different pointers. The most apparent comment that can be said after this figure is hypocentral depths that belong to greater magnitude values (especially M_W > 6.0) are lower. Depth distributions of middle and small magnitude recordings are generally behaving regular in-between 0 and 30 km.

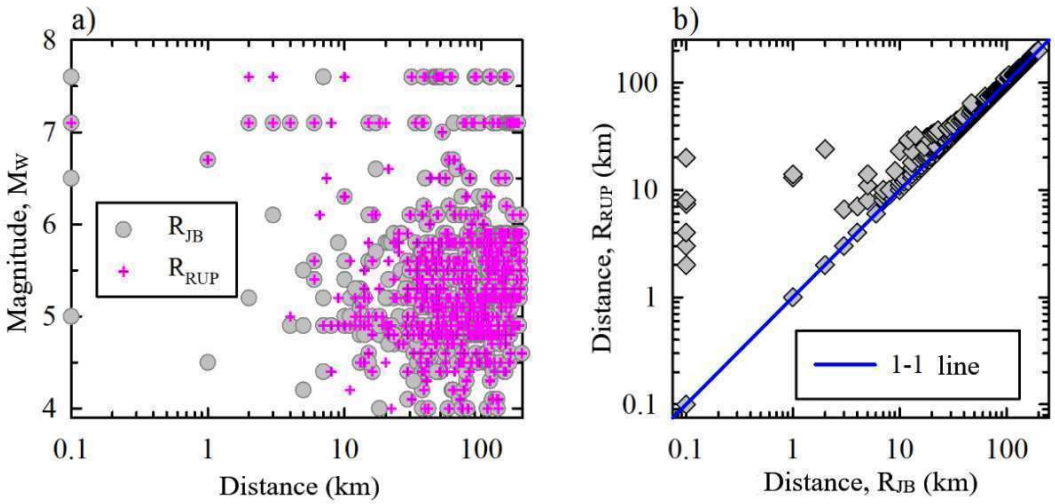

Figure 2.1. Ground-motion data that will be used in regression analyses: a) R_{RUP} and R_{JB} versus M_W distribution, b) R_{JB} versus R_{RUP} comparison.

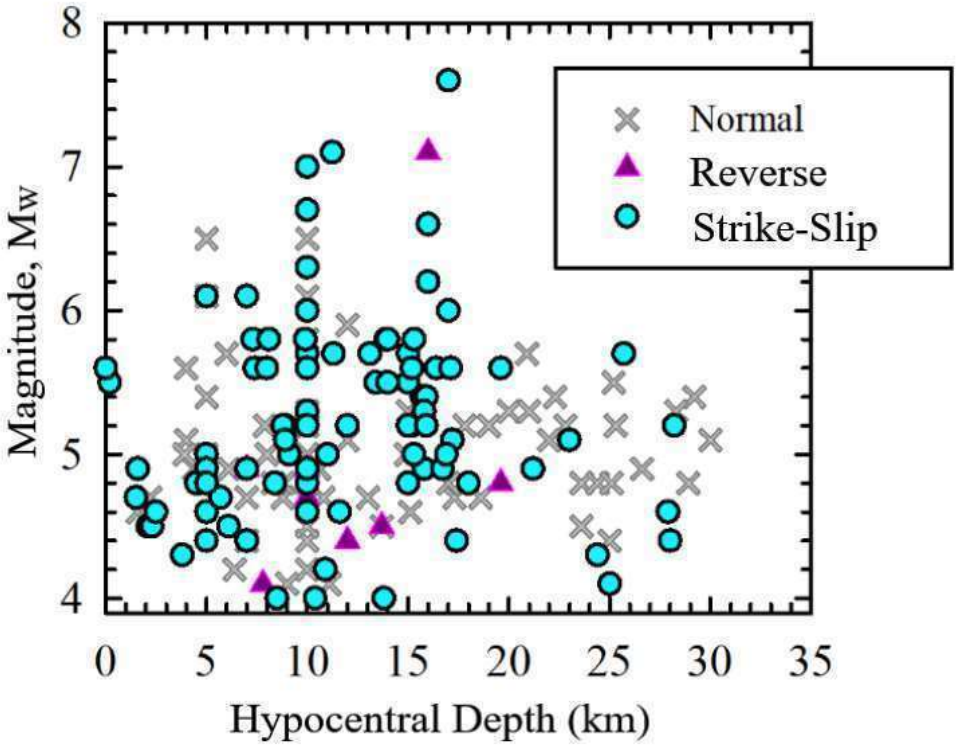

Figure 2.2. Hypocentral depth distribution of ground-motion database in terms of fault type.

2.2. Compilation of the Global Database

In the second part of this study, a global strong motion database has been compiled from NGA-West2 database (Ancheta et al., 2014) to use in evaluations of basic and complex forms of ground-motion prediction equations. The main goal in this study is application of basic and complex functional forms in GMPEs depending on distance-metric. Ancheta et al. (2014) database includes approximately 21000 acceleration records. To this main set, quality criteria of Campbell and Bozorgnia (2014) has been applied. In this context, these recording are excluded from main database to obtain an earthquake database to use in regressions:

- Recordings with no measured or estimated V_{S30} values
- Earthquakes with no rake angle or focal mechanism
- Earthquakes with hypocentral depth of more than 20 km or on the ocean plate or on the stable continental regions
- Recordings with non-realistic spectral shapes, late triggering, low quality, considered as unreliable because doesn't locate on the free surfaces
- Recordings that qualified as low quality according to criteria of $M_W < 5.5$ and $N < 5$ or $5.5 \leq M_W < 6.5$ and $N < 3$ (Earthquakes with one recording but with big magnitude have been included.) (N: number of recordings with closest distance to fault fracture plane (R_{RUP}) lower than 80 km or equal to 80 km)
- Earthquakes that moment magnitude values (M_W) have been empirically estimated from other magnitude types

Global database which is compiled with application of these criteria that are explained here, includes 13670 ground-motion acceleration recordings from 322 earthquakes with magnitude between 3.0 – 7.9. Comparisons of R_{JB} and R_{RUP} distance-metrics versus M_W and comparison of R_{JB} and R_{RUP} distance-metrics have been given in Figure 2.3. In this figure, R_{JB} or R_{RUP} values below 0.1 km have been shown as 0.1 km because logarithmic axis has been used but in

calculations, real values have been used. Chosen database includes mostly strike-slip and reverse style of faulting. Alongside with this, there are limited number of normal faults are included too. Most of the recordings in earthquake database are in ZC (360 m/s ≤ V_{S30} < 760 m/s) and ZD (180 m/s ≤ V_{S30} < 360 m/s) site conditions. This is a similar feature with Turkish database. Global database includes greater number of close distance acceleration records. When the slope between R_{JB} and R_{RUP} distance-metrics has been considered in Figure 2.3.b, it is similar to the behavior of Turkish database shown in Figure 2.1.b. In this context, R_{JB}-R_{RUP} relation in Turkish database can be considered as reliable. Here, the reasons to choose a global database are higher number of recordings and positive differences in quality of records.

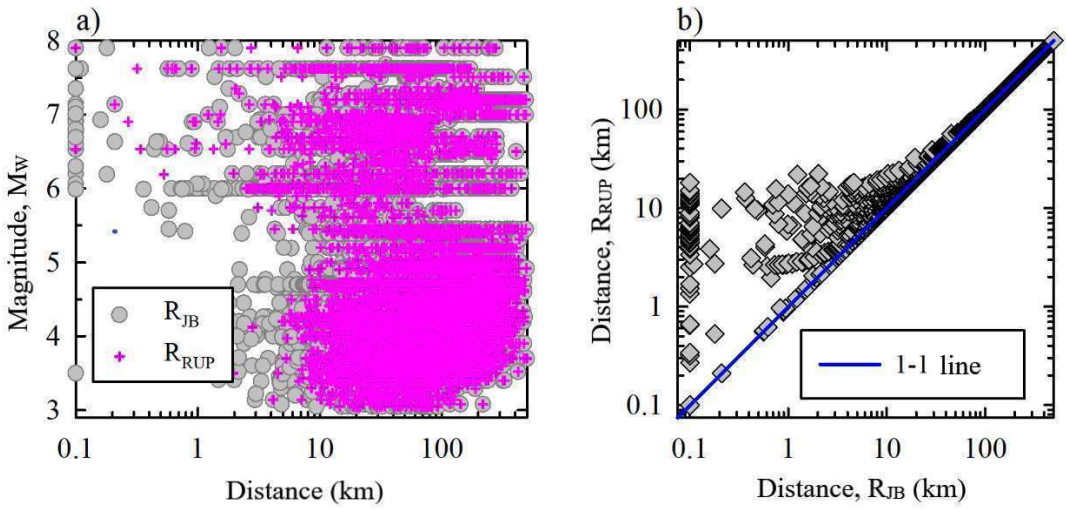

Figure 2.3. NGA-West 2 near source database that will be used in regression analyses: a) distribution of R_{JB} and R_{RUP} versus M_W, b) comparison of R_{JB} versus R_{RUP}.

Change of hypocentral depth dependent on magnitude according to style of faulting has been shown in Figure 2.4. This database is showing a decent distribution according to hypocentral depth. All of the recordings with magnitude lower than 5 have strike-slip fault mechanism, while similar distributions have been observed in other magnitude values.

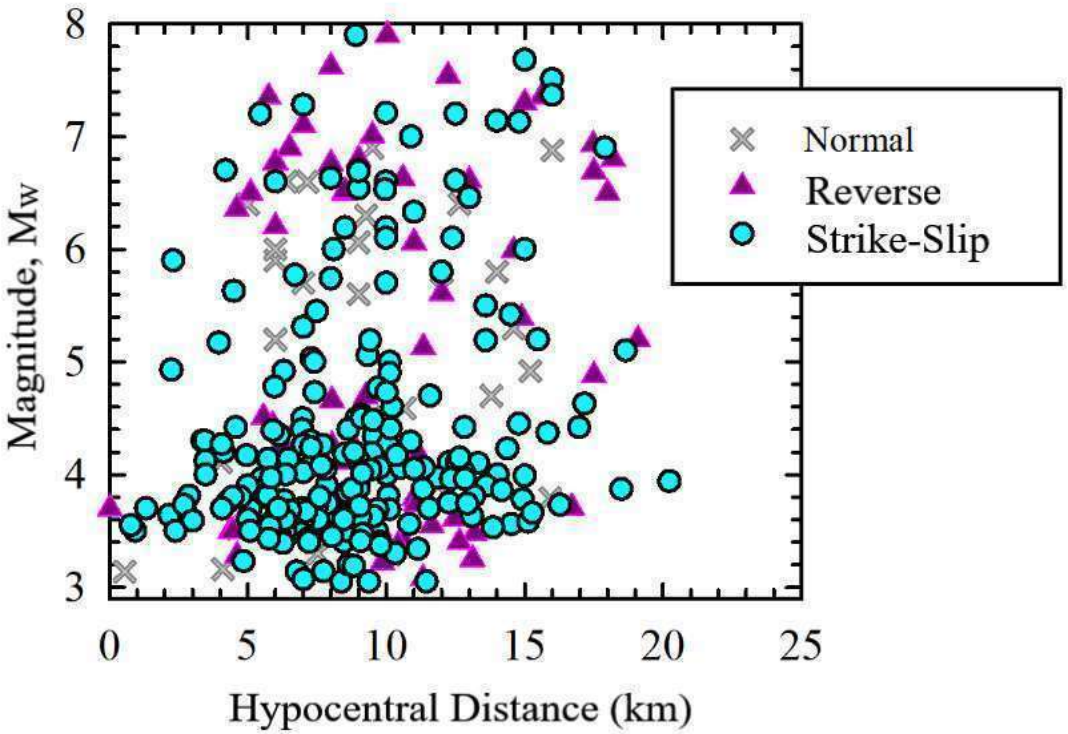

Figure 2.4. Distribution of hypocentral depth of ground-motion database dependent on magnitude in terms of style of faulting.

3. GMPE EVALUATIONS FOR TURKEY

In this part of this study, a R_{RUP} GMPE, which is equivalent to the R_{JB} model in Kale et al. (2015), has been developed with using the Turkish ground-motion earthquake data that recently compiled in the previous part. In addition to this model, hypocentral depth terms have also been added to the functional forms of R_{JB} and R_{RUP} models.

Abrahamson and Youngs (1992) mixed-effects algorithm has been chosen as regression method. Regression procedure implemented exactly same as in Kale et al. (2015). Thus, it is aimed to observe only the effect of change of distance metric in ground-motion model predictions. Weighted regression algorithm that depends on magnitude value has been used in Kale et al. (2015). Hereby, low uncertainty which is in high magnitude ground-motion data and high uncertainty which comes from low magnitude earthquakes can be controlled in random variable models of prediction equations. Ground-motion database has been evaluated as different grades: near source database (R_{JB} < 80 km), far source database (80 km ≤ R_{JB} ≤ 200 km) and complete database (R_{JB} ≤ 200 km). While the magnitude dependent regression coefficients and style of faulting coefficients have been derived from near source database, the distance scaling coefficient has been predicted from complete database. Besides, far source database has been used for acquiring anelastic distance attenuation term. After applying some smoothing to the regression coefficients, constant coefficient and standard deviation terms have been calculated with using complete database.

Dependency on hypocentral depth has also been investigated for developed and present prediction equations. In this stage, statistical dependency assessments for different depth groups has been done (e.g. 0-5 km, 5-10 km etc.) by the calculation of the difference between empirical data and prediction data (namely residual). Also, by adding the hypocentral depth term to the regression function,

effect of hypocentral depth term to the results has been discussed for both of the GMPEs.

In the scope of this study, comparison of the median prediction values of GMPEs has been done under several earthquake scenarios by using developed and present equations. In the earthquake scenarios that will be used for comparison, different types of distance metrics that are calculated consistent with the fault dimensions calculated from Wells and Coppersmith (1994) study have been taken into account. Moreover, to obtain the other earthquake parameters that will be needed for calculating the R_{RUP} distance metric (hypocentral distance; dipping angle of the fault; distance from the upper edge of the fault plane to the surface, Z_{TOR}), empirical connections from Kaklamanos et al. (2011) have been taken noticed.

3.1. Development of the R_{RUP} Dependent GMPE

The functional form of Kale et al. (2015) equation has been shown in Equation 3.1. This functional form includes magnitude scaling (f_{mag}, Equation 3.2), distance scaling (f_{dis}, Equation 3.3), style of faulting (f_{sof}, Equation 3.4), anelastic distance attenuation (f_{aat}, Equation 3.5) and linear and nonlinear site amplification (f_{site}, Equation 3.6) terms. F_{NM} and F_{RV} terms in Equation 3.4 are dummy variables that belongs to normal and reverse style of faultings and they take unit value for normal and reverse faulting types, respectively. Both of the parameters are zero for strike-slip faults. Nonlinear site amplification term is taken from Sandıkkaya et al. (2013). Function constants values are: V_{CON} = 1000 m/s, V_{REF} = 750 m/s, c = 2.5 and n = 3.2. In this equation, PGA_{REF} is the maximum ground acceleration value for reference rock that calculated for V_{S30} = 750 m/s from Equation 3.1.

Random variability model has been configured as heteroscedastic magnitude dependent and shown in Equation (3.7 - 3.9). Total random variability (standard

deviation, σ; Equation 3.7) is a combination of between-event standard deviation (τ) and within-event standard deviation (Φ). "*sd₁*" and "*sd₂*" are weighted standard deviation terms, meanwhile w is weighting function that obtained from pure error analysis and can be calculated with Equation 3.9.

$$lnY = f_{mag} + f_{dis} + f_{sof} + f_{aat} + f_{site} \tag{3.1}$$

$$f_{mag} = \begin{cases} b_1 + b_2(M_W - 6.75) + b_3(8.5 - M_W)^2, & M_W \leq 6.75 \\ b_1 + b_7(M_W - 6.75) + b_3(8.5 - M_W)^2, & M_W > 6.75 \end{cases} \tag{3.2}$$

$$f_{dis} = [b_4 + b_5 (M_W - 6.75)] \ln \sqrt{R_{RUP}^2 + b_6^2} \tag{3.3}$$

$$f_{sof} = b_8 F_{NM} + b_9 F_{RV} \tag{3.4}$$

$$f_{aat} = \begin{cases} 0, & R_{RUP} \leq 80 \\ b_{10}(R_{RUP} - 80), & R_{RUP} > 80 \end{cases} \tag{3.5}$$

$$f_{site} = \begin{cases} sb_1 \ln\left(\frac{V_{S30}}{V_{REF}}\right) + sb_2 \ln\left[\frac{PGA_{REF} + c\,(V_{S30}/V_{REF})^n}{(PGA_{REF} + c)(V_{S30}/V_{REF})^n}\right], & V_{S30} < V_{REF} \\ sb_1 \ln\left(\frac{\min(V_{S30}, V_{CON})}{V_{REF}}\right), & V_{S30} \geq V_{REF} \end{cases} \tag{3.6}$$

$$\sigma = \sqrt{\tau^2 + \Phi^2} \tag{3.7}$$

$$\Phi = w\, sd_1\,;\ \tau = w\, sd_2 \tag{3.8}$$

$$w = \begin{cases} a_1, & M_W < 6.0 \\ a_1 + (a_2 - a_1)[(M_W - 6)/0.5], & 6.0 \leq M_W < 6.5 \\ a_2, & M_W > 6.5 \end{cases} \quad (3.9)$$

List of period dependent nonlinear site amplification model coefficients that have been derived for Turkey and Middle East and used in regression analysis of Sandıkkaya et al. (2013), is given in Table 3.1. Constant model coefficients that come from regression analysis results are given in Table 3.2, as period dependent variables listed in Table 3.3.

Table 3.1. Period dependent nonlinear site effects model coefficients that defined in Sandıkkaya et al. (2013).

Period (s)	sb1	sb1
PGA	-0.41997	-0.28846
0.01	-0.41729	-0.28685
0.02	-0.39998	-0.28241
0.03	-0.34799	-0.26842
0.05	-0.21231	-0.22385
0.1	-0.26492	-0.28832
0.15	-0.48496	-0.39525
0.2	-0.64239	-0.44574
0.3	-0.82052	-0.45287
0.4	-0.90568	-0.41105
0.5	-0.95097	-0.37956
0.75	-1.00027	-0.32233
1	-1.01881	-0.28172
1.5	-0.96317	-0.22449
2	-0.91305	-0.18388
3	-0.84242	-0.12665
4	-0.79231	-0.08605

Table 3.2. Constant model coefficients of R_{RUP} equation that is in basic functional form.

b2	b5	b6	b7
0.193	0.17	8	-0.354

Table 3.3. Period dependent model coefficients of R_{RUP} equation that is in basic functional form.

Period (s)	b1	b3	b4	b7	b8	b9	b10	a1	a2	sd1	sd2
PGA	2.13572	-0.07049	-1.25932	-0.354	-0.01329	-0.09158	-0.00112	0.57	0.45	1.0778	0.718
0.01	2.15188	-0.06981	-1.2615	-0.354	-0.01349	-0.09158	-0.00112	0.574	0.453	1.0699	0.7127
0.02	2.18315	-0.07058	-1.26451	-0.354	-0.01189	-0.09158	-0.00112	0.577	0.455	1.0678	0.7113
0.03	2.27764	-0.06976	-1.27573	-0.354	-0.00748	-0.09158	-0.00112	0.581	0.458	1.0706	0.7107
0.05	2.57668	-0.06226	-1.32364	-0.354	0.03907	-0.09158	-0.00139	0.588	0.463	1.0836	0.7218
0.1	3.16877	-0.05217	-1.41831	-0.354	0.1	-0.09158	-0.00206	0.606	0.475	1.0649	0.7784
0.15	3.36364	-0.06397	-1.40713	-0.354	0.06727	-0.09158	-0.00257	0.624	0.488	1.0266	0.7483
0.2	3.29931	-0.07494	-1.35895	-0.354	0.0162	-0.09158	-0.00266	0.642	W0.5	0.9921	0.7252
0.3	2.85133	-0.09387	-1.24116	-0.354	-0.03697	-0.09158	-0.00204	0.678	0.525	0.9542	0.6511
0.4	2.33395	-0.10977	-1.12534	-0.354	-0.06582	-0.09158	-0.00161	0.7	0.55	0.9569	0.6352
0.5	1.87615	-0.12342	-1.03066	-0.354	-0.08511	-0.01297	-0.00127	0.673	0.55	0.9703	0.6464
0.75	1.10781	-0.15056	-0.88761	-0.354	-0.11756	0	-0.00066	0.62	0.55	1.0673	0.659
1	0.66829	-0.17099	-0.82253	-0.354	-0.14267	0	-0.00022	0.62	0.55	1.0721	0.6314
1.5	0.15868	-0.19999	-0.77308	-0.354	-0.14621	0	0	0.62	0.55	1.1167	0.618
2	-0.18563	-0.21978	-0.75629	-0.354	-0.14621	0	0	0.62	0.55	1.1779	0.5741
3	-0.66314	-0.2453	-0.74522	-0.354	-0.14621	0	0	0.62	0.55	1.1678	0.6296
4	-0.9687	-0.26119	-0.74175	-0.354	-0.14621	0	0	0.62	0.55	1.0381	0.5536

Between-event and within-event residuals of R_{RUP} equation that are derived from regression analysis are obtained according to mixed-effects algorithm that is given in Abrahamson and Youngs (1992). Change of between-event residuals versus magnitude (M_W) and hypocentral depth (Z_{HYP}) and also change of within-event residuals versus distance (R_{RUP}) have been shown in Figure 3.1 in different panels for peak ground acceleration (PGA), T = 0.2 s and 1.0 s. In these figures, red circles stand for residuals (within-event or between-event); black squares represent average values of different magnitudes, distances and depths and black lines show 95% confidence intervals for average values. If confidence intervals are crossing the zero line or the mean is very close to zero, that shows this model makes consistent predictions in related period value. In this context, it

is clear that there is no problem in the equation related to magnitude and distance. When the residuals dependent on depth have been evaluated, it can be seen that there is particular level of bias in trends for PGA and T = 0.2 s values for shallow earthquakes. Although this trend is in negligible level, a new version R_{RUP} equation with hypocentral depth term has been developed to investigate the option of decreasing the trend with adding the hypocentral depth term to Equation 3.1 and this process has been explained in the next section. The observations made for the periods that have been selected here are also overarching for other periods that are selected for the regression.

3.2. Development of the R_{RUP} Dependent GMPE with the Hypocentral Depth Term

For the purpose of investigating the effect of hypocentral depth term, Equation 3.10 has been obtained by adding hypocentral depth term (f_{hyp}) to the Equation 3.1, which is the R_{RUP} based ground-motion prediction equation that is developed in previous stage. The functional form of hypocentral depth term has been given in Equation 3.11. This function is a suitable function for tectonic structure of active shallow earthquakes that are recommended in Campbell and Bozorgnia (2014). In this equation, Z_{HYP} term stands for hypocentral depth of the earthquake in kilometers.

$$lnY = f_{mag} + f_{dis} + f_{sof} + f_{aat} + f_{site} + f_{hyp} \tag{3.10}$$

$$f_{hyp} = \begin{cases} 0, & Z_{HYP} < 0 \\ b_{11}(Z_{HYP} - 7), & 7 < Z_{HYP} \leq 20 \\ 13b_{11}, & Z_{HYP} > 20 \end{cases} \tag{3.11}$$

In this stage, regression coefficients of R_{RUP} equation with depth term (namely R_{RUP} + Z_{HYP}) has developed with the same regression steps that are used to

obtain the R_{RUP} based equation in the previous stage. Sandıkkaya et al. (2013) (see. Table 3.1) have been used again as nonlinear site amplification function. The most of the coefficients haven't been changed in the result of regression. Therefore, in Table 3.4, only the period dependent values of the coefficients that have changed are listed.

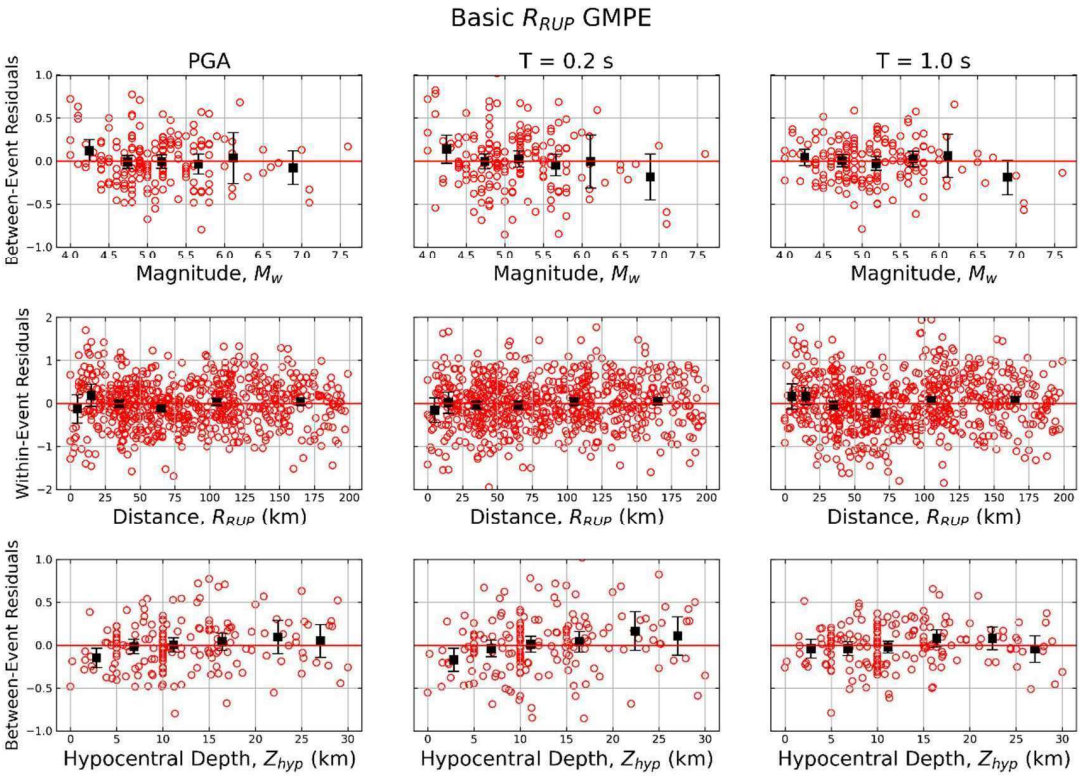

Figure 3.1. The distributions of between event residuals versus magnitude (top row), within-event residuals versus distance (middle row) and between event residuals versus hypocentral depth (bottom row) for basic functional form R_{RUP} equation.

Table 3.4. Model coefficients of the R_{RUP} equation that is in basic functional form with hypocentral depth term.

Period (s)	b1	b11	a1	a2	sd1	sd2
PGA	2.01966	0.02056	0.57	0.45	1.0769	0.7021
0.01	2.03497	0.02073	0.574	0.453	1.0689	0.6968
0.02	2.06461	0.0209	0.577	0.455	1.0674	0.6933
0.03	2.15661	0.02105	0.581	0.458	1.0701	0.6925
0.05	2.44944	0.0224	0.588	0.463	1.0833	0.701
0.1	3.02391	0.0255	0.606	0.475	1.0646	0.7551
0.15	3.20897	0.02785	0.624	0.488	1.0254	0.7251
0.2	3.14893	0.02796	0.642	0.5	0.9903	0.7046
0.3	2.73199	0.02079	0.678	0.525	0.9527	0.6413
0.4	2.2539	0.01607	0.7	0.55	0.9563	0.628
0.5	1.78509	0.01679	0.673	0.55	0.97	0.637
0.75	1.01853	0.01708	0.62	0.55	1.0675	0.6455
1	0.57059	0.01683	0.62	0.55	1.0718	0.6198
1.5	0.07143	0.01476	0.62	0.55	1.1167	0.6084
2	-0.23942	0.0098	0.62	0.55	1.1785	0.5667
3	-0.7409	0.00737	0.62	0.55	1.1667	0.629
4	-1.02983	0.00893	0.62	0.55	1.0392	0.5449

Residual evaluations of derived ground-motion prediction equation are repeated especially for the purpose of research to investigate the effect of hypocentral depth term. Residual evaluations are given in the same format as in Figure 3.2. In this context, an apparent change has been observed in magnitude and distance dependent distributions. As seen in hypocentral depth versus between-event residuals graph, the trend in shallow depths that has been observed in the basic functional form R_{RUP} equation has been diminished as well. Besides, there are closer results to zero line for average residual values of Z_{HYP} > 20 km. All those observations show that, hypocentral depth term has enhanced the prediction capability of equation.

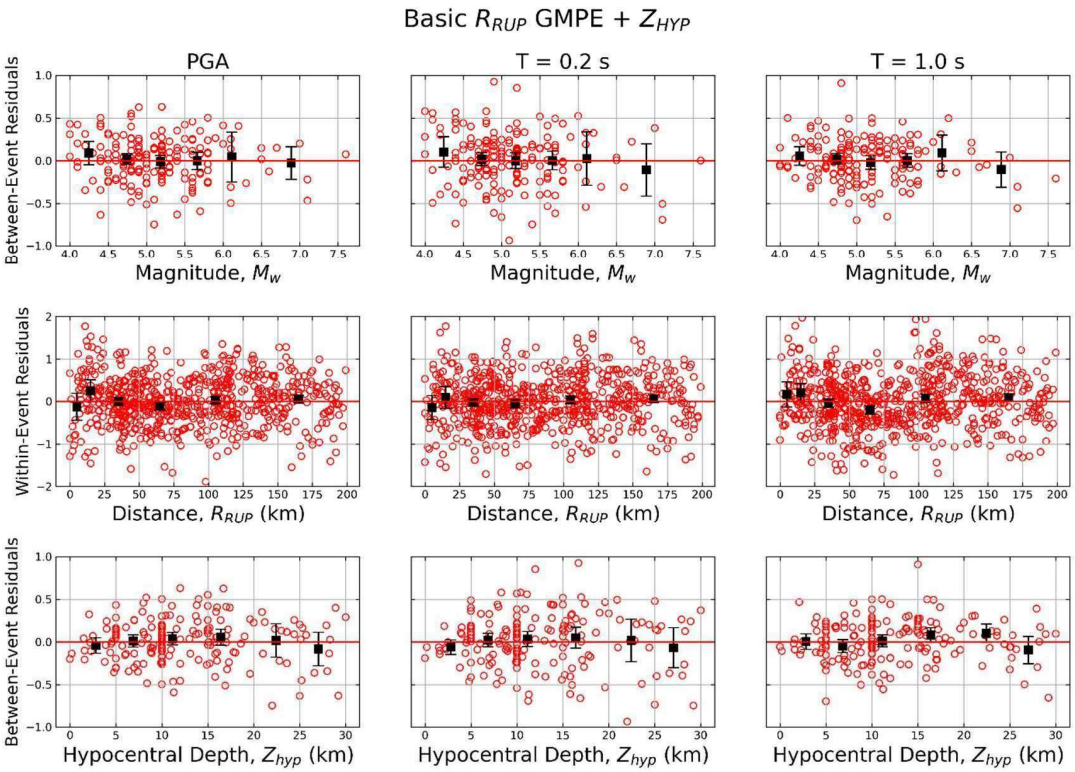

Figure 3.2. The distributions of between event residuals versus magnitude (top row), within-event residuals versus distance (middle row) and between event residuals versus hypocentral depth (bottom row) for basic functional form R_{RUP} equation with depth term add-on.

To observe more clearly the effects of hypocentral depth term to the total standard deviations of the R_{RUP} based ground-motion prediction equations, Figure 3.3 has been prepared. In this figure, standard deviation values of basic R_{RUP} equation and R_{RUP} with Z_{HYP} add-on equation has been shown for two different magnitude values (M_W 5.0 and 7.5) with change of period. Here, it can be seen that hypocentral depth term has an effect to decrease the random variability even if just a bit.

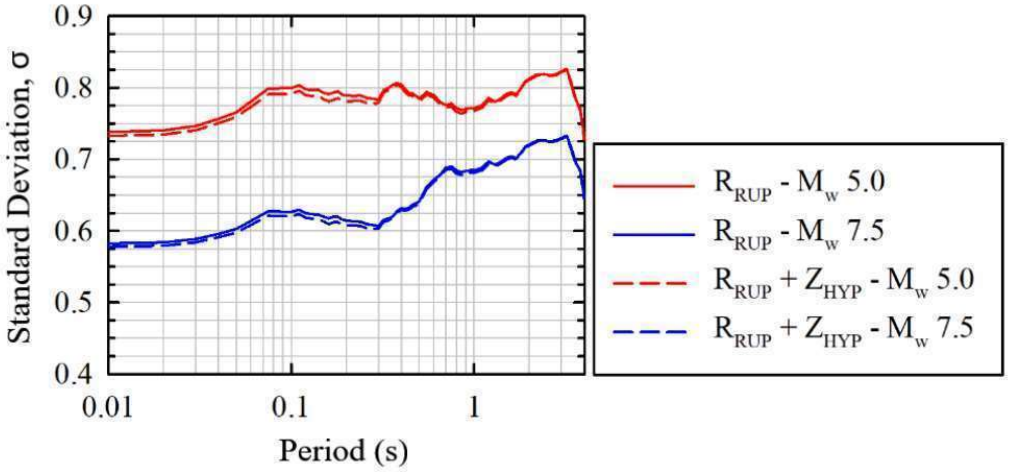

Figure 3.3. Period dependent total standard deviation comparisons for R_{RUP} equations.

3.3. Development of R_{JB} Distance Metric Dependent Kale et al. (2013) Equation's Version with Hypocentral Depth Term

When taken into account the effects of the hypocentral depth term to the R_{RUP} based ground-motion prediction equation, it is a reasonable approach to investigate the same effects in present R_{JB} based Kale et al. (2015) equation. In Figure 3.4, the distribution of between-event and within-event residuals versus magnitude, distance and hypocentral depth of R_{JB} based Kale et al. (2015) ground-motion prediction equation has been shown. Here, comparing the R_{RUP} version of the same equation (see. 3rd row of Figure 3.1), there are less trend has been observed. Average residual values (black squares) generally scatter around zero line. Even though there's a fair amount of divergence from zero for Z_{HYP} values between 0 and 5 km, confidence intervals are still crossing the zero line. In this situation, it's not possible to speak of dependence of hypocentral distance for R_{JB} equation, in this database.

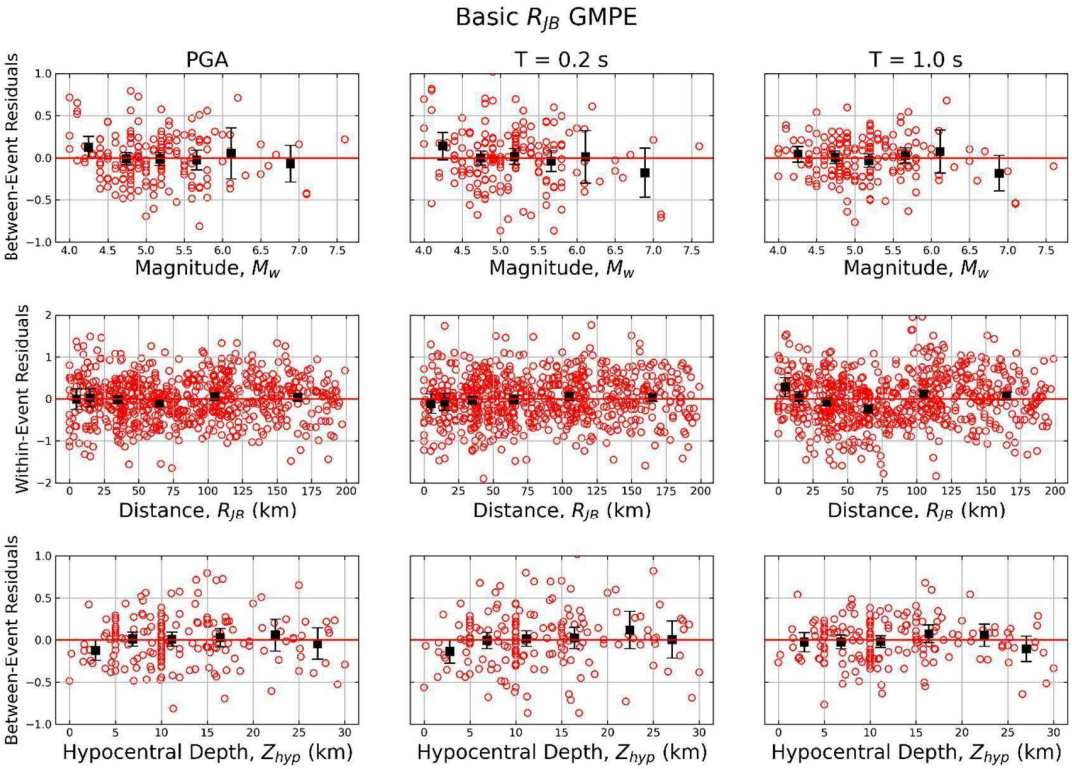

Figure 3.4. The distributions of between event residuals versus magnitude (top row), within-event residuals versus distance (middle row) and between event residuals versus hypocentral depth (bottom row) for basic functional form Kale et al. (2015) R_{JB} equation.

Despite the observation above, regressions have been repeated for the purpose of investigating the effect of hypocentral depth term on the R_{JB} equation in basic functional form. While developing the R_{JB} based equation with hypocentral depth term, the steps (Equations 3.1 - 3.11) that are used to develop the R_{RUP} based equation with hypocentral depth term have been followed. The only difference between R_{RUP} equation and this equation is utilization of R_{JB} as distance metric in regression steps. In other words, instead of R_{RUP} distance parameter in Equation 3.3 and 3.5, R_{JB} has been used. This derived equation should be treated as a version of the equation that is developed in Kale et al. (2015) which takes into account of hypocentral depth term. Regression coefficients of the developed equation have been listed in Table 3.5 and 3.6. Sandıkkaya et al. (2013) has been taken as site amplification function (see. Table 3.1).

Table 3.5. Constant model coefficients of the hypocentral depth term included version of Kale et al. (2015) equation that uses R_{JB} as distance metric.

b2	b5	b6	b7
0.193	0.17	8	-0.354

Residual distributions of developed R_{JB} based equation with hypocentral depth term (namely R_{JB} + Z_{HYP}) have been given in Figure 3.5. Negative average residual values of R_{JB} equation have been observed notably close to zero between 0 – 5 km in this situation. In general, when analyzing the hypocentral depth term dependent residual distributions, it is possible to say that hypocentral term is enhancing the prediction capability of R_{JB} equation as well. For the purpose of investigating the effect of hypocentral depth term to total standard deviation values of R_{JB} based equations, comparisons have been done in Figure 3.6. Here, the findings are similar to the observations that have been done for R_{RUP} equations. Hypocentral depth term has shown the effect of lowering the total random variability of equations.

Table 3.6. Period dependent model coefficients of the hypocentral depth term included version of Kale et al. (2015) equation that uses R_{JB} as distance metric.

Period (s)	b1	b3	b4	b8	b9	b10	b11	a1	a2	sd1	sd2
PGA	1.7063	-0.07049	-1.18164	-0.01329	-0.09158	-0.00156	0.0069	0.57	0.45	1.0516	0.72
0.01	1.7208	-0.06981	-1.18362	-0.01349	-0.09158	-0.00156	0.00705	0.574	0.453	1.0443	0.7126
0.02	1.75065	-0.07058	-1.18653	-0.01189	-0.09158	-0.0016	0.00722	0.577	0.455	1.0423	0.7113
0.03	1.84118	-0.06976	-1.19699	-0.00748	-0.09158	-0.0017	0.0073	0.581	0.458	1.0459	0.7088
0.05	2.11844	-0.06226	-1.24101	0.03907	-0.09158	-0.00197	0.00814	0.588	0.463	1.0608	0.714
0.1	2.66984	-0.05217	-1.32996	0.1	-0.09158	-0.00267	0.01034	0.606	0.475	1.0429	0.769
0.15	2.85177	-0.06397	-1.31888	0.06727	-0.09158	-0.00296	0.01278	0.624	0.488	1.0058	0.7395
0.2	2.78768	-0.07494	-1.27072	0.0162	-0.09158	-0.00275	0.01315	0.642	0.5	0.9776	0.7167
0.3	2.39812	-0.09387	-1.16008	-0.03697	-0.09158	-0.00204	0.00712	0.678	0.525	0.9401	0.6543
0.4	1.96571	-0.10977	-1.05535	-0.06582	-0.09158	-0.00161	0.0035	0.7	0.55	0.9432	0.6392

Table 3.6. (Cont'd)

0.5	1.53587	-0.12342	-0.97014	-0.08511	-0.01297	-0.00127	0.00508	0.673	0.55	0.9521	0.6475
0.75	0.81441	-0.15056	-0.83799	-0.11756	0	-0.00066	0.00669	0.62	0.55	1.049	0.6556
1	0.37218	-0.17099	-0.77438	-0.14267	0	-0.00022	0.00707	0.62	0.55	1.0534	0.6315
1.5	-0.13571	-0.19999	-0.72272	-0.14621	0	0	0.00527	0.62	0.55	1.0991	0.6144
2	-0.45584	-0.21978	-0.70389	-0.14621	0	0	0.00048	0.62	0.55	1.1594	0.5724
3	-0.96705	-0.2453	-0.69065	-0.14621	0	0	-0.00087	0.62	0.55	1.1588	0.628
4	-1.25689	-0.26119	-0.6862	-0.14621	0	0	0.00036	0.62	0.55	1.0364	0.5404

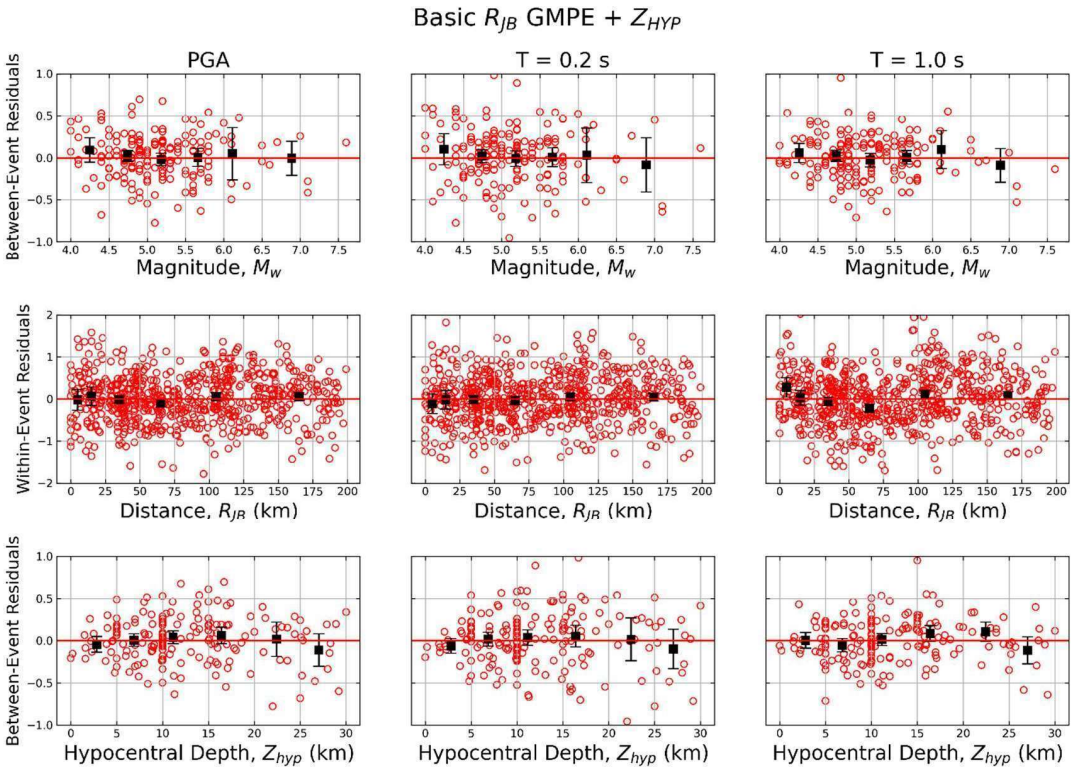

Figure 3.5. The distributions of between event residuals versus magnitude (top row), within-event residuals versus distance (middle row) and between event residuals versus hypocentral depth (bottom row) for basic functional form R_{JB} equation with depth term add-on.

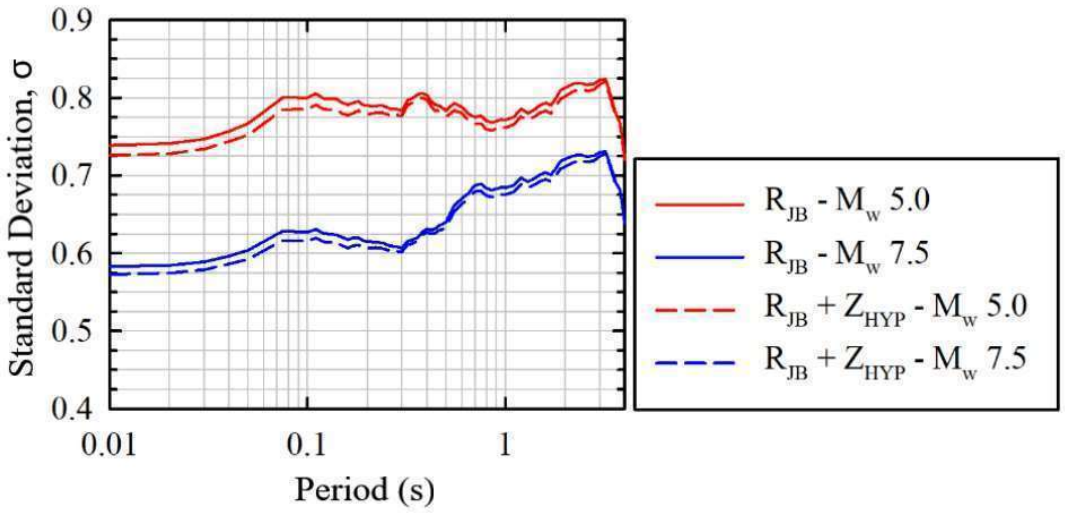

Figure 3.6. Period dependent total standard deviation comparisons for R_{JB} equations.

To compare the contribution of hypocentral depth term on R_{JB} and R_{RUP} equations, regression coefficients that are controlling the hypocentral depth term has been compared in Figure 3.7. In this figure, solid orange line stands for hypocentral depth term added functional form of R_{RUP} equation (Basic R_{RUP} GMPE + Depth), while solid blue line stands for hypocentral depth term added functional form of R_{JB} equation (Basic R_{JB} GMPE + Depth). While the general behavior is same, the line stands for R_{JB} equation is clearly under the R_{RUP} equations. Therefore, it can be said that, the contribution of hypocentral depth term in R_{JB} equation is lower than the R_{RUP} ones, under Turkish Strong-Motion database.

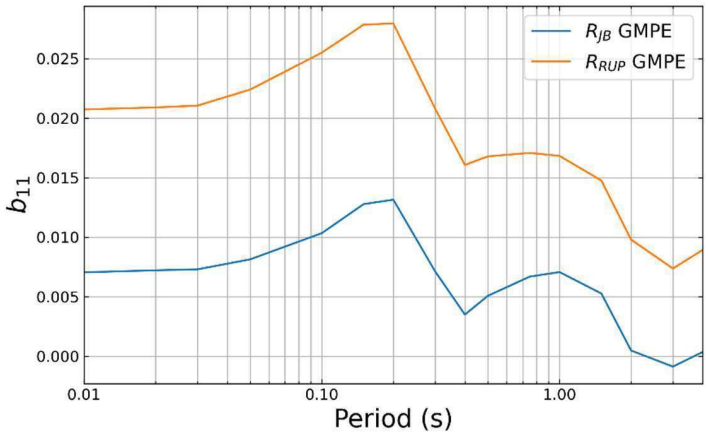

Figure 3.7. Comparison of b_{11} regression coefficients, which controls the hypocentral depth term, from the analyses that are held under Turkish Strong-Motion database for both equations.

In addition to evaluations have been made above, random variability comparisons have been made for R_{JB} and R_{RUP} equations with hypocentral depth term add-on versions (R_{JB} + Z_{HYP} and R_{RUP} + Z_{HYP}, respectively). These comparisons have been shown in Figure 3.8. Here, standard deviations values of R_{JB} based equation is slightly lower than the R_{RUP} equations. In the light of these observations, if a comparison must be made for R_{JB} and R_{RUP} distance metrics, it is not so possible to speak of superiority to one another in terms of modelling the ground-motion under the earthquake database of Turkey.

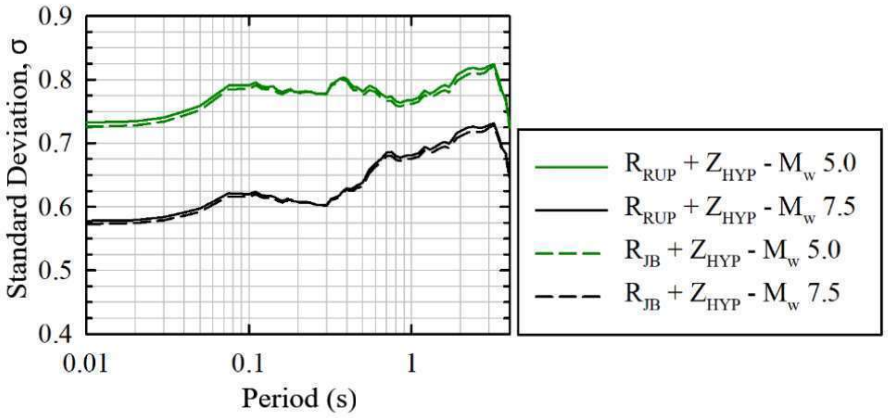

Figure 3.8. Period dependent total standard deviation comparisons for depth term added versions of R_{JB} and R_{RUP} equations.

3.4. General Evaluations

When considering the general situation of the Turkish earthquake database, it is possible to sort the most reliable parameters as: moment magnitude values (M_W), R_{JB} and R_{RUP} distance metrics, style of faulting, site classifications in terms of V_{S30} and hypocentral depth values. Generally, ground-motion prediction equations in literature from Europe and Middle East regions use functional forms that include M_W, R_{JB} or R_{RUP}, V_{S30} and style of faulting parameters for predicting the ground-motions. From global GMPEs, especially NGA-West2 equations (see. Gregor et al. 2014), are also modelling hanging wall, hypocentral depth, basin effects and dipping angle of the fault effects. Distance between upper edge of the fault plane to the surface (Z_{TOR}), sediment depth (depth to shear wave velocity of 1.0 km/s or 2.5 km/s), hypocentral depth (Z_{HYP}), width of the fault plane, dipping angle of the fault (dip) can be the necessary parameters for these modellings. From these parameters, hypocentral depth is the only one that has trustworthy amount of data to use in Turkish database. Even though empiric equations are given for other parameters in different studies, it is not suitable to use them in ground-motion prediction equation development phase while they might increase the uncertainty. Considering these matters, only the equations that are developed by adding Z_{HYP} term to present functional forms under Turkish database has been evaluated in this study.

Average residual values (with 95% confidence intervals) of four different equations (Basic R_{JB}, Basic R_{RUP}, R_{JB} + Z_{HYP} and R_{RUP} + Z_{HYP}) that have been evaluated in Figure 3.9 versus their magnitude and hypocentral depth comparisons are given. While it is not possible to talk about superiority of R_{JB} and R_{RUP} to one another according to residual distributions dependent on magnitude; average residual values of equations with hypocentral depth term are closer to zero than the basic form R_{JB} and R_{RUP} equations', especially for high magnitude intervals. This situation can be interpreted as positive effect of hypocentral depth term. As it is discussed in previous sections, adding the hypocentral depth term

to function rectified the trend of residual values and contributed as a small amount of decrement to the random variability.

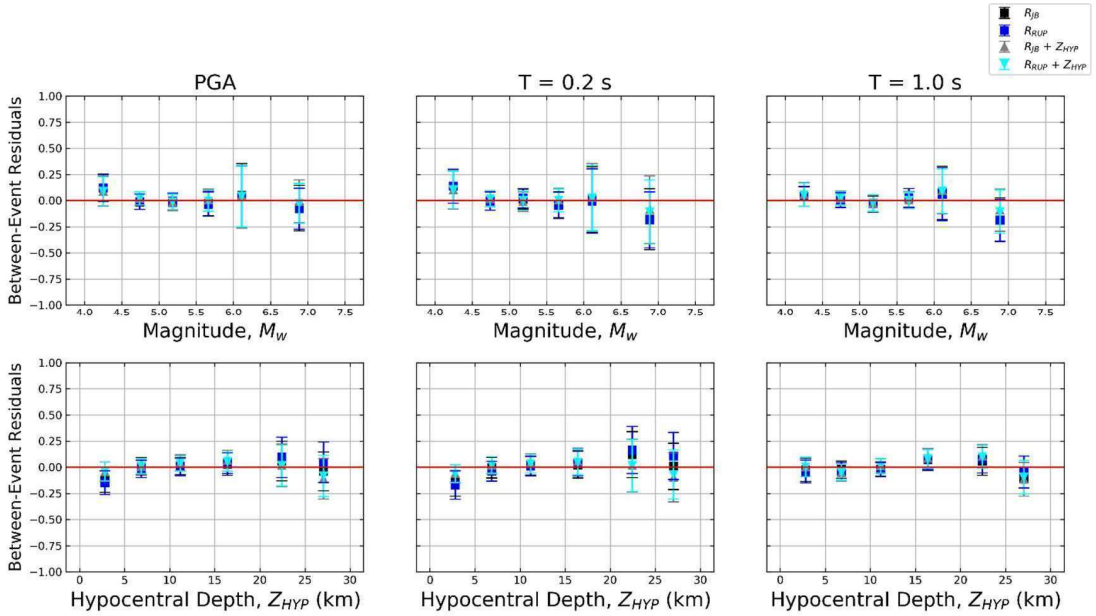

Figure 3.9. Distributions with comparisons of between-event residuals versus magnitude (top row) and hypocentral depth (bottom row) of Basic R_{JB}, Basic R_{RUP}, R_{JB} + Z_{HYP} and R_{RUP} + Z_{HYP} equations.

3.5. Comparisons of the Median Prediction Values for Turkish GMPEs

To compare the median predictions of the ground-motion prediction equations that are considered in this study, there are different earthquake scenarios have been produced. Different situations of the fault rupture and different positions of the site have been shown in Figure 3.10. Here, the distance between the edge of the fault rupture that close to the surface and the site has been represented with R_X. Median comparisons have been evaluated based on this distance-metric. In Figure 3.10, while in scenarios a and b dipping angle of the fault (Dip) is lower than 90 degrees, in scenario c it is 90 degrees and this situation is a clear example of strike-slip fault. In the situations that dipping angle is lower than 90 degrees (Figure 3.10.a and b); while R_X is positive (Figure 3.10.a), site is located

on hanging wall; while R_X is negative (Figure 3.10.b), site is located on footing wall.

Chosen earthquake scenarios have been used for distance calculations between site and fault plane. For this purpose, 4 different magnitude values (M_W 4.5, 5.5, 6.5, 7.5) have been considered. Width value of the fault rupture (RW) has been taken from magnitude dependent empirical formulas that are recommended by Wells and Coppersmith (1994). Z_{TOR} values have been calculated by the help of empirical formulas which are recommended by Kaklamanos et al. (2011) and they are dependent on hypocentral depth (Z_{HYP}), dipping angle and RW values. Considering Kaklamanos et al. (2011); dipping angles of planes in normal, reverse and strike-slip fault types are taken as 50, 40 and 90 degrees, respectively. Z_{HYP}, RW and Z_{TOR} values that are obtained from empirical formulas for earthquake scenarios and their corresponding magnitude values are listed in Table 3.7.

Table 3.7. Values of fault parameters that changes dependent on magnitude.

M_W	Z_{HYP} (km)	RW (km)	Z_{TOR} (km)
4.5	8.7	2.9	7
5.5	9.4	5.3	6.2
6.5	10.1	9.9	4.2
7.5	10.7	18.4	0

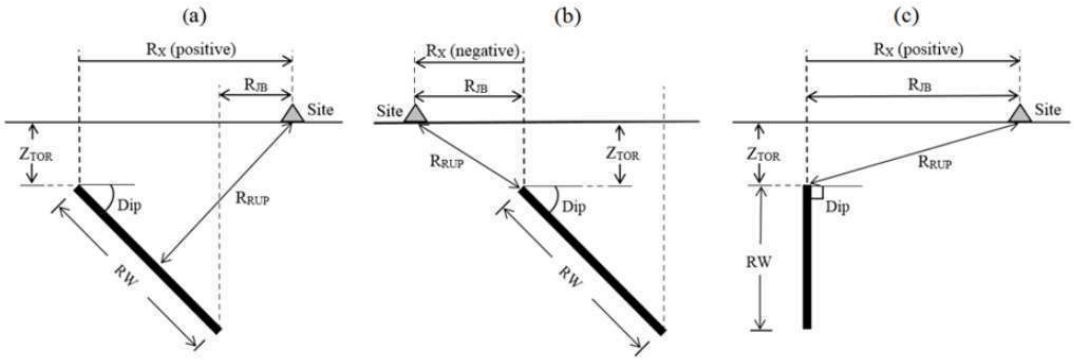

Figure 3.10. Drawings of fault geometries for a) site on hanging wall for dipping fault, b) site on footing wall for dipping fault and c) site near the vertical fault (adopted from Campbell and Bozorgnia, 2014).

In Figure 3.11, change of R_{JB} and R_{RUP} distance values are given according to R_X distances that are generated with earthquake scenarios given in Table 3.7 and Figure 3.10. Different fault geometries are given in Figure 3.10.a, 3.10.b and 3.10.c and they are used to calculate the distance-metrics that are given in Figure 3.11.a, 3.11.b and 11.c, respectively. R_{JB} and R_{RUP} values for the hanging wall side of the fault rupture are showing apparent differences (R_{JB} = 0 km values are shown as R_{JB} = 0.1 km because y axis is in logarithmic scale). R_{JB} values are equal to R_X values for the situations that are shown in Figure 3.10.b and Figure 3.10.c. Again, in these situations, while R_{JB} and R_{RUP} values are showing discrepancies for M_W 4.5, 5.5 and 6.5 scenarios up to $R_X \sim 10$ km, all the distance-metrics are reaching the same values for M_W 7.5 scenario. This is because Z_{TOR} parameter is taking value of 0 km while fault rupture is reaching the surface.

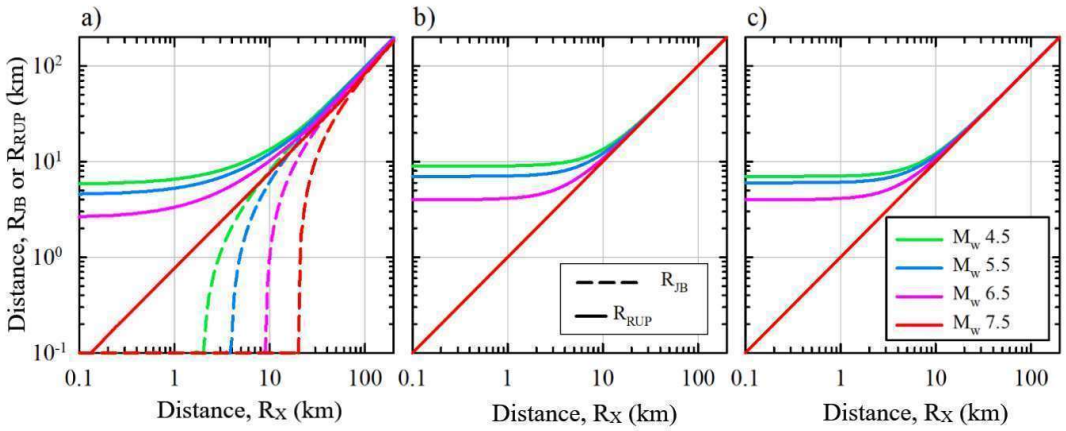

Figure 3.11. Comparisons of R_{JB} and R_{RUP} distance-metrics versus R_X distance-metric that is calculated for situations in Figure 3.10.

As one can see in Figure 3.11.b and c, variations of R_{JB} and R_{RUP} distance-metrics are similar. To reduce the complexity of comparing the R_{JB} and R_{RUP} based ground-motion prediction equations; strike-slip (which is the dominant seismotectonic structure of Turkey) and normal (Figure 3.11.a and c) fault type scenarios are taken into account. Comparisons are made for V_{S30} = 760 m/s reference rock site condition and PGA, T = 0.2 s and T = 1.0 s periods.

R_X distance dependent median spectral acceleration (PSA) predictions of GMPEs for 4 different magnitudes and strike-slip earthquake scenarios are shown for PGA, T = 0.2 s and T = 1.0 s values in Figure 3.12, 3.13 and 3.14, respectively. In Figure 3.15, 3.16 and 3.17, comparisons of the same scenarios but with normal faults are given. The most notable matter in these comparisons, equations with Z_{HYP} add-on are generating lower values than basic functional form equations, especially for close distances. This difference changes also for both type of distance-metric equations, dependent on magnitude. While magnitude is increasing, difference between them is decreasing. Decrease observed in R_{RUP} based equation is lower than the one in R_{JB} based equation. The difference observed in R_{JB} based equation in M_W 7.5 value is on substantially low level. This situation can be explained with the observation that hypocentral depth dependence of R_{JB} based Kale et al. (2015) equation is on very low levels in

residual evaluations phase. General behavior of change is nearly the same for both basic functional form and depth term added functional form equations.

Even though R_{JB} and R_{RUP} based equations are derived from the same database, they predict very different spectral values from each other especially for close and middle distances, as seen clearly in comparison graphs plotted here (Figure 3.12-3.17). In this phase, for the purpose of making a more detailed evaluation, earthquake scenarios are divided into low (M_W 4.5; M_{low}), middle (M_W 5.5; M_{mid}) and high (M_W 6.5 and 7.5; M_{high}) magnitude levels and dipping (normal fault) and vertical (strike-slip) plane fault types. For M_{low} and M_{mid} magnitude levels, ground-motion predictions of R_{JB} prediction model are greater than R_{RUP} equations for strike-slip fault type scenarios (Figure 3.12, 3.13 and 3.14) on specific distances. None the less, behavior is changing completely in M_{high} magnitude level. In these scenarios, ground-motion predictions of the R_{RUP} model are greater than the R_{JB} models. This observation is similar for all the period values.

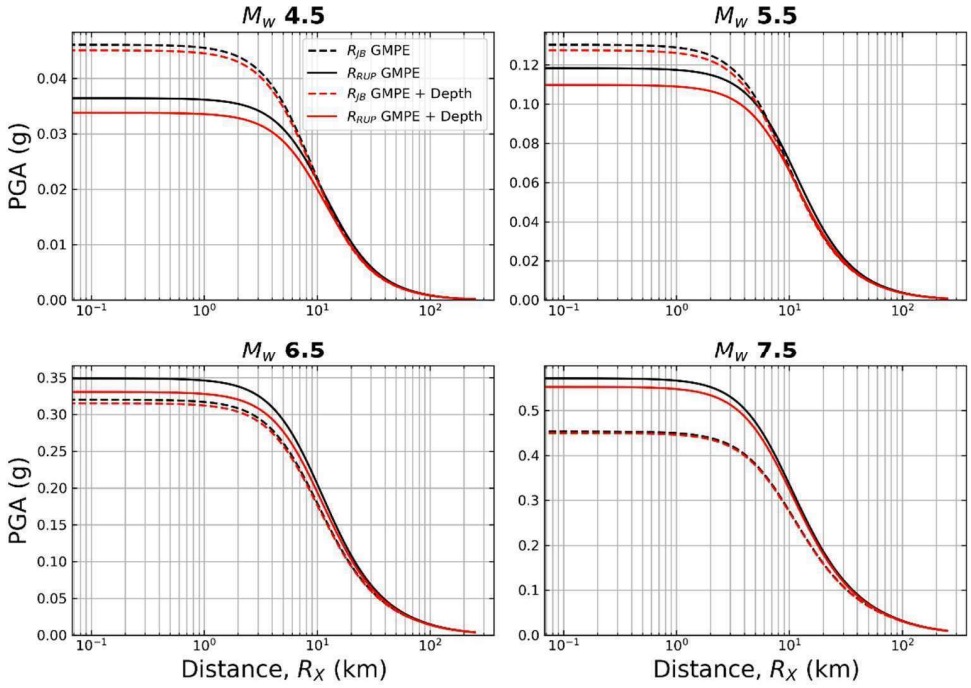

Figure 3.12. Distance dependent change of PGA for different magnitude values (V_{S30} = 760 m/s; strike-slip fault).

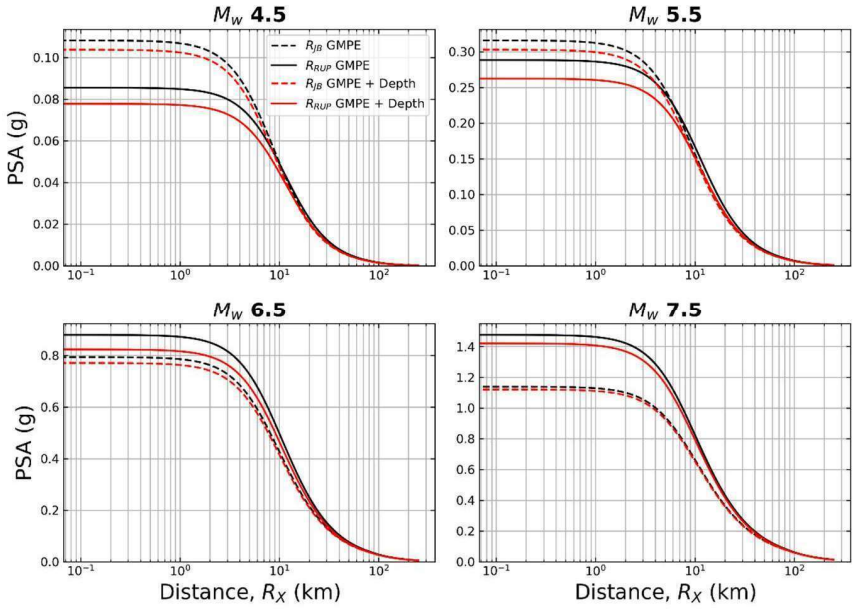

Figure 3.13. Distance dependent change of spectral acceleration (T = 0.2 s) values for different magnitude values (V_{S30} = 760 m/s; strike-slip fault).

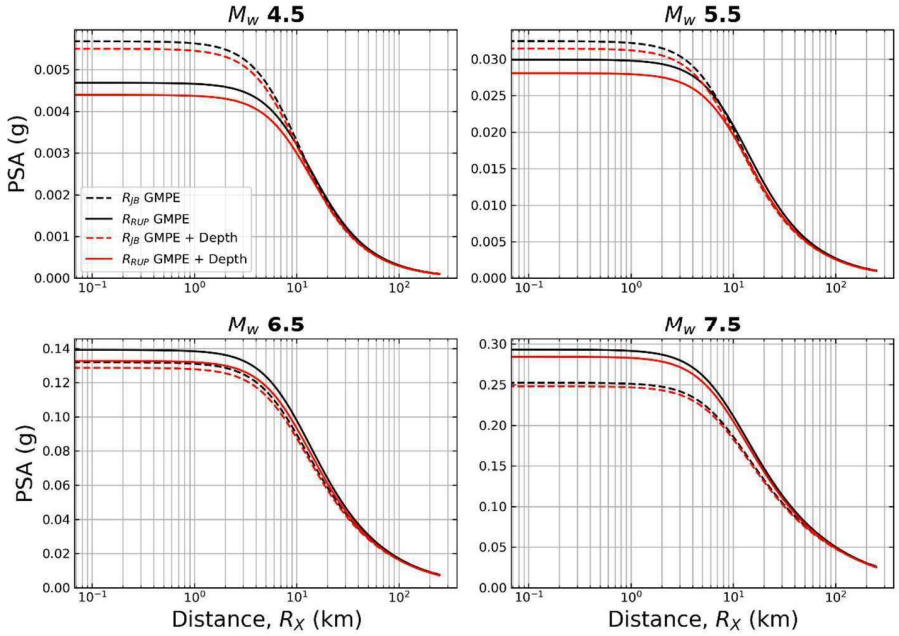

Figure 3.14. Distance dependent change of spectral acceleration (T = 1.0 s) values for different magnitude values (V_{S30} = 760 m/s; strike-slip fault).

Ground-motion behaviors are more complicated for dipping fault type situations that are given in Figure 3.15, 3.16 and 3.17. R_{JB} model predicts constant values until R_{JB} distance takes greater values than zero, along the surface projection of the fault rupture. In this constant part, for M_{mid} and M_{high} magnitude levels, there's a distance value (R_{eq}) that ground-motion predictions of R_{JB} and R_{RUP} models are the same. R_{eq} gets higher values as magnitude increases. When distance is lower than R_{eq}, ground-motion predictions of R_{RUP} model is greater than R_{JB} models. After the R_{eq} intersection point, there are apparent differences between two models as the predictions of R_{RUP} model rapidly decreases. Dependent on magnitude level, until certain distances, R_{JB} model predicts higher ground-motion intensity measure predictions than R_{RUP} model. In specific distance value, spectral values come to a convergence point. It has been already shown that R_{JB} and R_{RUP} values are the same in the database for these values (see. Figure 2.1.b and 2.3.b). Predictions of R_{JB} model are always greater than R_{RUP} models in closer distances for M_{low} situation.

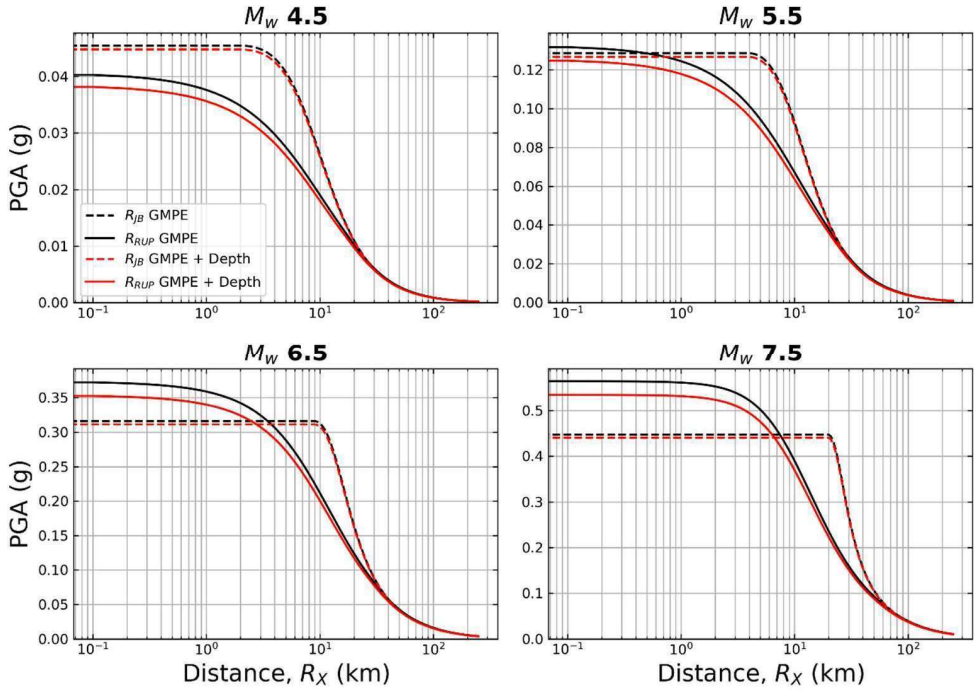

Figure 3.15. Distance dependent change of PGA for different magnitude values (V_{S30} = 760 m/s; normal fault).

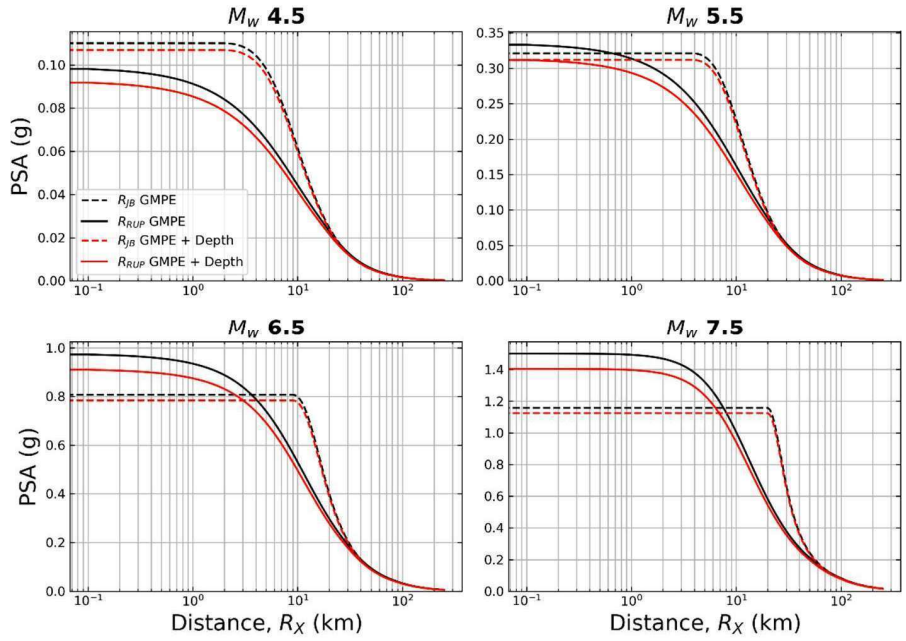

Figure 3.16. Distance dependent change of spectral acceleration (T = 0.2 s) values for different magnitude values (V_{S30} = 760 m/s; normal fault).

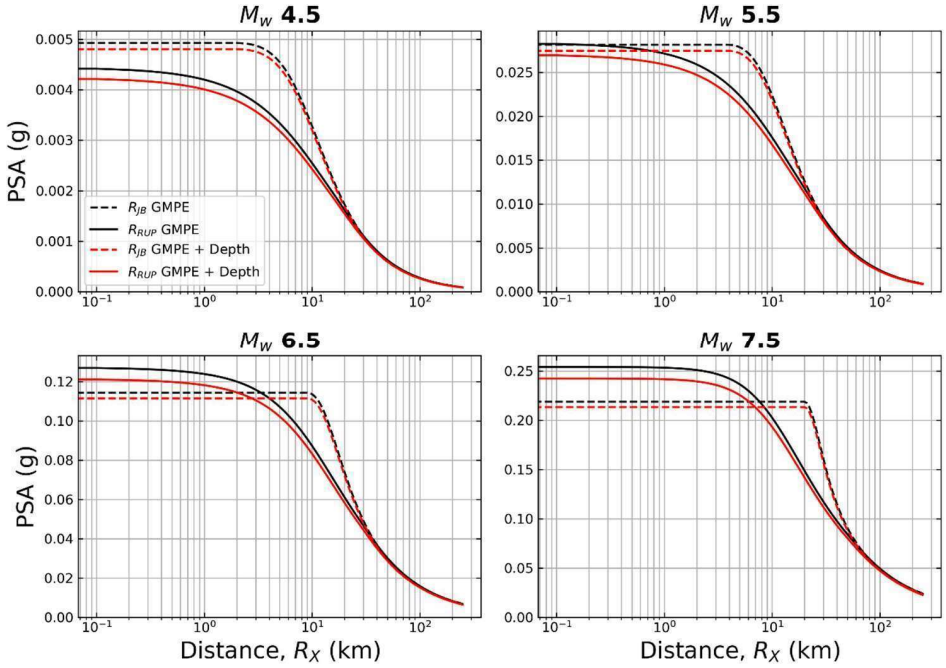

Figure 3.17. Distance dependent change of spectral acceleration (T = 1.0 s) values for different magnitude values (V_{S30} = 760 m/s; normal fault).

To determine the differences between the prediction equations more clearly, PSA ratios of basic functional form R_{JB} and R_{RUP} equations have been calculated and shown in Figure 3.18. Here, ratios of spectral accelerations of R_{RUP} equation to R_{JB} equation from Figure 3.13, 3.14, 3.16 and 3.17 have been calculated and shown in different panels. There's no significant difference between ratios of equations with depth term and ratios of basic equations. In these figures, PSA_{RRUP} and PSA_{RJB} are stand for PSA values of predictions of R_{RUP} and R_{JB} equations, respectively. While unit value represents $PSA_{RRUP} = PSA_{RJB}$ situation, $PSA_{RRUP} > PSA_{RJB}$ and $PSA_{RRUP} < PSA_{RJB}$ represent above and below ratios of unit value, respectively. The difference between ground-motion intensity measure predictions between R_{JB} and R_{RUP} equations reaches up to 50% for high magnitude earthquake scenarios. Plots of PSA ratios show that the differences are more critical for the sites that are on the hanging wall side of the dipping normal faults.

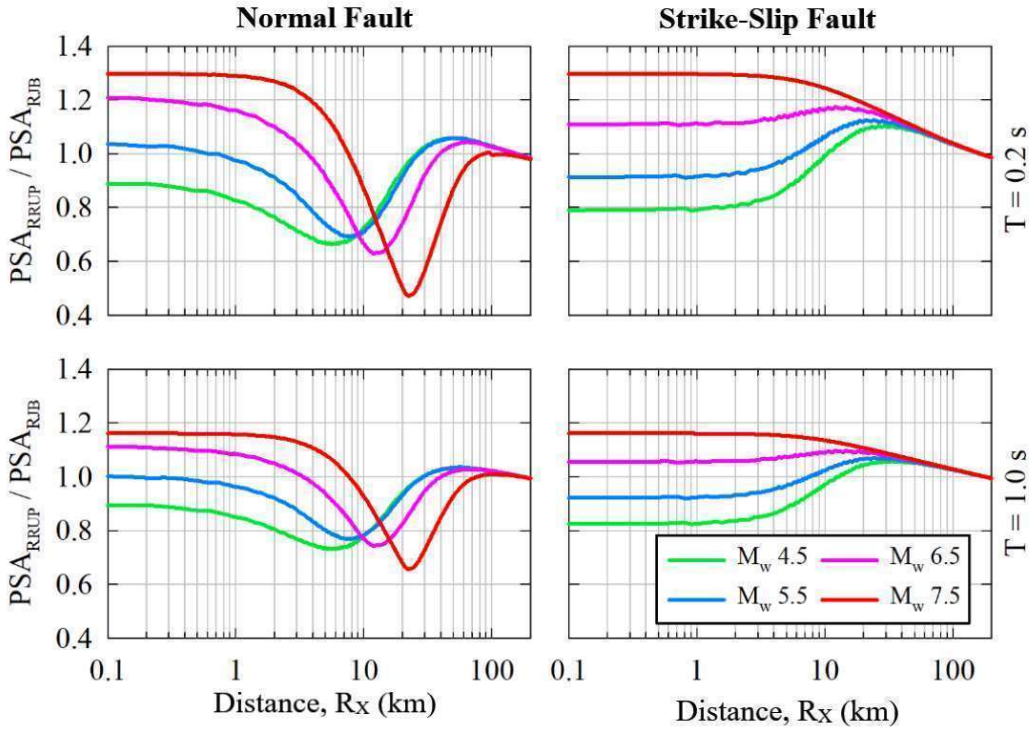

Figure 3.18. Comparisons of PSA ratios: a) Normal fault type for T = 0.2 s, b) Strike-slip fault type for T = 0.2 s, c) Normal fault type for T = 1.0 s, d) Strike-slip fault type for T = 1.0 s.

The clear result that is obtained from these evaluations, ground-motion prediction equations that are developed using R_{JB} and R_{RUP} distance metrics (with hypocentral depth term or not) generates different spectral amplitude values, especially for close and middle distances. General spectral behavior is more complicated in hanging wall side of the faults. However, the factors like inadequacy of number of acceleration records and earthquake parameters both are limiting the investigations of these matters in more detailed way. Therefore, it's been chosen to do evaluations with a global database, in the next stages of this study.

4. DEVELOPMENT OF GLOBAL GMPES

In this part of study, derivation of GMPEs in different functional forms with using the strong ground-motion database that is compiled from NGA-West2 database (Ancheta et al. 2014) has been explained. In the first stage, considering the recently compiled database, basic functional forms of GMPEs for R_{JB} and R_{RUP} distance-metrics have been developed. In the next stages, with using the same database, hypocentral depth term, dipping angle and hanging wall terms are added to the main functional form. As linear mixed-effects regression method, lme4.0 (Bates et al., 2013) in R programming language has been used.

4.1. Development of R_{JB} and R_{RUP} based GMPEs in Basic Functional Form

In this section, a different functional form, which has been proven that it's more compatible with global database in statistical tests (see. Kale et al., 2017), has been used. Considered functional form has been shown in Equation 4.1. This functional form includes magnitude scaling (f_{mag}, Equation 4.2), distance scaling (f_{dis}, Equation 4.3), style of faulting (f_{sof}, Equation 4.4), anelastic distance attenuation (f_{aat}, Equation 4.5) and linear and nonlinear site effects (f_{site}, Equation 4.6) terms. F_{NM} and F_{RV} terms in Equation 4.4 are dummy variables belongs to normal and reverse faults and they take unit values for normal and reverse faults, respectively. They are both zero for strike-slip faults. PSA_{1130} that is given in Equation 4.6.c represents spectral acceleration value on reference rock for related period. Random variability model is in homoscedastic structure and total standard deviation (σ) is given in terms of between-event (τ), within-event (ϕ) and site-to-site (ϕ_{S2S}) standard deviations in Equation 4.7.

$$ln\,Y = f_{mag} + f_{dis} + f_{sof} + f_{aat} + f_{site} \qquad (4.1)$$

$$f_{mag} = \begin{cases} a_0 + a_1 M_w, & M_w \le 4.5 \\ a_0 + a_1 M_w + a_2(M_w - 4.5), & 4.5 < M_w \le 5.5 \\ a_0 + a_1 M_w + a_2(M_w - 4.5) + a_3(M_w - 5.5), & 5.5 < M_w \le 6.5 \\ a_0 + a_1 M_w + a_2(M_w - 4.5) + a_3(M_w - 5.5) + a_4(M_w - 6.5), & M_w > 6.5 \end{cases} \quad (4.2)$$

$$f_{dis} = [a_5 + a_6(M_w)] \, ln\sqrt{R_{JB}^2 + h^2} \quad (4.3)$$

$$f_{sof} = [\, a_8 F_{NM} + a_9 F_{RV}] \, f_{sof,M} \quad (4.4.a)$$

$$f_{sof,M} = \begin{cases} 0; & M_w \le 4.5 \\ M_w - 4.5; & 4.5 < M_w \le 5.5 \\ 1; & M_w > 5.5 \end{cases} \quad (4.4.b)$$

$$f_{aat} = \begin{cases} 0, & R_{JB} \le 80 \\ a_{10}(R_{JB} - 80), & R_{JB} > 80 \end{cases} \quad (4.5)$$

$$f_{site} = f_{lin} + f_{nl} \quad (4.6.a)$$

$$f_{lin} = a_7 \, min\left\{\ln\left(\frac{V_{S30}}{1130}\right), 0\right\} \quad (4.6.b)$$

$$f_{nl} = s_4\left[e^{s_5(\min(V_{S30},1130)-360)} - e^{s_5(1130-360)}\right]\ln\left(\frac{PSA_{1130} + s_3}{s_3}\right) \quad (4.6.c)$$

$$\sigma = \sqrt{\tau^2 + \phi^2 + \phi_{S2S}^2} \quad (4.7)$$

Model coefficients of R_{JB} based equation, obtained in the result of regression analyses, have been given in Table 4.1. From these coefficients, a_0-a_4 belong to magnitude scaling, a_5-a_6 belong to distance scaling, a_7 belongs to linear site effects and a_{10} belongs to anelastic distance attenuation. In Equation 4.3, *h* is

fictitious depth and independent of period, it is takes as 7 km for R_{JB} equation. In Equation 4.4.a above, a_8 and a_9 are coefficients of style of faulting, and they take values of *-0.1* and *0* for normal and reverse faults, respectively. Nonlinear site effects (Equation 4.6.c) coefficients are listed in Table 4.2 and they are dependent on period, mutual for all distance-metrics and functional forms.

With using R_{RUP} instead of R_{JB} in the sub-functions of Equation 4.1 (namely, Equation 4.3 and 4.5), R_{RUP} based basic functional form ground-motion prediction equation has been obtained. Regression coefficients belong to this equation has been listed in Table 4.3 depending on period. Fictitious depth (*h*) is taken as 5 km after the results of regression calculations (see. Equation 4.3). Style of faulting coefficients in Equation 4.4.a, a_8 and a_9 are -0.1 and 0 for normal and reverse faults, respectively, similar as R_{JB} equation. Coefficients that are listed on Table 4.2 have been used to calculate nonlinear site effects.

Table 4.1. Model coefficients of basic functional form R_{JB} equation.

Period (s)	a0	a1	a2	a3	a4	a5	a6	a7	a10
PGA	-4.69919	1.047288	0.04007	-1.19049	-0.35161	-2.52415	0.233693	-0.36196	-0.00651
0.01	-4.65286	1.041856	0.037317	-1.17704	-0.35722	-2.52669	0.233865	-0.35928	-0.00653
0.02	-4.5679	1.036607	0.051108	-1.1897	-0.35278	-2.53502	0.233704	-0.3434	-0.00648
0.03	-4.13085	0.987781	0.097431	-1.20466	-0.33722	-2.56925	0.234684	-0.29361	-0.00644
0.05	-3.31758	0.913326	0.130273	-1.17728	-0.32917	-2.64143	0.237859	-0.23043	-0.00679
0.1	-3.41554	0.980842	0.190614	-1.32657	-0.26642	-2.5104	0.216629	-0.34295	-0.00813
0.15	-4.91897	1.240999	0.029093	-1.25924	-0.37279	-2.26706	0.186	-0.45042	-0.00825
0.2	-5.9808	1.368361	0.02284	-1.26891	-0.46031	-2.12713	0.173708	-0.55023	-0.00777
0.3	-7.76721	1.609627	-0.06757	-1.31576	-0.5452	-2.00052	0.163883	-0.68524	-0.00662
0.4	-9.36437	1.842926	-0.23819	-1.13899	-0.75	-1.86548	0.146076	-0.73484	-0.00562
0.5	-10.5009	1.99609	-0.32014	-1.12372	-0.82113	-1.79937	0.138188	-0.78622	-0.00489
0.75	-12.345	2.213366	-0.26118	-1.23179	-0.95833	-1.69208	0.122272	-0.83853	-0.00357
1	-13.5989	2.362536	-0.23156	-1.26573	-1.07618	-1.62168	0.108396	-0.84708	-0.0027
1.5	-14.8509	2.437209	-0.17745	-1.15282	-1.31887	-1.62461	0.10891	-0.87252	-0.00157
2	-15.3417	2.418154	-0.12915	-1.06369	-1.46474	-1.71279	0.123041	-0.87901	-0.00073
3	-15.937	2.367119	-0.05611	-0.87076	-1.70394	-1.80914	0.135512	-0.88489	-0.00013

Table 4.1. (Cont'd)

4	-16.172	2.290024	0.018453	-0.81665	-1.78987	-1.90597	0.153166	-0.88421	-0.00035
5	-16.4841	2.254559	0.035378	-0.76189	-1.83982	-1.93853	0.160223	-0.8627	-0.00036

Table 4.2. Nonlinear site effects coefficients that are mutual for all equations.

Period (s)	s4	s5	s3
PGA	-0.1417	-0.00701	0.102151
0.01	-0.1417	-0.00701	0.102151
0.02	-0.1364	-0.00728	0.10836
0.03	-0.1403	-0.00735	0.119888
0.05	-0.1862	-0.00647	0.148927
0.1	-0.2943	-0.0056	0.230662
0.15	-0.3113	-0.00585	0.266468
0.2	-0.2927	-0.00614	0.255253
0.3	-0.2405	-0.0067	0.207277
0.4	-0.1975	-0.00713	0.165464
0.5	-0.1633	-0.00744	0.133828
0.75	-0.1028	-0.00812	0.085153
1	-0.0699	-0.00844	0.058595
1.5	-0.0425	-0.00771	0.031787
2	-0.0302	-0.00479	0.019716
3	-0.0129	-0.00183	0.009643
4	-0.0016	-0.00152	0.005379
5	0	-0.00144	0.003223

Table 4.3. Model coefficients of basic functional form R_{RUP} equation.

Period (s)	a0	a1	a2	a3	a4	a5	a6	a7	a10
PGA	-3.74218	0.923795	-0.00721	-1.22051	-0.132	-2.77761	0.270858	-0.35212	-0.006
0.01	-3.69537	0.918367	-0.01013	-1.20685	-0.13761	-2.78031	0.271041	-0.34949	-0.00602
0.02	-3.60835	0.913171	0.002583	-1.21867	-0.13319	-2.78947	0.270966	-0.33356	-0.00596
0.03	-3.1632	0.864119	0.046106	-1.23256	-0.11587	-2.82655	0.272269	-0.28394	-0.00592
0.05	-2.33705	0.789637	0.075294	-1.20433	-0.10447	-2.90311	0.275795	-0.22198	-0.00625
0.1	-2.4387	0.857096	0.143529	-1.35905	-0.05035	-2.76965	0.253982	-0.33647	-0.00759
0.15	-3.98	1.11968	-0.01047	-1.29143	-0.17533	-2.51538	0.22216	-0.44391	-0.00774
0.2	-5.07263	1.24932	-0.01122	-1.30145	-0.27244	-2.36563	0.208636	-0.54338	-0.00729

Table 4.3. (Cont'd)

0.3	-6.87426	1.490154	-0.09984	-1.3459	-0.36428	-2.23485	0.198744	-0.6773	-0.00616
0.4	-8.50116	1.725565	-0.27233	-1.16336	-0.58032	-2.09248	0.180465	-0.72577	-0.0052
0.5	-9.65828	1.882184	-0.35709	-1.14593	-0.65563	-2.02108	0.171778	-0.77572	-0.00447
0.75	-11.5154	2.100652	-0.30317	-1.25007	-0.79838	-1.91123	0.155938	-0.82563	-0.00316
1	-12.8018	2.256341	-0.27666	-1.28356	-0.9224	-1.83264	0.140586	-0.83263	-0.0023
1.5	-14.0759	2.334637	-0.22469	-1.17115	-1.16469	-1.83024	0.140353	-0.85732	-0.00118
2	-14.5697	2.317067	-0.17686	-1.08358	-1.30463	-1.91744	0.154094	-0.86386	-0.00034
3	-15.1836	2.270968	-0.10331	-0.89412	-1.53931	-2.00819	0.165133	-0.87036	0
4	-15.4446	2.200208	-0.02815	-0.84242	-1.62088	-2.0977	0.180959	-0.87068	0
5	-15.7725	2.167568	-0.01093	-0.78786	-1.67001	-2.12578	0.187166	-0.84971	0

Between-event and within-event residuals of R_{JB} and R_{RUP} based ground-motion prediction equations are obtained considering mixed-effects algorithm from Bates el al. (2013). As main prediction parameters for residual evaluations magnitude (M_W), distance (R_{JB} and R_{RUP}), average shear wave velocity of upper 30 m of the soil (V_{S30}), hypocentral depth (Z_{HYP}) and dipping angle (Dip) are considered. Change of M_W, Z_{HYP} and dipping angle depending on between-event residuals and change of V_{S30} and distance (R_{JB} and R_{RUP}) depending on within-event residuals have been shown in Figure 4.1 and Figure 4.2, for R_{JB} and R_{RUP} based equations, respectively, in different columns for peak ground acceleration (PGA) and periods of 0.2 s and 1.0 s. The format of these plots is the same as in evaluations that are made for compiled Turkish database. As you may recall, crossing zero or following quite close trends to zero for confident intervals of these residuals are enough to show this model predicts consistent values for related period.

In this context, according to residual distributions, there's no problem in equations in terms of magnitude, distance, V_{S30} and dipping angle. When evaluating residual distributions dependent on hypocentral distance, there's a trend seen in shallow earthquakes for PGA and T = 0.2 s values. This trend shows the similar behavior for both R_{JB} and R_{RUP} based equations. To eliminate this trend, a hypocentral depth term has been added to both R_{JB} and R_{RUP} equations and these versions of equations have been explained in the next section.

Observations that are made for the selected period values in here are overarching for other period values that are chosen for regression.

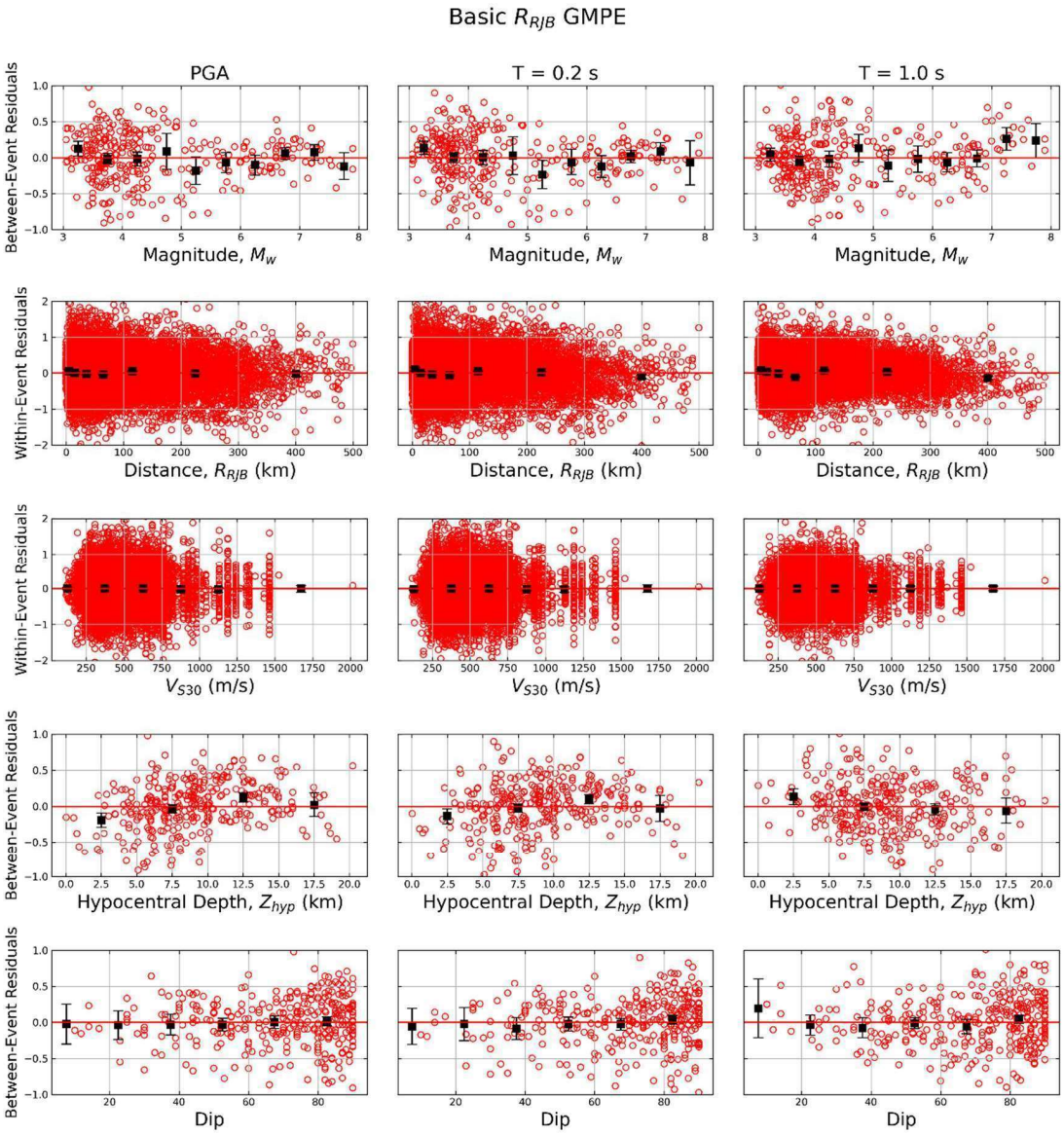

Figure 4.1. Distributions of between-event residuals versus magnitude (1st row), within-event residuals versus distance (2nd row), within-event residuals versus V_{S30} (3rd row), between-event residuals versus hypocentral depth (4th row) and between-event residuals versus dipping angle (5th row) for basic functional form R_{JB} equation.

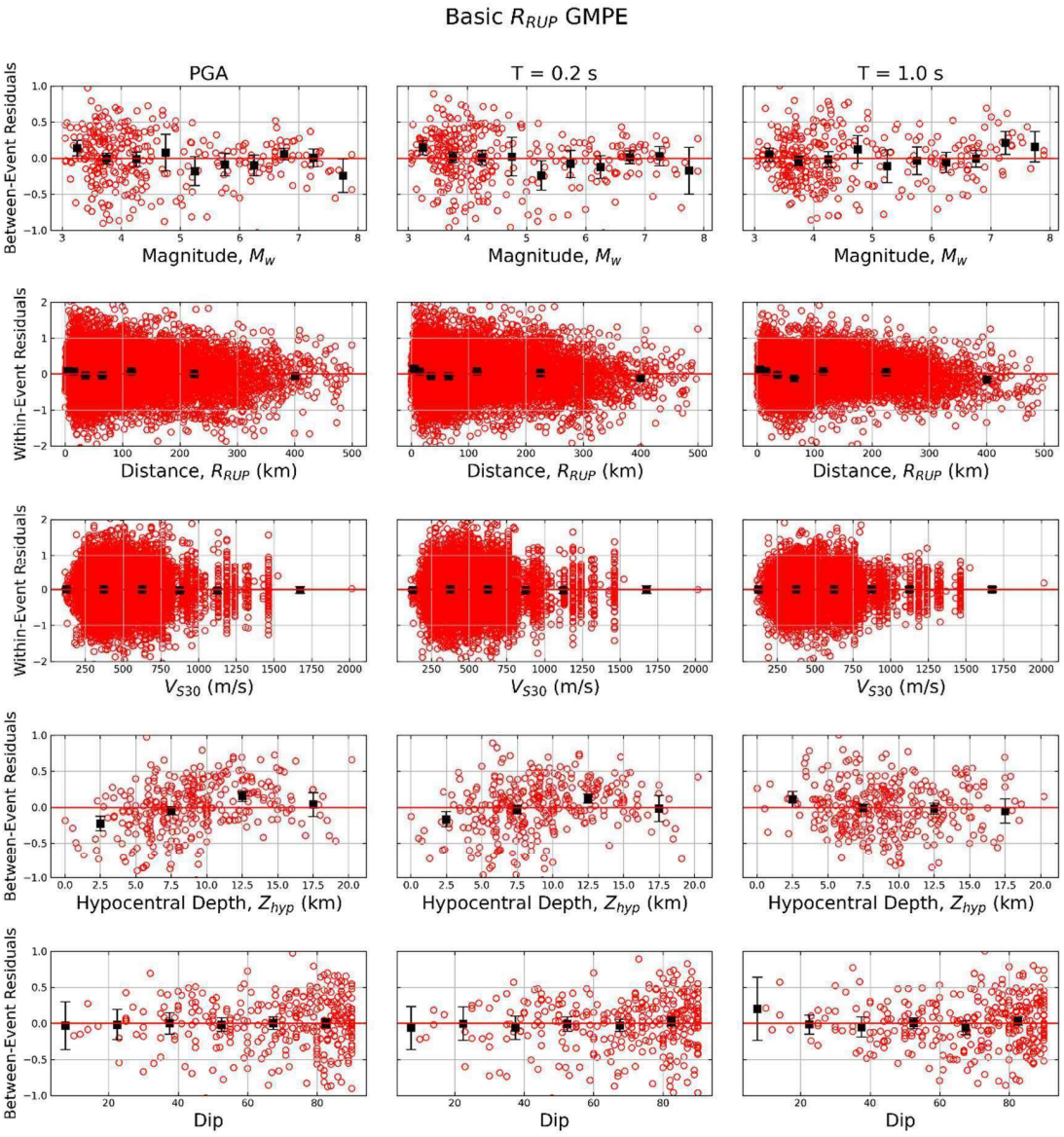

Figure 4.2. Distributions of between-event residuals versus magnitude (1st row), within-event residuals versus distance (2nd row), within-event residuals versus V_{S30} (3rd row), between-event residuals versus hypocentral depth (4th row) and between-event residuals versus dipping angle (5th row) for basic functional form R_{RUP} equation.

To evaluate the random variability model components of both of these equations, change of total standard deviation (σ), between-event standard deviation (τ), within-event standard deviation (ϕ) and site-to-site standard deviation (ϕ_{S2S}) depending on period have been listed in Table 4.4 and plotted in Figure 4.3. In the comparison that is given in this figure, it has been seen that, in short period

values, between-event standard deviation of R_{RUP} equation is higher than the R_{JB} equations with a small amount. This difference is also the reason of small difference in the total standard deviation.

Table 4.4. Random variability values of basic functional form R_{JB} and R_{RUP} GMPEs.

Period (s)	R_{JB} based GMPE				R_{RUP} based GMPE			
	τ	Φ_{S2S}	Φ	σ	τ	Φ_{S2S}	Φ	σ
PGA	0.3909	0.4094	0.5326	0.7773	0.4074	0.4091	0.5344	0.7867
0.01	0.3917	0.4090	0.5331	0.7778	0.4083	0.4087	0.5349	0.7873
0.02	0.3944	0.4131	0.5343	0.7821	0.4115	0.4128	0.5360	0.7919
0.03	0.4069	0.4210	0.5399	0.7965	0.4246	0.4210	0.5418	0.8069
0.05	0.4382	0.4428	0.5492	0.8305	0.4566	0.4431	0.5511	0.8417
0.1	0.4472	0.4581	0.5492	0.8435	0.4623	0.4581	0.5503	0.8523
0.15	0.4244	0.4588	0.5492	0.8320	0.4381	0.4586	0.5505	0.8398
0.2	0.4000	0.4564	0.5481	0.8177	0.4128	0.4561	0.5497	0.8250
0.3	0.3603	0.4483	0.5398	0.7888	0.3702	0.4484	0.5414	0.7945
0.4	0.3423	0.4606	0.5170	0.7724	0.3486	0.4617	0.5192	0.7774
0.5	0.3360	0.4712	0.5059	0.7687	0.3394	0.4720	0.5079	0.7720
0.75	0.3554	0.4804	0.4733	0.7623	0.3530	0.4829	0.4747	0.7636
1	0.3854	0.4872	0.4515	0.7680	0.3810	0.4894	0.4526	0.7678
1.5	0.4349	0.4731	0.4417	0.7798	0.4272	0.4757	0.4430	0.7779
2	0.4554	0.4650	0.4475	0.7899	0.4459	0.4684	0.4490	0.7873
3	0.4744	0.4501	0.4672	0.8037	0.4623	0.4517	0.4692	0.7987
4	0.4911	0.4351	0.4808	0.8134	0.4778	0.4362	0.4833	0.8076
5	0.5160	0.4335	0.4906	0.8336	0.5017	0.4343	0.4937	0.8271

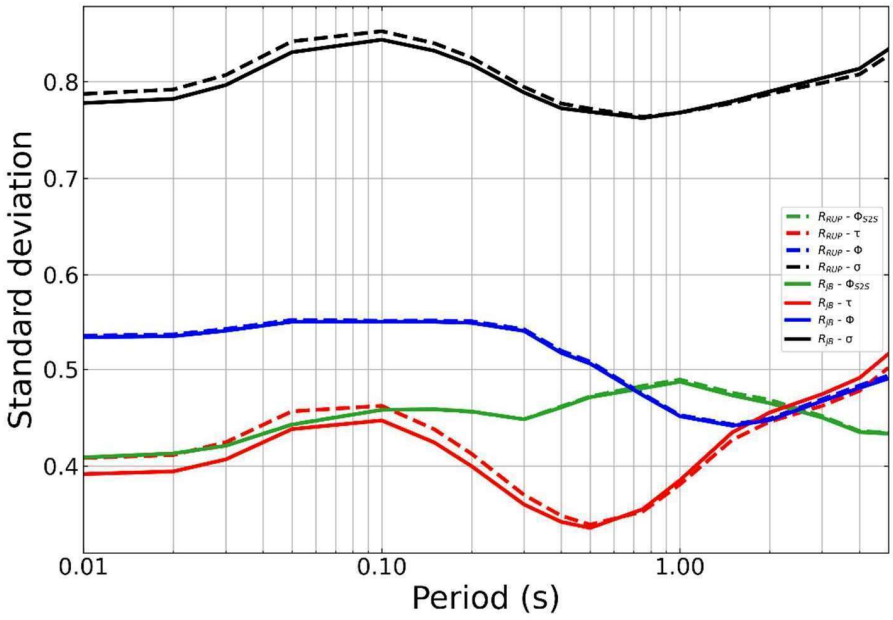

Figure 4.3. Random variability comparisons of basic functional form R_{JB} and R_{RUP} GMPEs.

4.2. Development of R_{JB} and R_{RUP} Based GMPEs in Basic Functional Form with Hypocentral Depth Term

To observe the effect of hypocentral depth term to the equations that are derived in the previous section, Equation 4.8 has been obtained with adding hypocentral depth term (f_{hyp}) to the Equation 4.1. Functional form of hypocentral depth term has been given in Equation 4.9. In this equation, $f_{hyp,H}$ ve $f_{hyp,M}$ terms represent variables that are related to Z_{hyp} and magnitude dependent hypocentral depth modelling. This equation proposed in Campbell and Bozorgnia (2014) and chosen because of the suitability of ground-motion database which has been working on this study.

$$ln\,Y = f_{mag} + f_{dis} + f_{sof} + f_{aat} + f_{hyp} + f_{site} \tag{4.8}$$

$$f_{hyp} = f_{hyp,H}\, f_{hyp,M} \tag{4.9.a}$$

$$f_{hyp,H} = \begin{cases} 0; & Z_{HYP} \leq 7 \\ (Z_{HYP} - 7); & 7 < Z_{HYP} \leq 20 \\ 13; & Z_{HYP} > 20 \end{cases} \quad (4.9.b)$$

$$f_{hyp,M} = \begin{cases} a_{11}, & M_w \leq 5.5 \\ [a_{11} + (a_{12} - a_{11})(M_w - 5.5)], & 5.5 < M_w \leq 6.5 \\ a_{12}, & M_w > 6.5 \end{cases} \quad (4.9.c)$$

The model coefficients of R_{JB} based equation that are obtained in the results of regression has been listed in Table 4.5. From these coefficients, the coefficients between a_0 and a_{10} are the new values in new functional form that are explained in previous section. Hypocentral depth related coefficients are listed in a_{11} and a_{12} columns of the table. R_{RUP} based ground-motion prediction equation which considers hypocentral depth effects has been developed in the similar way as previous section. In the sub-functions of terms that are given in Equation 4.8, R_{RUP} has been used instead of R_{JB}. Regression coefficients belong to this equation has been given in Table 4.6 for selected period values. Fictitious depth (h), style of faulting and nonlinear site effects coefficients are exactly same as the ones that are obtained in basic functional form section.

Residual distributions of equations that are derived in this stage are given in Figure 4.4 and 4.5, for R_{JB} and R_{RUP} based equations, respectively. The chosen format and considered periods are equivalent as in previous section (namely Figure 4.1 and 4.2).

Table 4.5. Model coefficients of basic functional form R_{JB} equation with hypocentral depth term.

T (s)	a0	a1	a2	a3	a4	a5	a6	a7	a10	a11	a12
PGA	-4.675	1.0037	0.0161	-0.9400	-0.5336	-2.5228	0.2332	-0.3624	-0.00650	0.061	0.022
0.01	-4.629	0.9980	0.0133	-0.9256	-0.5400	-2.5253	0.2334	-0.3597	-0.00652	0.062	0.022
0.02	-4.541	0.9907	0.0262	-0.9207	-0.5501	-2.5337	0.2332	-0.3438	-0.00647	0.064	0.021
0.03	-4.098	0.9362	0.0718	-0.9052	-0.5585	-2.5678	0.2342	-0.2942	-0.00644	0.071	0.022
0.05	-3.271	0.8526	0.1025	-0.8047	-0.6125	-2.6407	0.2375	-0.2316	-0.00678	0.080	0.017
0.1	-3.389	0.9352	0.1646	-1.0544	-0.4659	-2.5091	0.2161	-0.3442	-0.00812	0.064	0.022
0.15	-4.911	1.2124	0.0112	-1.1210	-0.4634	-2.2648	0.1853	-0.4508	-0.00824	0.043	0.026

Table 4.5. (Cont'd)

0.2	-5.983	1.3505	0.0119	-1.2234	-0.4755	-2.1241	0.1730	-0.5500	-0.00776	0.030	0.031
0.3	-7.774	1.6028	-0.0669	-1.3881	-0.4652	-1.9973	0.1631	-0.6847	-0.00660	0.013	0.036
0.4	-9.369	1.8403	-0.2350	-1.2146	-0.6739	-1.8632	0.1456	-0.7343	-0.00561	0.006	0.027
0.5	-10.507	2.0001	-0.3116	-1.2462	-0.7105	-1.7977	0.1378	-0.7860	-0.00488	-0.005	0.024
0.75	-12.355	2.2271	-0.2466	-1.4325	-0.7856	-1.6911	0.1221	-0.8388	-0.00356	-0.019	0.025
1	-13.612	2.3804	-0.2155	-1.5001	-0.8755	-1.6209	0.1083	-0.8476	-0.00270	-0.024	0.026
1.5	-14.872	2.4628	-0.1596	-1.4383	-1.0767	-1.6240	0.1088	-0.8735	-0.00157	-0.034	0.027
2	-15.365	2.4481	-0.1127	-1.3326	-1.2424	-1.7128	0.1231	-0.8805	-0.00073	-0.040	0.015
3	-15.960	2.3977	-0.0384	-1.1554	-1.4677	-1.8092	0.1356	-0.8864	-0.00013	-0.041	0.017
4	-16.195	2.3202	0.0351	-1.0844	-1.5691	-1.9062	0.1533	-0.8858	-0.00035	-0.041	0.014
5	-16.505	2.2837	0.0498	-0.9943	-1.6513	-1.9390	0.1604	-0.8643	-0.00036	-0.039	0.006

Table 4.6. Model coefficients of basic functional form R_{RUP} equation with hypocentral depth term.

T (s)	a0	a1	a2	a3	a4	a5	a6	a7	a10	a11	a12
PGA	-3.687	0.8603	-0.0379	-0.8635	-0.3956	-2.7809	0.2713	-0.3531	-0.00599	0.082	0.024
0.01	-3.640	0.8547	-0.0407	-0.8490	-0.4019	-2.7836	0.2715	-0.3505	-0.00602	0.082	0.024
0.02	-3.550	0.8472	-0.0286	-0.8434	-0.4120	-2.7927	0.2714	-0.3345	-0.00596	0.085	0.023
0.03	-3.096	0.7917	0.0154	-0.8267	-0.4193	-2.8295	0.2726	-0.2850	-0.00592	0.092	0.024
0.05	-2.256	0.7073	0.0441	-0.7240	-0.4718	-2.9059	0.2761	-0.2237	-0.00625	0.102	0.019
0.1	-2.386	0.7919	0.1103	-0.9782	-0.3332	-2.7717	0.2542	-0.3385	-0.00758	0.085	0.024
0.15	-3.949	1.0737	-0.0380	-1.0495	-0.3441	-2.5169	0.2223	-0.4449	-0.00774	0.063	0.028
0.2	-5.058	1.2163	-0.0339	-1.1559	-0.3622	-2.3661	0.2086	-0.5435	-0.00728	0.048	0.032
0.3	-6.869	1.4699	-0.1112	-1.3229	-0.3553	-2.2342	0.1985	-0.6767	-0.00615	0.031	0.038
0.4	-8.496	1.7105	-0.2799	-1.1485	-0.5723	-2.0919	0.1803	-0.7250	-0.00519	0.023	0.028
0.5	-9.657	1.8745	-0.3580	-1.1806	-0.6119	-2.0200	0.1715	-0.7750	-0.00447	0.012	0.026
0.75	-11.520	2.1028	-0.2957	-1.3660	-0.6916	-1.9098	0.1556	-0.8252	-0.00316	-0.002	0.026
1	-12.809	2.2626	-0.2666	-1.4354	-0.7864	-1.8312	0.1403	-0.8325	-0.00230	-0.008	0.028
1.5	-14.089	2.3481	-0.2115	-1.3746	-0.9875	-1.8289	0.1401	-0.8576	-0.00118	-0.018	0.028
2	-14.585	2.3346	-0.1647	-1.2691	-1.1486	-1.9164	0.1539	-0.8645	-0.00034	-0.023	0.016
3	-15.200	2.2891	-0.0901	-1.0939	-1.3706	-2.0070	0.1649	-0.8711	0.00000	-0.024	0.019
4	-15.460	2.2178	-0.0160	-1.0246	-1.4682	-2.0966	0.1808	-0.8714	0.00000	-0.023	0.015
5	-15.787	2.1842	-0.0011	-0.9348	-1.5494	-2.1250	0.1871	-0.8505	0.00000	-0.022	0.008

There's no problem seen in magnitude, distance, V_{S30} and dipping angle; after analyzing these distributions, similarly as in the basic functional form equation that is derived in the previous section. When considering residual distributions dependent on hypocentral depth, it's been seen that the trend in basic functional form has been vanished. In this context, it occurs that Z_{HYP} term is necessary for both of the distance-metrics.

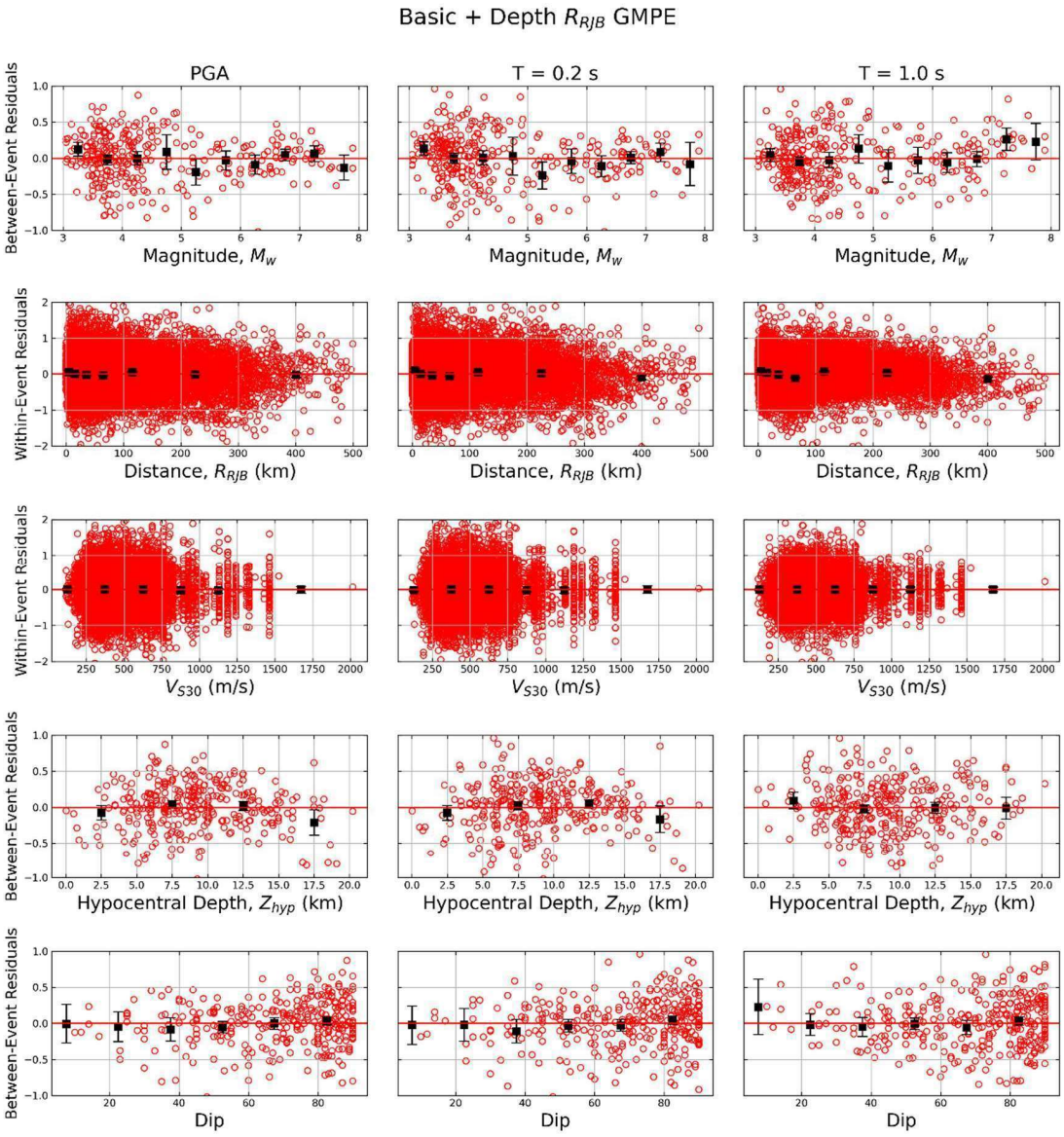

Figure 4.4. Distributions of between-event residuals versus magnitude (1st row), within-event residuals versus distance (2nd row), within-event residuals versus V_{S30} (3rd row), between-event residuals versus hypocentral depth (4th row) and between-event residuals versus dipping angle (5th row) for basic + Z_{HYP} functional form R_{JB} equation.

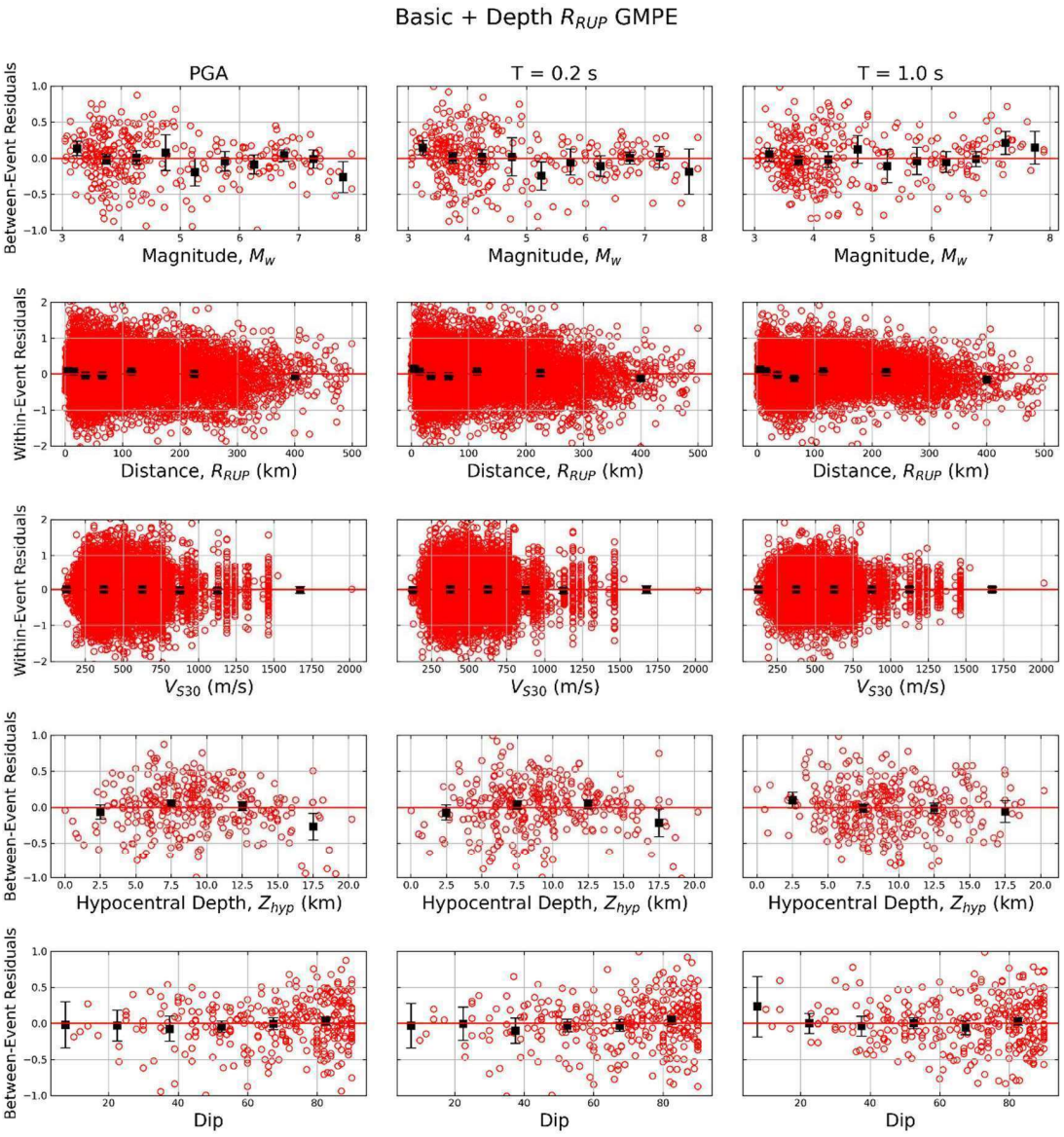

Figure 4.5. Distributions of between-event residuals versus magnitude (1st row), within-event residuals versus distance (2nd row), within-event residuals versus V_{S30} (3rd row), between-event residuals versus hypocentral depth (4th row) and between-event residuals versus dipping angle (5th row) for basic + Z_{HYP} functional form R_{RUP} equation.

To evaluate the components of random variability model of Z_{HYP} term added functional form, change of total standard deviation (σ), between-event standard deviation (τ), within-event standard deviation (ϕ) and site-to-site standard deviation (ϕ_{S2S}) with period are listed in Table 4.7 and given in Figure 4.6. In the comparison that is given in this figure, likewise in the basic functional form, it's

been seen that between-event standard deviation values of R_{RUP} equation are slightly higher than the R_{JB} ones, in the short period values. This difference is also the reason for the difference in total standard deviation. While it has been seen that this observation still continues and cannot be resolved with the addition of hypocentral depth term in this section. Although, it's been observed that discrepancy is smaller than the one in previous section.

Table 4.7. Random variability values of hypocentral depth term added functional form R_{JB} and R_{RUP} GMPEs.

Period (s)	R_{JB} based GMPE				R_{RUP} based GMPE			
	τ	Φ_{S2S}	Φ	σ	τ	Φ_{S2S}	Φ	σ
PGA	0.3778	0.4083	0.5326	0.7702	0.3892	0.4076	0.5345	0.7768
0.01	0.3785	0.4079	0.5332	0.7706	0.3899	0.4072	0.5350	0.7772
0.02	0.3806	0.4118	0.5343	0.7746	0.3923	0.4112	0.5362	0.7813
0.03	0.3914	0.4196	0.5400	0.7879	0.4034	0.4191	0.5419	0.7950
0.05	0.4192	0.4411	0.5492	0.8197	0.4311	0.4409	0.5513	0.8271
0.1	0.4304	0.4567	0.5490	0.8338	0.4391	0.4562	0.5503	0.8390
0.15	0.4124	0.4580	0.5490	0.8253	0.4200	0.4574	0.5504	0.8298
0.2	0.3926	0.4561	0.5479	0.8139	0.4008	0.4554	0.5497	0.8187
0.3	0.3569	0.4482	0.5396	0.7871	0.3636	0.4481	0.5414	0.7913
0.4	0.3405	0.4607	0.5169	0.7716	0.3450	0.4617	0.5192	0.7757
0.5	0.3349	0.4713	0.5059	0.7682	0.3374	0.4721	0.5079	0.7711
0.75	0.3533	0.4803	0.4733	0.7612	0.3514	0.4830	0.4747	0.7629
1	0.3817	0.4869	0.4515	0.7659	0.3789	0.4893	0.4526	0.7667
1.5	0.4280	0.4726	0.4417	0.7756	0.4235	0.4755	0.4430	0.7757
2	0.4456	0.4646	0.4475	0.7841	0.4404	0.4682	0.4490	0.7840
3	0.4653	0.4496	0.4672	0.7981	0.4572	0.4513	0.4692	0.7956
4	0.4832	0.4346	0.4808	0.8084	0.4734	0.4359	0.4833	0.8048
5	0.5086	0.4332	0.4906	0.8289	0.4977	0.4341	0.4937	0.8246

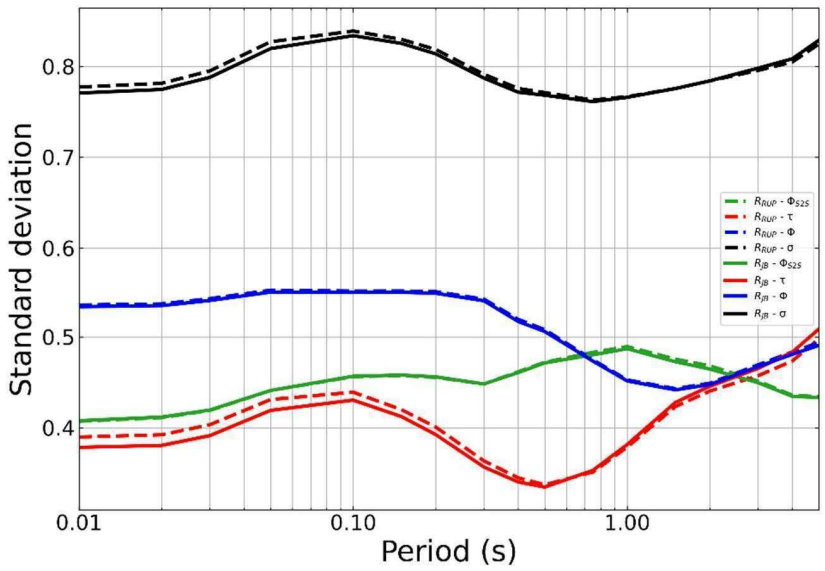

Figure 4.6. Random variability comparisons of hypocentral depth term added functional form R_{JB} and R_{RUP} GMPEs.

To compare the contribution of hypocentral depth term on R_{JB} and R_{RUP} equations, regression coefficients that are controlling the hypocentral depth term has been compared in Figure 4.7 and Figure 4.8. In these figures, solid orange line stands for hypocentral depth term added functional form of R_{RUP} equation (Basic + Depth R_{RUP} GMPE), while solid blue line stands for hypocentral depth term added functional form of R_{JB} equation (Basic + Depth R_{JB} GMPE). While the general behaviors are similar, the lines stand for R_{JB} equation are clearly under the R_{RUP} equations'. Therefore, it can be said that, the contribution of hypocentral depth term in R_{JB} equation is lower than the R_{RUP} ones, under global database. This situation has also been observed under Turkish database (see. Figure 3.7).

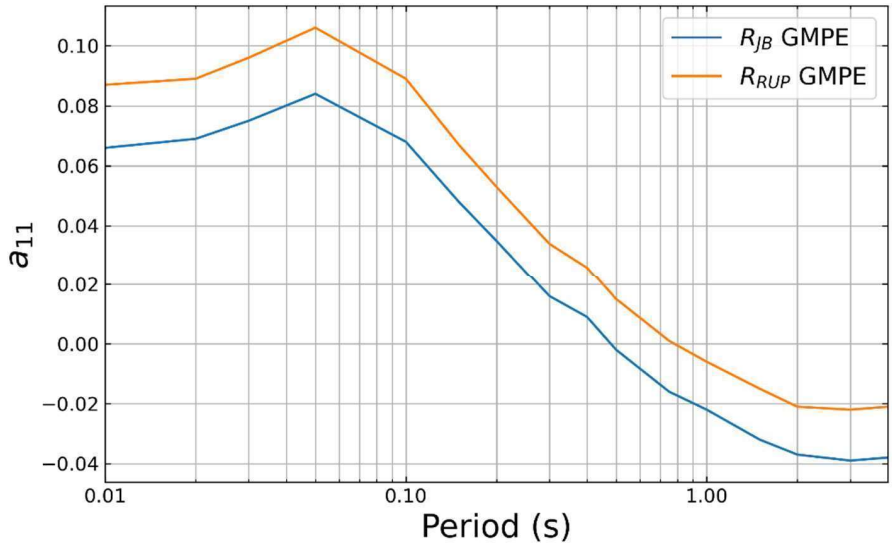

Figure 4.7. Comparison of a_{11} regression coefficients, which controls the hypocentral depth term, from the analyses that are held under Global database for both equations.

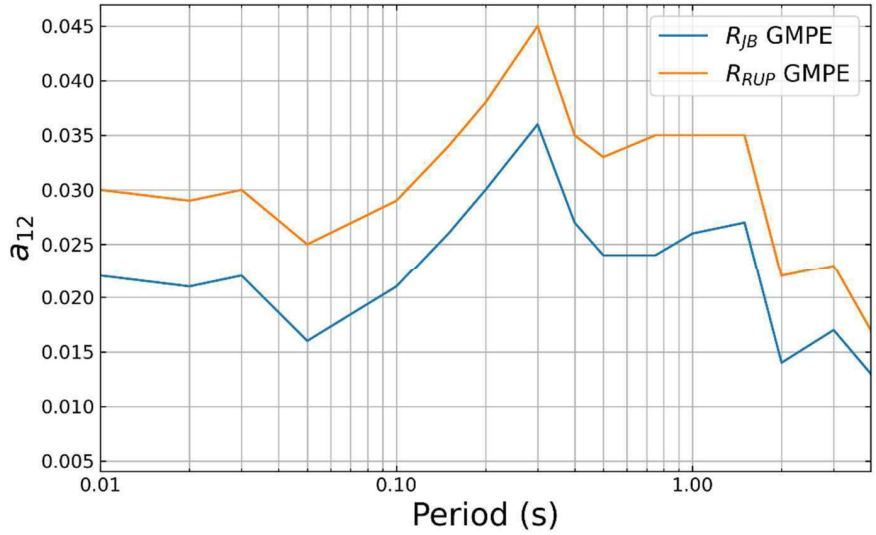

Figure 4.8. Comparison of a_{12} regression coefficients, which controls the hypocentral depth term, from the analyses that are held under Global database for both equations.

4.3. Development of R_{JB} and R_{RUP} based GMPEs with Dipping Angle Term

In the result of residual distributions, there's no trend has been observed in dipping angle distributions (as seen in previous sections). However, Campbell and Bozorgnia (2014) suggests using dipping angle term in functional form. It is indicated that there's a correction required especially for small magnitude earthquakes. For the purpose of investigating this term, dipping angle term (f_{dip}) has been added to Equation 4.8 and Equation 4.10 has been obtained. Dipping angle function has been given in Equation 4.11.

$$ln\, Y = f_{mag} + f_{dis} + f_{sof} + f_{aat} + f_{hyp} + f_{dip} + f_{site} \tag{4.10}$$

$$f_{dip} = \begin{cases} a_{13}\,\delta; & M_w \leq 4.5 \\ a_{13}\,(5.5 - M_w)\delta; & 4.5 < M_w \leq 5.5 \\ 0; & M_w > 5.5 \end{cases} \tag{4.11}$$

Model coefficients of R_{JB} equation that are acquired in the result of regression analyses which considers current functional form, has been listed in Table 4.8. From these regression coefficients, the ones between a_0-a_{12} are the new values of coefficients, which are explained in the previous section, in this new functional form. The coefficient of dipping angle has been listed on a_{13} column of the table. As in previous stages, R_{RUP} distance-metric has been used instead of R_{JB} distance-metric (in Equation 4.3 and 4.5) in sub-functions of Equation 4.10 and R_{RUP} based equation, which considers hypocentral depth term and dipping angle term, has been developed. Model coefficients of this equations have also been listed in Table 4.9 with corresponding period values. Fictitious depth (h), style of faulting and nonlinear site effects coefficients are exactly same as the ones that are obtained in basic functional form section.

Residual distributions of equations derived in this stage have been given in Figure 4.9 and Figure 4.10 for R_{JB} and R_{RUP} based equations, respectively. Here, format

and considered periods in the residual distributions are the same as the ones in previous stage.

Table 4.8. Model coefficients of basic functional form R_{JB} equation with hypocentral depth term and dipping angle term version.

T (s)	a0	a1	a2	a3	a4	a5	a6	a7	a10	a11	a12	a13
PGA	-4.931	0.9830	0.3680	-1.2521	-0.5522	-2.5212	0.2330	-0.3633	-0.0065	0.066	0.022	0.0046
0.01	-4.884	0.9774	0.3652	-1.2376	-0.5586	-2.5237	0.2331	-0.3606	-0.0065	0.066	0.022	0.0046
0.02	-4.793	0.9704	0.3722	-1.2277	-0.5683	-2.5320	0.2330	-0.3447	-0.0065	0.069	0.021	0.0045
0.03	-4.348	0.9159	0.4169	-1.2114	-0.5765	-2.5663	0.2339	-0.2950	-0.0064	0.075	0.022	0.0045
0.05	-3.510	0.8331	0.4332	-1.0983	-0.6296	-2.6393	0.2372	-0.2323	-0.0068	0.084	0.016	0.0043
0.1	-3.627	0.9159	0.4919	-1.3443	-0.4836	-2.5078	0.2159	-0.3450	-0.0081	0.068	0.021	0.0043
0.15	-5.170	1.1913	0.3683	-1.4371	-0.4827	-2.2632	0.1851	-0.4518	-0.0082	0.048	0.026	0.0046
0.2	-6.259	1.3287	0.3886	-1.5567	-0.4964	-2.1222	0.1726	-0.5512	-0.0078	0.035	0.030	0.0049
0.3	-7.944	1.5895	0.1644	-1.5928	-0.4780	-1.9960	0.1629	-0.6853	-0.0066	0.016	0.036	0.0030
0.4	-9.527	1.8278	-0.0197	-1.4056	-0.6853	-1.8621	0.1453	-0.7349	-0.0056	0.009	0.027	0.0028
0.5	-10.660	1.9881	-0.1023	-1.4323	-0.7213	-1.7966	0.1376	-0.7865	-0.0049	-0.002	0.024	0.0027
0.75	-12.507	2.2153	-0.0391	-1.6171	-0.7963	-1.6902	0.1219	-0.8392	-0.0036	-0.016	0.024	0.0027
1	-13.744	2.3703	-0.0368	-1.6595	-0.8845	-1.6203	0.1081	-0.8479	-0.0027	-0.022	0.026	0.0023
1.5	-14.989	2.4539	-0.0009	-1.5799	-1.0847	-1.6236	0.1087	-0.8738	-0.0016	-0.032	0.027	0.0021
2	-15.512	2.4371	0.0857	-1.5097	-1.2523	-1.7123	0.1230	-0.8808	-0.0007	-0.037	0.014	0.0026
3	-16.096	2.3873	0.1455	-1.3194	-1.4771	-1.8087	0.1355	-0.8867	-0.0001	-0.039	0.017	0.0024
4	-16.338	2.3093	0.2288	-1.2570	-1.5791	-1.9056	0.1531	-0.8860	-0.0004	-0.038	0.013	0.0025
5	-16.648	2.2729	0.2426	-1.1660	-1.6614	-1.9385	0.1603	-0.8646	-0.0004	-0.037	0.006	0.0025

Table 4.9. Model coefficients of basic functional form R_{RUP} equation with hypocentral depth term and dipping angle term version.

T (s)	a0	a1	a2	a3	a4	a5	a6	a7	a10	a11	a12	a13
PGA	-3.928	0.8410	0.2926	-1.1567	-0.4132	-2.7792	0.2710	-0.3539	-0.0060	0.086	0.024	0.0043
0.01	-3.881	0.8354	0.2898	-1.1421	-0.4195	-2.7819	0.2712	-0.3513	-0.0060	0.087	0.024	0.0043
0.02	-3.786	0.8282	0.2959	-1.1313	-0.4292	-2.7911	0.2711	-0.3352	-0.0060	0.089	0.023	0.0042
0.03	-3.331	0.7728	0.3383	-1.1133	-0.4363	-2.8279	0.2724	-0.2857	-0.0059	0.096	0.024	0.0042
0.05	-2.479	0.6893	0.3518	-0.9972	-0.4879	-2.9046	0.2759	-0.2243	-0.0063	0.105	0.018	0.0040
0.1	-2.607	0.7741	0.4151	-1.2482	-0.3498	-2.7704	0.2540	-0.3392	-0.0076	0.088	0.023	0.0040
0.15	-4.194	1.0540	0.2983	-1.3472	-0.3624	-2.5153	0.2221	-0.4458	-0.0077	0.067	0.028	0.0044
0.2	-5.320	1.1957	0.3232	-1.4719	-0.3822	-2.3642	0.2083	-0.5445	-0.0073	0.053	0.032	0.0047
0.3	-7.025	1.4577	0.1011	-1.5109	-0.3671	-2.2329	0.1983	-0.6772	-0.0062	0.034	0.038	0.0028
0.4	-8.641	1.6992	-0.0829	-1.3233	-0.5828	-2.0907	0.1800	-0.7255	-0.0052	0.026	0.028	0.0026
0.5	-9.798	1.8635	-0.1668	-1.3506	-0.6219	-2.0189	0.1713	-0.7754	-0.0045	0.015	0.025	0.0025
0.75	-11.659	2.0921	-0.1063	-1.5346	-0.7014	-1.9089	0.1555	-0.8256	-0.0032	0.000	0.026	0.0025
1	-12.928	2.2535	-0.1053	-1.5792	-0.7946	-1.8306	0.1402	-0.8328	-0.0023	-0.006	0.028	0.0021
1.5	-14.193	2.3402	-0.0700	-1.5009	-0.9947	-1.8284	0.1400	-0.8578	-0.0012	-0.016	0.028	0.0018
2	-14.719	2.3246	0.0166	-1.4309	-1.1578	-1.9158	0.1538	-0.8648	-0.0003	-0.021	0.016	0.0024

Table 4.9. (Cont'd)

3	-15.323	2.2797	0.0775	-1.2433	-1.3792	-2.0064	0.1648	-0.8713	0.0000	-0.022	0.018	0.0022
4	-15.592	2.2079	0.1618	-1.1830	-1.4775	-2.0960	0.1807	-0.8717	0.0000	-0.021	0.015	0.0023
5	-15.918	2.1743	0.1762	-1.0927	-1.5587	-2.1244	0.1869	-0.8507	0.0000	-0.020	0.008	0.0023

After analyzing these distributions, as in the previous sections, there's no problem in equations about magnitude, distance, V_{S30}, hypocentral distance and dipping angle. It is not that possible to talk about apparent effects of f_{dip} term.

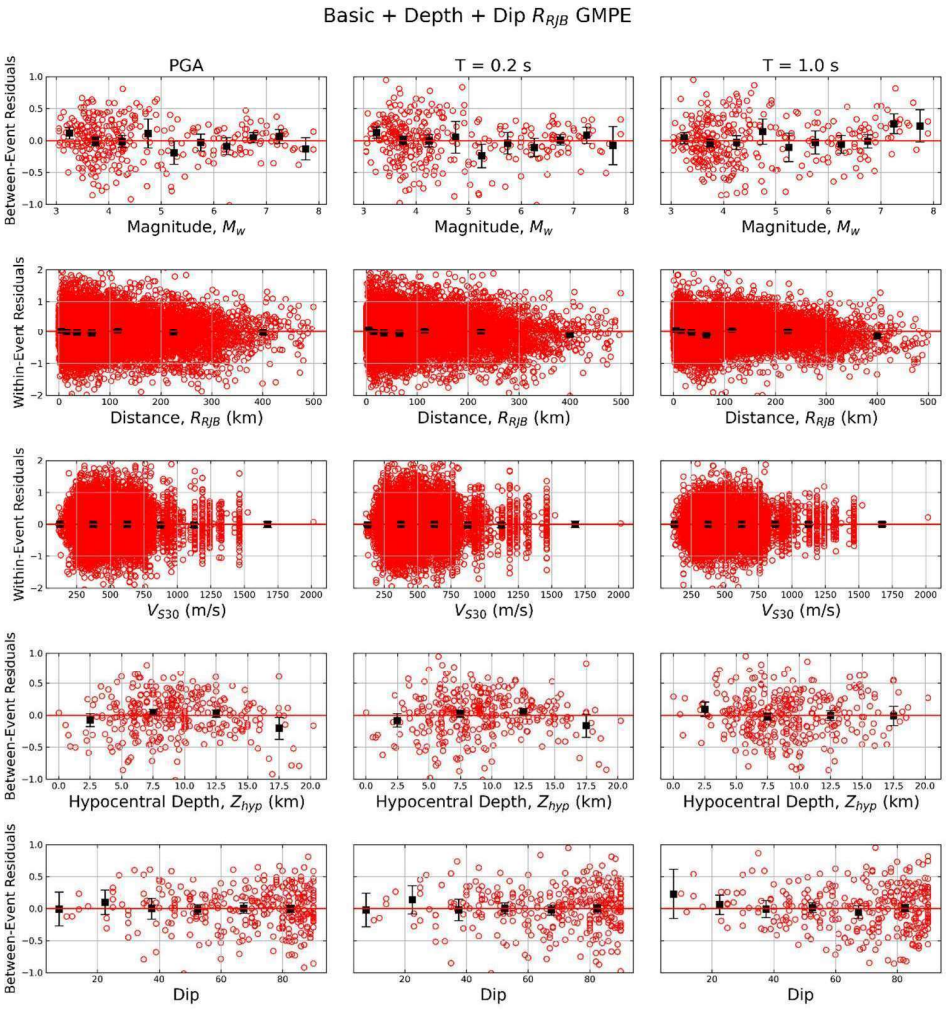

Figure 4.9. Distributions of between-event residuals versus magnitude (1st row), within-event residuals versus distance (2nd row), within-event residuals versus V_{S30} (3rd row), between-event residuals versus hypocentral depth (4th row) and between-event residuals versus dipping angle (5th row) for basic + Z_{HYP} + Dip functional form R_{JB} equation.

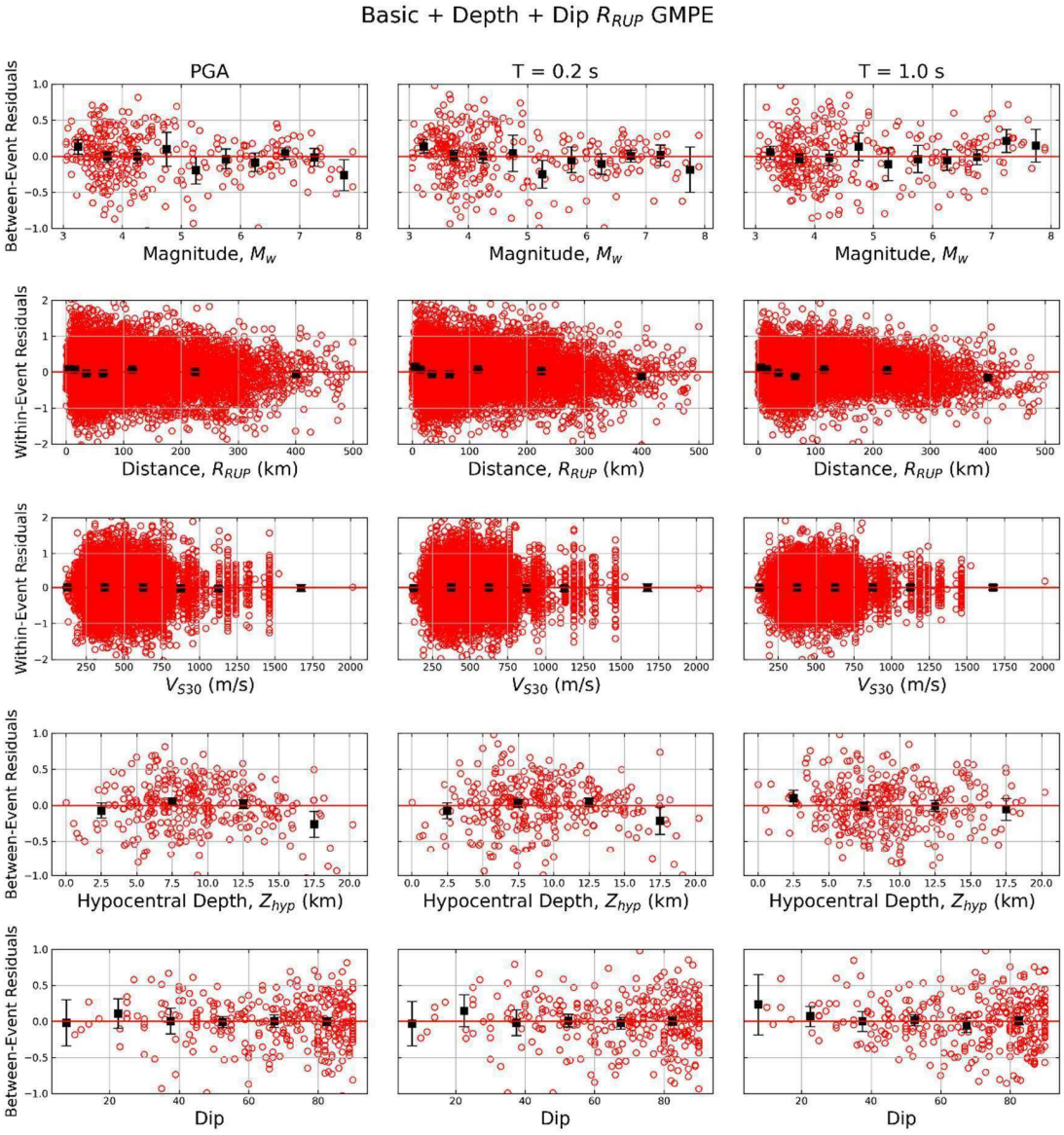

Figure 4.10. Distributions of between-event residuals versus magnitude (1st row), within-event residuals versus distance (2nd row), within-event residuals versus V_{S30} (3rd row), between-event residuals versus hypocentral depth (4th row) and between-event residuals versus dipping angle (5th row) for basic + Z_{HYP} + Dip functional form R_{RUP} equation.

To evaluate the components of random variability model of Z_{HYP} and dip terms added functional form, change of total standard deviation (σ), between-event standard deviation (τ), within-event standard deviation (ϕ) and site-to-site standard deviation (ϕ_{S2S}) with period are listed in Table 4.10 and they are given

in Figure 4.11. In the comparison that is given in this figure, likewise in the basic functional form, it's been seen that between-event standard deviation values of R_{RUP} equation are slightly higher than the R_{JB} ones in the short period values as it was for basic and Z_{HYP} added functional form GMPEs. This difference is also the reason of the difference in total standard deviation. It is possible to say that the effect of dipping angle term on standard deviation is quite small.

Table 4.10. Random variability values of hypocentral depth and dipping angle terms added functional form R_{JB} and R_{RUP} GMPEs.

Period (s)	R_{JB} based GMPE				R_{RUP} based GMPE			
	τ	Φ_{S2S}	Φ	σ	τ	Φ_{S2S}	Φ	σ
PGA	0.3737	0.4084	0.5326	0.7682	0.3857	0.4077	0.5345	0.7750
0.01	0.3744	0.4080	0.5331	0.7687	0.3864	0.4072	0.5350	0.7755
0.02	0.3767	0.412	0.5343	0.7727	0.3890	0.4112	0.5362	0.7797
0.03	0.3878	0.4197	0.5400	0.7862	0.4004	0.4192	0.5419	0.7936
0.05	0.4160	0.4412	0.5492	0.8181	0.4285	0.4411	0.5513	0.8259
0.1	0.4263	0.4569	0.5490	0.8318	0.4356	0.4564	0.5503	0.8372
0.15	0.4075	0.4582	0.5490	0.8230	0.4158	0.4575	0.5504	0.8277
0.2	0.3869	0.4562	0.5479	0.8112	0.3958	0.4555	0.5496	0.8162
0.3	0.3542	0.4483	0.5396	0.7859	0.3613	0.4481	0.5413	0.7902
0.4	0.3384	0.4607	0.5169	0.7706	0.3432	0.4616	0.5192	0.7749
0.5	0.3328	0.4713	0.5058	0.7673	0.3356	0.4721	0.5079	0.7703
0.75	0.3521	0.4802	0.4732	0.7606	0.3504	0.4829	0.4746	0.7624
1	0.3808	0.4869	0.4515	0.7654	0.3781	0.4893	0.4526	0.7663
1.5	0.4270	0.4726	0.4417	0.7751	0.4227	0.4754	0.4430	0.7752
2	0.4447	0.4646	0.4475	0.7835	0.4396	0.4681	0.4490	0.7836
3	0.4647	0.4496	0.4672	0.7977	0.4568	0.4513	0.4693	0.7953
4	0.4824	0.4346	0.4808	0.8079	0.4728	0.4358	0.4833	0.8044
5	0.5076	0.4332	0.4906	0.8283	0.4969	0.4341	0.4937	0.8241

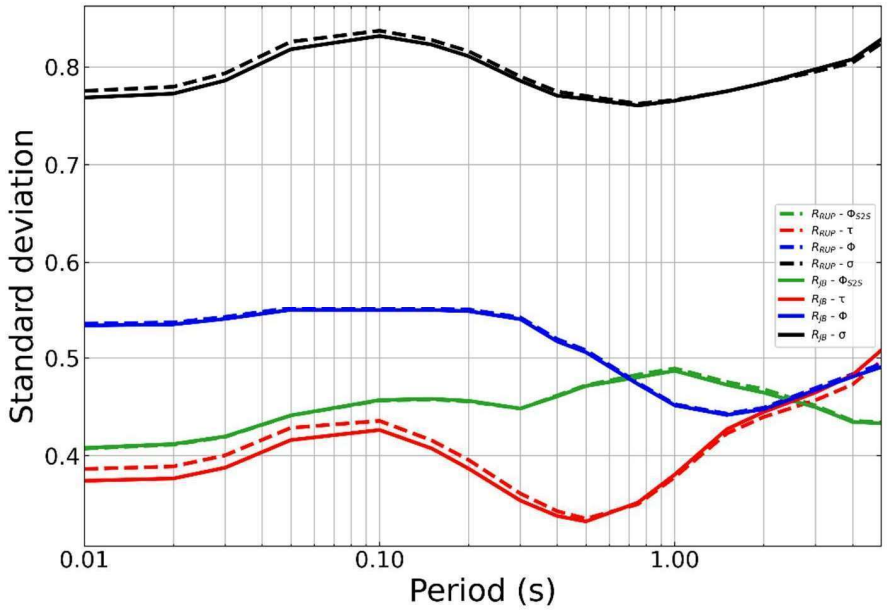

Figure 4.11. Random variability comparisons of hypocentral depth and dipping angle terms added functional form R_{JB} and R_{RUP} GMPEs.

4.4. Development of R_{RUP} Based GMPE in Complex Functional Form

In this stage of the study, terms that will provide hanging wall corrections which are necessary for R_{RUP} based equation have been added to the functional form. R_{JB} based equations can consider the hanging wall effects on average because they take R_{JB} distance-metric as 0 km on the surface projection of the fault. (Donahue and Abrahamson, 2014). Residual distributions for the hanging wall earthquake data of basic form which is derived in the first stage of this study have been shown in Figure 4.12, Figure 4.13 and Figure 4.14 for PGA, T = 0.2 s and T = 1.0 s values, respectively. In these figures, residual values of earthquake recordings that are on the fault projection (namely R_{JB} = 0 km) and outside of this place (namely R_{JB} > 0 km) are evaluated separately. In this context, when analyzing the residual distributions, a serious trend has been seen in R_{RUP} based equation, especially for R_{JB} = 0 km (left column). This fact about R_{JB} based equations has been seen in evaluations that are made after the result of regression analyses, as it has been explained physically in Donahue and Abrahamson (2014).

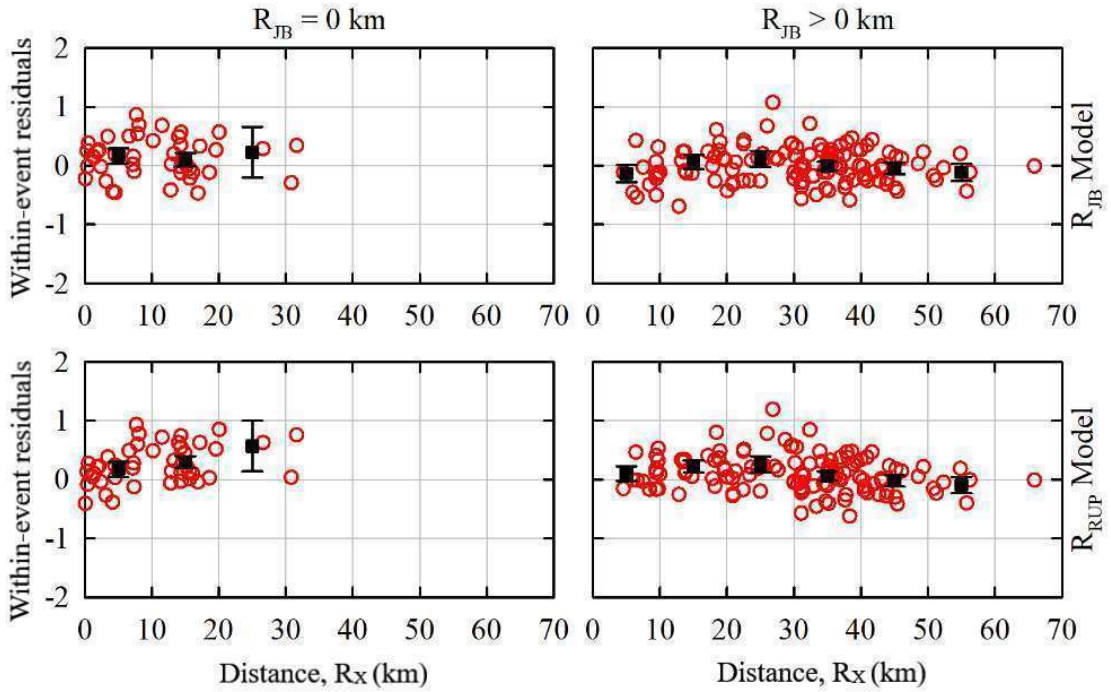

Figure 4.12. Within-event distributions of basic functional form R_{JB} (top row) and R_{RUP} (bottom row) equations for R_{JB} = 0 km (left column) and R_{JB} > 0 km (right column) situations depending on R_X distance for PGA.

In this stage, to enhance the modelling capability of R_{RUP} equation, hanging wall term (HW) has been added to Basic + Z_{HYP} + Dip functional form and this form represented with Basic + Z_{HYP} + Dip + HW ground-motion prediction equation. From now onward, this hanging wall effects term which has been added to the functional form, turns this functional form to a complex version.

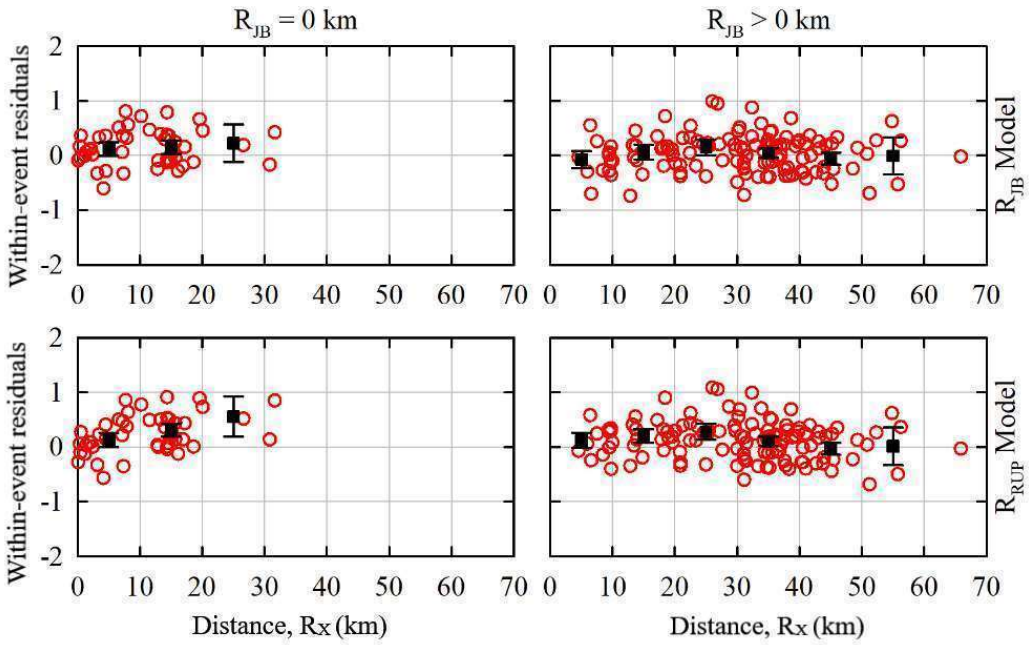

Figure 4.13. Within-event distributions of basic functional form R_{JB} (top row) and R_{RUP} (bottom row) equations for R_{JB} = 0 km (left column) and R_{JB} > 0 km (right column) situations depending on R_X distance for T = 0.2s.

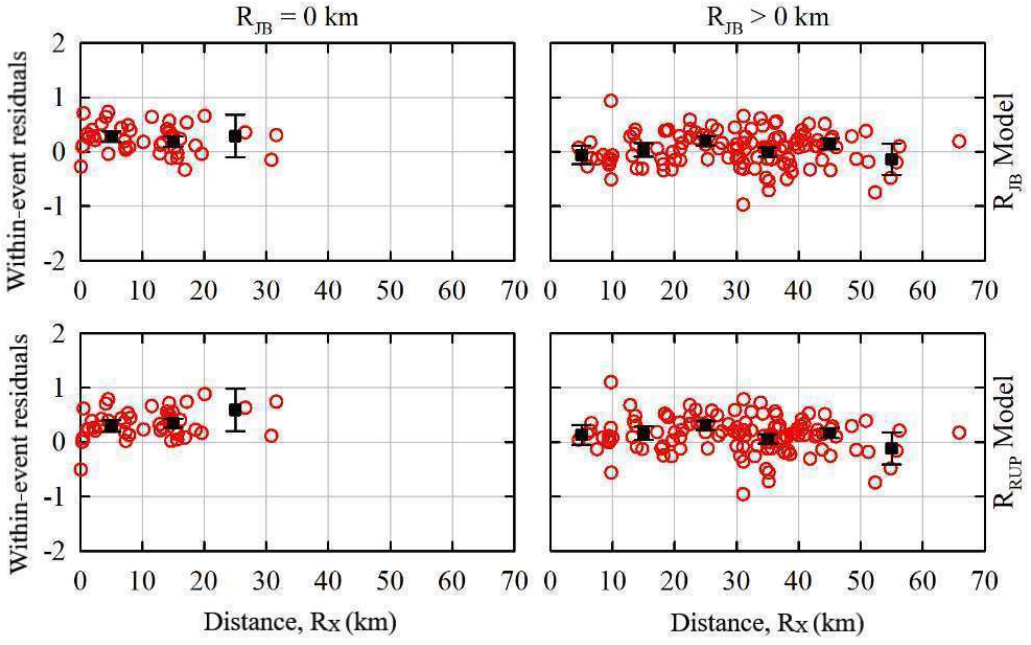

Figure 4.14. Within-event distributions of basic functional form R_{JB} (top row) and R_{RUP} (bottom row) equations for R_{JB} = 0 km (left column) and R_{JB} > 0 km (right column) situations depending on R_X distance for T = 1.0s.

New functional form has been turned into a complex form given in Equation 4.12 with adding f_{hng} (hanging wall) to Equation 4.10. With the hanging wall model that is given in Equation 4.13; R_X distance (Equation 4.14; W fault rupture width and δ dipping angle), R_{RUP} distance (Equation 4.15), M_W magnitude scaling (Equation 4.16), Z_{TOR} (Equation 4.17) and dipping angle (Equation 4.18) effects have been taken into account. This model is the function that have been used to consider hanging wall effects in Campbell and Bozorgnia (2014).

$$ln\, Y = f_{mag} + f_{dis} + f_{sof} + f_{aat} + f_{hyp} + f_{dip} + f_{site} + f_{hng} \tag{4.12}$$

$$f_{hng} = a_{14}\, f_{hng,R_X}\, f_{hng,R_{RUP}}\, f_{hng,M_W}\, f_{hng,Z_{TOR}}\, f_{hng,\delta} \tag{4.13}$$

$$f_{hng,R_X} = \begin{cases} 0; & R_X < 0 \\ f_1(R_X); & 0 \le R_X < R_1 \\ \max[f_2(R_X), 0]; & R_X \ge R_1 \end{cases} \tag{4.14.a}$$

$$f_1(R_X) = h_1 + h_2\,(R_X/R_1) + h_3(R_X/R_1)^2 \tag{4.14.b}$$

$$f_2(R_X) = 1 + h_5\left(\frac{R_X - R_1}{R_2 - R_1}\right) + h_6\left(\frac{R_X - R_1}{R_2 - R_1}\right)^2 \tag{4.14.c}$$

$$R_1 = W\,\cos(\delta) \tag{4.14.d}$$

$$R_1 = 62\,M_W - 350 \tag{4.14.e}$$

$$f_{hng,R_{RUP}} = \begin{cases} 1; & R_{RUP} = 0 \\ (R_{RUP} - R_{JB})/R_{RUP}\,; & R_{RUP} > 0 \end{cases} \tag{4.15}$$

$$f_{hng,M_W} = \begin{cases} 0\ ; & 5.5 \leq M_W \\ (M_W - 5.5)[1 + a_{2HW}(M_W - 6.5)]\ ; & 5.5 < M_W \leq 6.5 \\ 1 + a_{2HW}(M_W - 6.5)\ ; & M_W > 6.5 \end{cases} \quad (4.16)$$

$$f_{hng,Z_{TOR}} = \begin{cases} 1 - 0.06Z_{TOR}\ ; & Z_{TOR} \leq 16.66 \\ 0\ ; & Z_{TOR} > 16.66 \end{cases} \quad (4.17)$$

$$f_{hng,\delta} = (90 - \delta)\ /\ 45 \quad (4.18)$$

Complex functional form has been used to develop R_{RUP} based equation. In the light of the information that is given in the beginning of the section, the model developed in the previous section will be used as the last version of the R_{JB} based equation. Period dependent model coefficients of R_{RUP} equation that has been developed in the results of regression analyses have been listen in Table 4.11 and 4.12. The coefficients that are given in Table 4.12 are directly the coefficients used to calculate hanging wall effects.

Table 4.11. Model coefficients of R_{RUP} based equation in complex functional form.

T (s)	a0	a1	a2	a3	a4	a5	a6	a7	a10	a11	a12	a13
PGA	-3.700	0.7819	0.3101	-1.2295	-0.3240	-2.8436	0.2867	-0.3652	-0.0061	0.086	0.030	0.0043
0.01	-3.653	0.7762	0.3072	-1.2149	-0.3304	-2.8462	0.2869	-0.3626	-0.0061	0.087	0.030	0.0043
0.02	-3.557	0.7687	0.3136	-1.2049	-0.3393	-2.8558	0.2869	-0.3466	-0.0061	0.089	0.029	0.0042
0.03	-3.097	0.7122	0.3568	-1.1893	-0.3439	-2.8940	0.2885	-0.2974	-0.0060	0.096	0.030	0.0042
0.05	-2.241	0.6275	0.3708	-1.0767	-0.3921	-2.9719	0.2923	-0.2365	-0.0063	0.106	0.025	0.0040
0.1	-2.377	0.7135	0.4334	-1.3271	-0.2545	-2.8358	0.2701	-0.3514	-0.0077	0.089	0.029	0.0039
0.15	-3.986	0.9975	0.3158	-1.4244	-0.2703	-2.5749	0.2370	-0.4587	-0.0078	0.067	0.034	0.0044
0.2	-5.071	1.1310	0.3415	-1.5520	-0.2833	-2.4348	0.2254	-0.5578	-0.0074	0.053	0.038	0.0046
0.3	-6.766	1.3906	0.1212	-1.5998	-0.2598	-2.3066	0.2161	-0.6922	-0.0062	0.034	0.045	0.0028
0.4	-8.390	1.6325	-0.0603	-1.4217	-0.4687	-2.1631	0.1977	-0.7432	-0.0053	0.026	0.035	0.0025
0.5	-9.498	1.7879	-0.1439	-1.4459	-0.5062	-2.1038	0.1914	-0.7917	-0.0046	0.015	0.033	0.0025
0.75	-11.332	2.0090	-0.0784	-1.6462	-0.5701	-2.0016	0.1775	-0.8445	-0.0033	0.001	0.035	0.0024
1	-12.668	2.1847	-0.0790	-1.6709	-0.6897	-1.9050	0.1583	-0.8498	-0.0024	-0.006	0.035	0.0021
1.5	-13.954	2.2770	-0.0452	-1.5867	-0.8973	-1.8967	0.1567	-0.8732	-0.0013	-0.015	0.035	0.0018
2	-14.507	2.2685	0.0384	-1.5064	-1.0718	-1.9765	0.1686	-0.8781	-0.0004	-0.021	0.022	0.0023
3	-15.174	2.2407	0.0920	-1.2940	-1.3206	-2.0487	0.1751	-0.8801	0.0000	-0.022	0.023	0.0022
4	-15.525	2.1906	0.1680	-1.2050	-1.4518	-2.1147	0.1852	-0.8754	0.0000	-0.021	0.017	0.0023
5	-15.886	2.1661	0.1792	-1.1030	-1.5466	-2.1332	0.1891	-0.8525	0.0000	-0.020	0.008	0.0023

Table 4.12. Hanging wall coefficients of R_{RUP} based equation in complex functional form.

T (s)	a14	a2hw	h1	h2	h3	h5	h6
PGA	0.600	0.596	0.117	1.616	-0.733	-0.128	-0.756
0.01	0.600	0.168	0.242	1.471	-0.714	-0.336	-0.270
0.02	0.600	0.166	0.244	1.467	-0.711	-0.339	-0.263
0.03	0.600	0.167	0.246	1.467	-0.713	-0.338	-0.259
0.05	0.600	0.173	0.251	1.449	-0.701	-0.338	-0.263
0.1	0.600	0.174	0.259	1.449	-0.708	-0.391	-0.201
0.15	0.600	0.198	0.254	1.461	-0.715	-0.449	-0.099
0.2	0.600	0.204	0.237	1.484	-0.721	-0.393	-0.198
0.3	0.600	0.164	0.210	1.586	-0.795	-0.447	-0.121
0.4	0.600	0.160	0.226	1.544	-0.770	-0.525	-0.086
0.5	0.600	0.184	0.217	1.554	-0.770	-0.407	-0.281
0.75	0.700	0.216	0.154	1.626	-0.780	-0.371	-0.285
1	0.657	0.596	0.117	1.616	-0.733	-0.128	-0.756
1.5	0.607	0.596	0.117	1.616	-0.733	-0.128	-0.756
2	0.538	0.596	0.117	1.616	-0.733	-0.128	-0.756
3	0.370	0.596	0.117	1.616	-0.733	-0.128	-0.756
4	0.163	0.596	0.117	1.616	-0.733	-0.128	-0.756
5	0.077	0.596	0.117	1.616	-0.733	-0.128	-0.756

General residual distributions belong to R_{RUP} equation derived in this stage have been given in Figure 4.15. Followed format and considered periods are equivalent to the residual distributions given in previous sections. After analyzing these distributions, there's no problem seen in equations about magnitude, distance, V_{S30}, hypocentral distance and dipping angle.

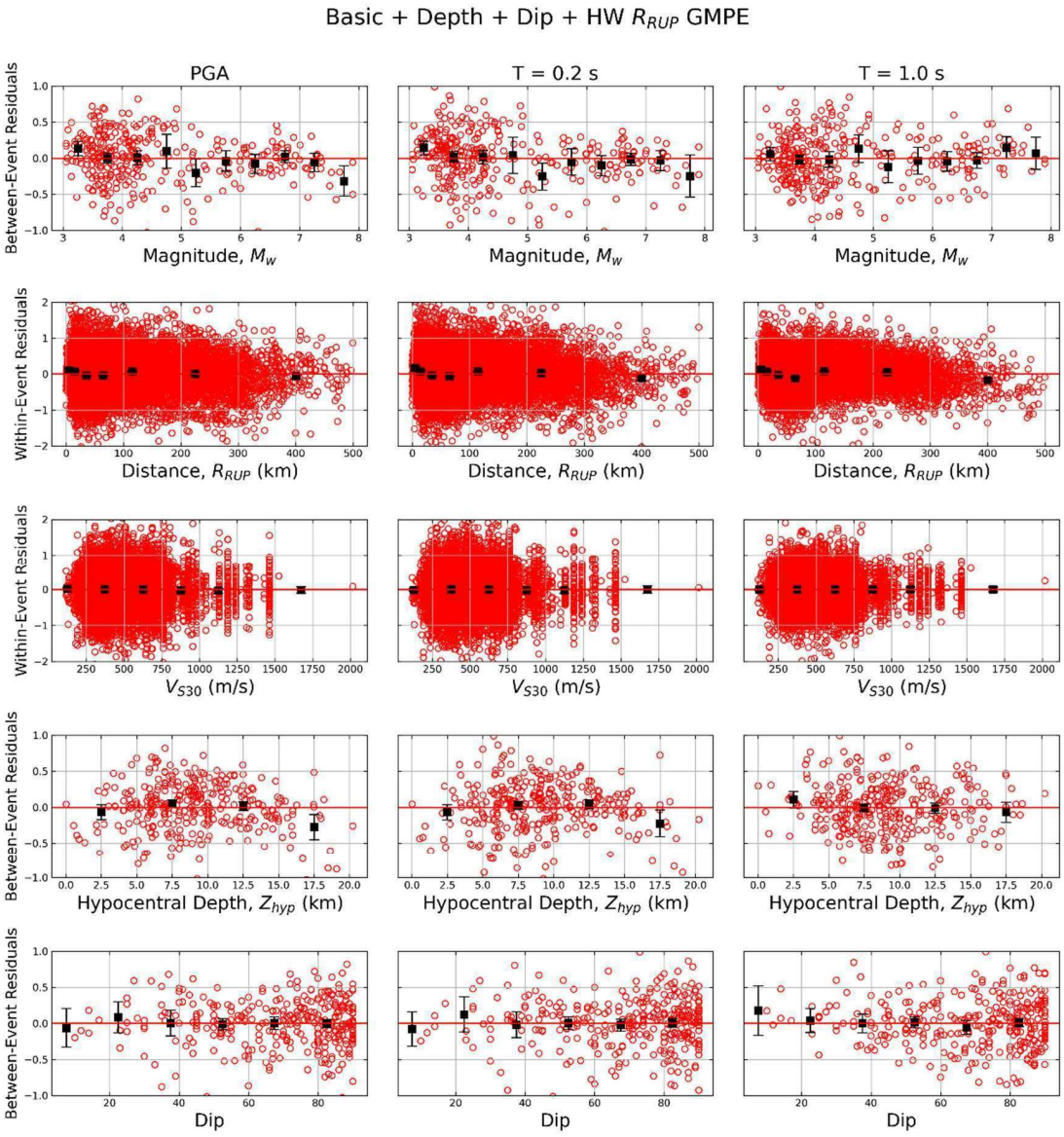

Figure 4.15. Distributions of between-event residuals versus magnitude (1st row), within-event residuals versus distance (2nd row), within-event residuals versus V_{S30} (3rd row), between-event residuals versus hypocentral depth (4th row) and between-event residuals versus dipping angle (5th row) for basic + Z_{HYP} + Dip + HW functional form R_{RUP} equation.

Residual distributions belong to R_{RUP} based equation in current functional form and R_{JB} based equation in functional form that considers hypocentral depth and dipping angle have been plotted for earthquake recordings on the hanging wall side in Figure 4.16, Figure 4.17 and Figure 4.18. These figures are up-to-date

versions of residual distributions in Figure 4.12, Figure 4.13 and Figure 4.14 that are examined in the previous paragraphs. It is evident that the trend of R_{RUP} equation has been vanished with the usage of complex form. In this context, it is obvious that complex functional form is a necessity for R_{RUP} based equation.

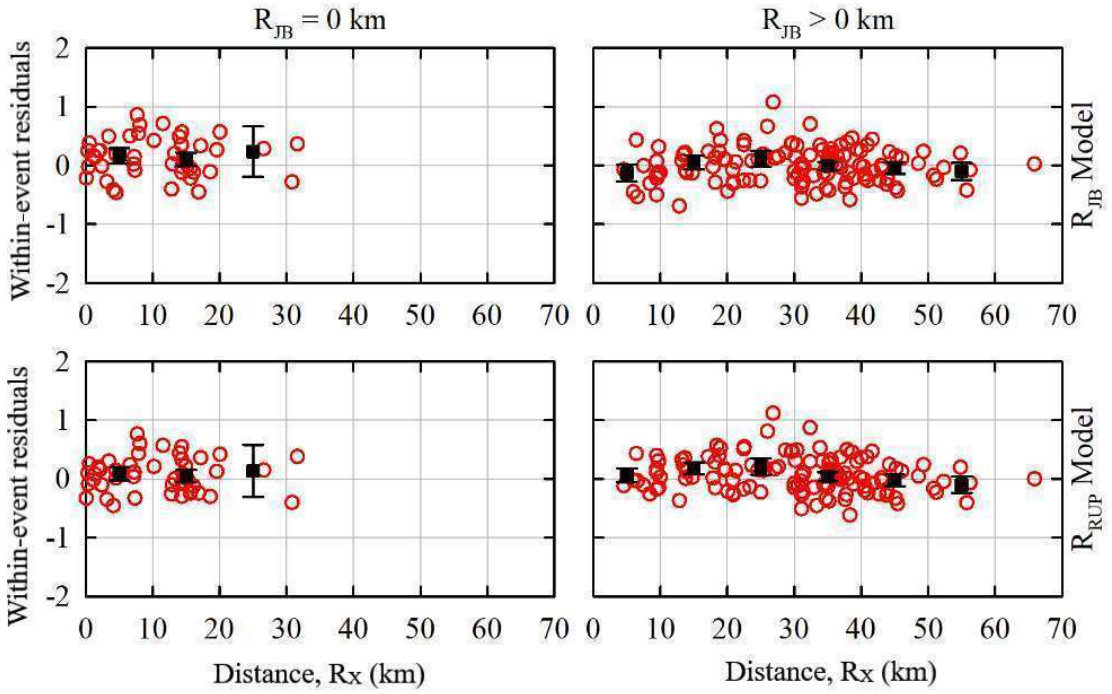

Figure 4.16. Within-event distributions of complex functional form R_{JB} (top row) and R_{RUP} (bottom row) equations for R_{JB} = 0 km (left column) and R_{JB} > 0 km (right column) situations depending on R_X distance for PGA.

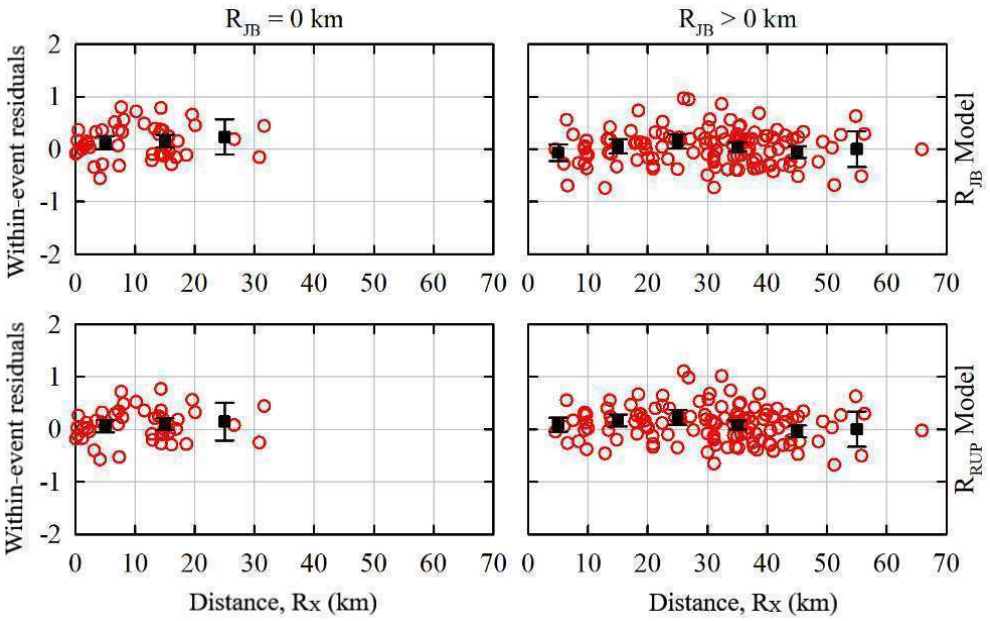

Figure 4.17. Within-event distributions of complex functional form R_{JB} (top row) and R_{RUP} (bottom row) equations for R_{JB} = 0 km (left column) and R_{JB} > 0 km (right column) situations depending on R_X distance for T = 0.2 s.

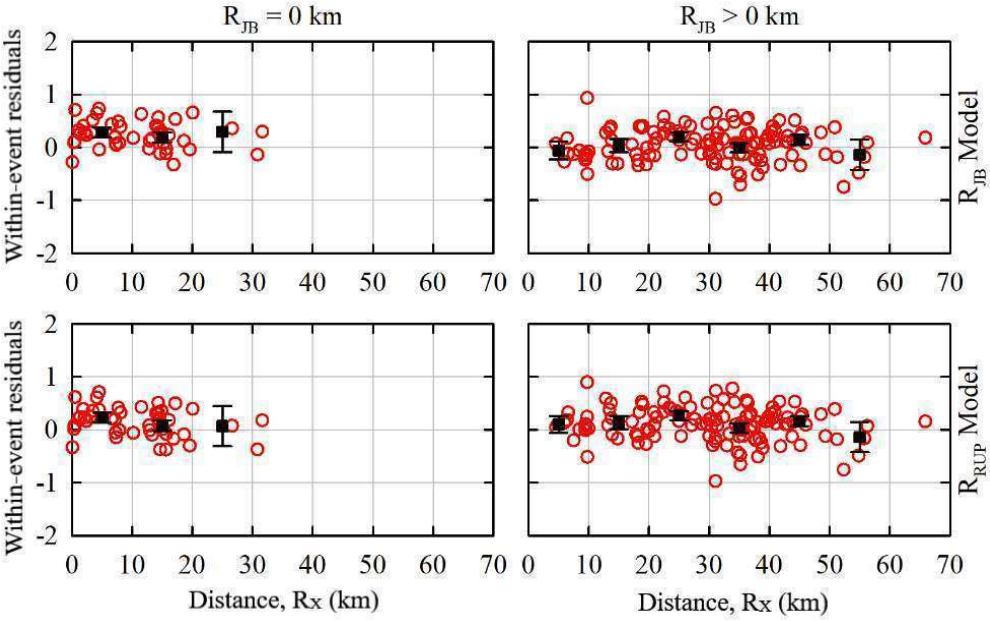

Figure 4.18. Within-event distributions of complex functional form R_{JB} (top row) and R_{RUP} (bottom row) equations for R_{JB} = 0 km (left column) and R_{JB} > 0 km (right column) situations depending on R_X distance for T = 1.0 s.

To evaluate the components of random variability models, change of total standard deviation (σ), between-event standard deviation (τ), within-event standard deviation (ϕ) and site-to-site standard deviation (ϕ_{S2S}) values of both Z_{HYP} and dip terms added R_{JB} equation (equation that is given in previous section) and R_{RUP} equation in complex functional form have been listed in Table 4.13 and given in Figure 4.19 depending on period. In this comparison, similarly as in the previous comparisons, between-event standard deviation value of R_{RUP} equation is slightly higher than the R_{JB} equations.

Table 4.13. Random variability values of R_{JB} and R_{RUP} GMPEs in complex forms.

Period (s)	R_{JB} based GMPE				R_{RUP} based GMPE			
	τ	Φ_{S2S}	Φ	σ	τ	Φ_{S2S}	Φ	σ
PGA	0.3737	0.4084	0.5326	0.7682	0.3874	0.4053	0.5347	0.7748
0.01	0.3744	0.4080	0.5331	0.7687	0.3881	0.4049	0.5352	0.7752
0.02	0.3767	0.412	0.5343	0.7727	0.3906	0.4089	0.5363	0.7794
0.03	0.3878	0.4197	0.5400	0.7862	0.4020	0.4168	0.5420	0.7932
0.05	0.4160	0.4412	0.5492	0.8181	0.4305	0.4388	0.5513	0.8257
0.1	0.4263	0.4569	0.5490	0.8318	0.4377	0.4542	0.5506	0.8373
0.15	0.4075	0.4582	0.5490	0.8230	0.4171	0.4557	0.5508	0.8276
0.2	0.3869	0.4562	0.5479	0.8112	0.3974	0.4534	0.5502	0.8161
0.3	0.3542	0.4483	0.5396	0.7859	0.3627	0.4452	0.5419	0.7895
0.4	0.3384	0.4607	0.5169	0.7706	0.3437	0.4577	0.5197	0.7730
0.5	0.3328	0.4713	0.5058	0.7673	0.3352	0.4684	0.5084	0.7679
0.75	0.3521	0.4802	0.4732	0.7606	0.3486	0.4772	0.4749	0.7579
1	0.3808	0.4869	0.4515	0.7654	0.3743	0.4841	0.4526	0.7611
1.5	0.4270	0.4726	0.4417	0.7751	0.4171	0.4710	0.4426	0.7692
2	0.4447	0.4646	0.4475	0.7835	0.4342	0.4648	0.4486	0.7783
3	0.4647	0.4496	0.4672	0.7977	0.4524	0.4503	0.4687	0.7919
4	0.4824	0.4346	0.4808	0.8079	0.4707	0.4358	0.4831	0.8031
5	0.5076	0.4332	0.4906	0.8283	0.4958	0.4342	0.4936	0.8234

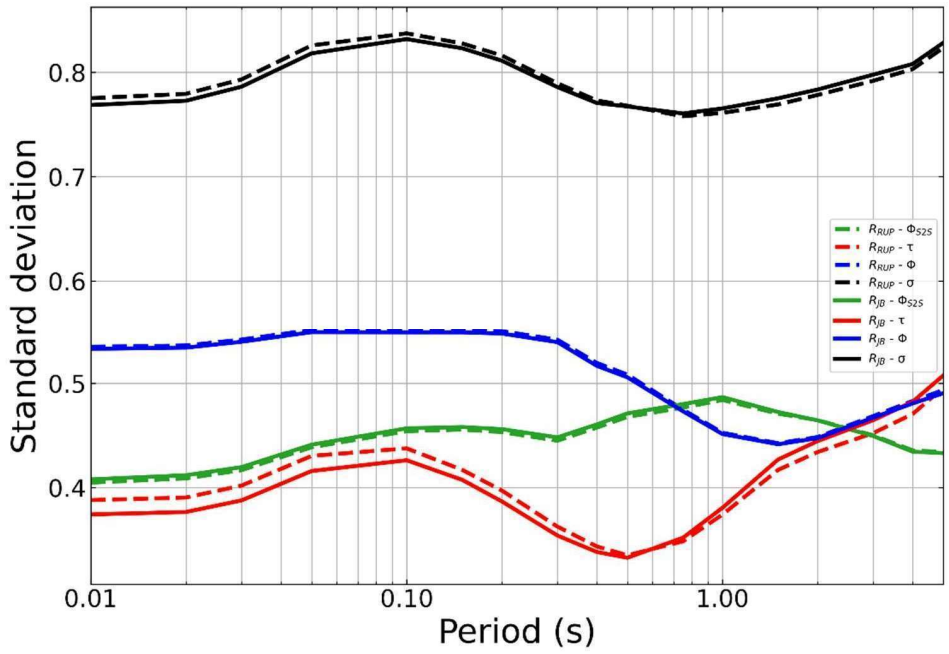

Figure 4.19. Random variability comparisons of R_{JB} and R_{RUP} GMPEs in complex forms.

4.5. Comparisons of the Median Prediction Values for Global GMPEs

In the first part of this study, it is observed that there has been always a difference between spectral value predictions of two distance-metrics in the evaluations that are held using Turkish database. While this difference is an indicator of an epistemic uncertainty depends on distance-metric; to show that this difference is independent of database, comparisons have been done for equations derived from global database under virtual earthquake scenarios (see. Chapter 3.5) of strike-slip fault situation and reference rock site (V_{S30} = 760 m/s) for PGA, T = 0.2 s and 1.0 s periods. These comparisons are given in Figure 4.20, Figure 4.21 and Figure 4.22.

In these comparisons, while additions to basic functional forms (hypocentral distance, dipping angle terms) are changing the median predictions of equations in the close distances substantially, these effects are getting lower in middle and far distances. In the comparisons that are made here, even though R_{JB} and R_{RUP}

based equations are derived from the same database, especially for close and middle-distance ranges, they predict quite different spectral values than each other, as it happened similarly in equations derived from Turkish database. To make a more effective observation in this stage, spectral value ratios of given complex functions have been calculated and given in Figure 4.21 and Figure 4.22. These ratios are the ratio of spectral values of R_{RUP} equation (PSA_{RRUP}) to R_{JB} (PSA_{RJB}) equations. Change of these values according to distance has been given in Figure 4.23. Here, observed changes are different than the ones observed in Turkish database (see. Figure 3.18). Convergence of spectral values and getting constant values have not been seen, especially for high magnitudes (M_W 6.5 and 7.5). It is highly possible that database is the source of this observation. Here, it's been seen that R_{RUP} equation is generating higher spectral values particularly in M_W 7.5 value. Setting aside these additional observations, it is evident that there's an epistemic uncertainty originating from distance-metrics.

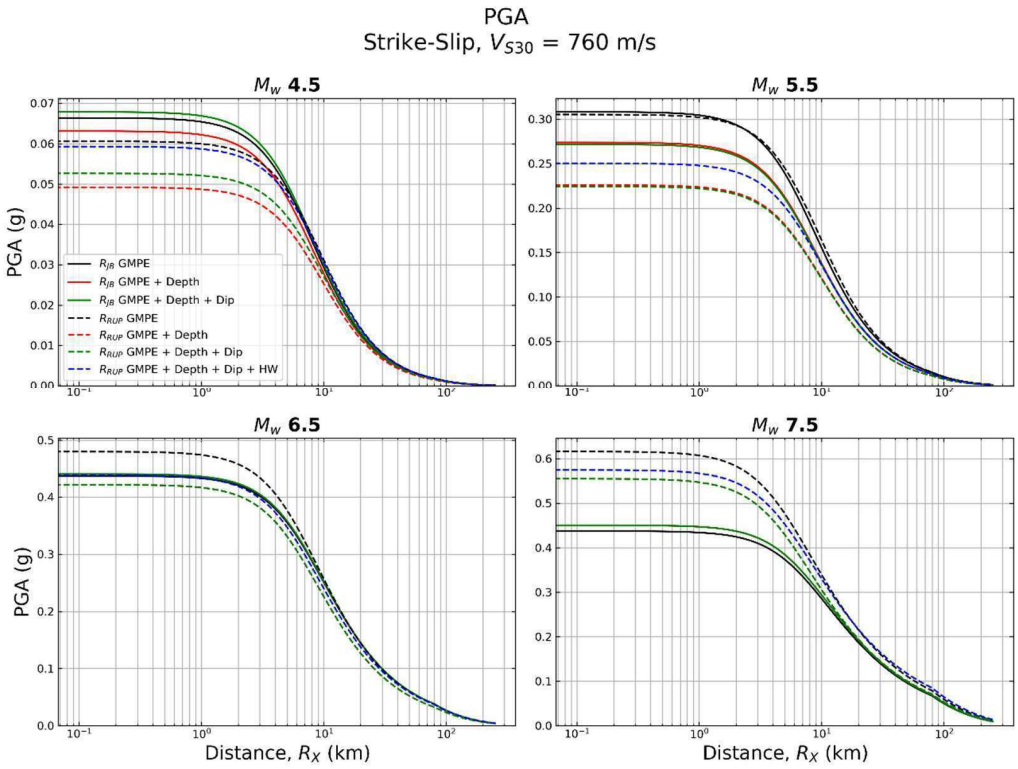

Figure 4.20. Change of PGA values for different magnitude values according to distance (V_{S30} = 760 m/s; strike-slip fault).

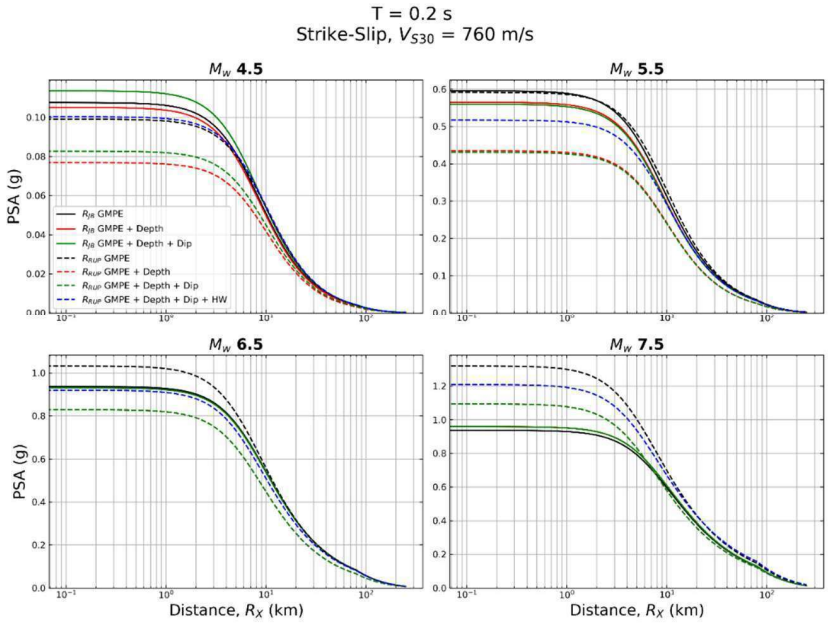

Figure 4.21. Change of spectral acceleration values (T = 0.2 s) for different magnitude values according to distance (V_{S30} = 760 m/s; strike-slip fault).

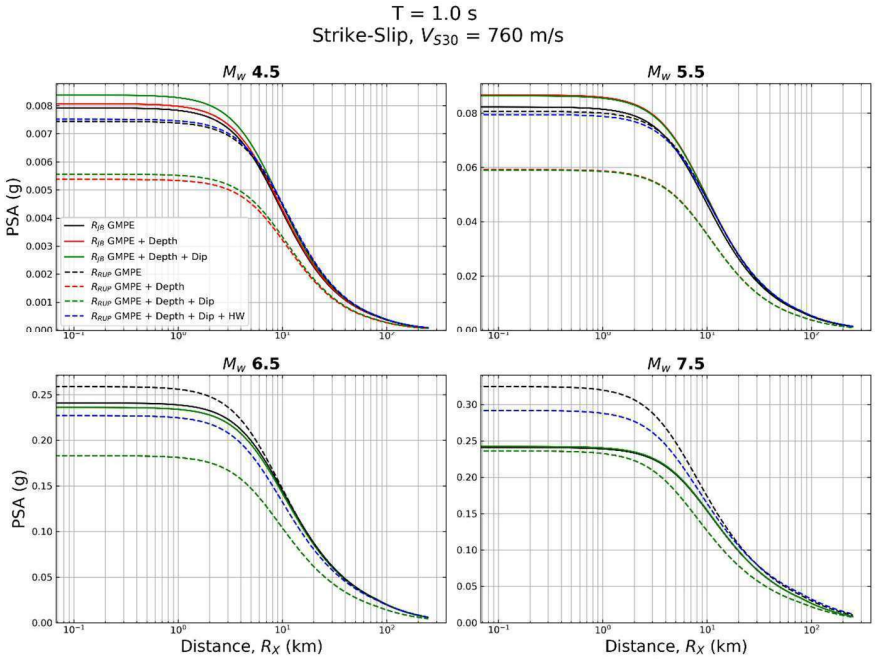

Figure 4.22. Change of spectral acceleration values (T = 1.0 s) for different magnitude values according to distance (V_{S30} = 760 m/s; strike-slip fault)

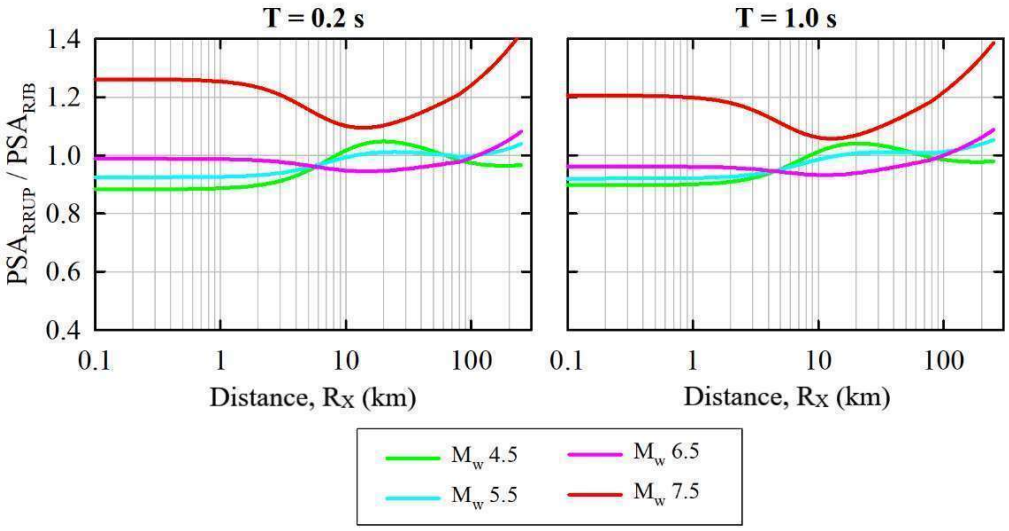

Figure 4.23. Comparisons of PSA values: Strike-slip fault type and reference rock site condition for T = 0.2 s (left column) and T = 1.0 s (right column).

To observe the change in distance-metrics to spectral values again, comparisons have been prepared for reverse virtual earthquake scenario considering sites that are located on hanging wall (positive R_X) and footing wall (negative R_X) of the fault in Figure 4.24. Changes of functional forms, from basic to complex, are similar as in previous sections. In this figure, serious differences have been noted on the hanging wall side of fault projection between behaviors of R_{RUP} (Basic + Z_{HYP} + Dip + HW) and R_{JB} (Basic + Z_{HYP} + Dip) equations represented with solid pink line and dotted green line, respectively. For instance, maximum spectral ordinate of R_{JB} equation is around 0.95 g level when dipping angle is 30° (1st row), corresponding R_{RUP} equations ordinate is around 1.6g level. With increasing dipping angle, projection area above the fault decreases and spectral ordinates of the equations are getting closer. These differences are getting higher with increasing magnitudes because of the similar reasons. Namely, surface area of the fractured fault is increasing with higher earthquake magnitudes.

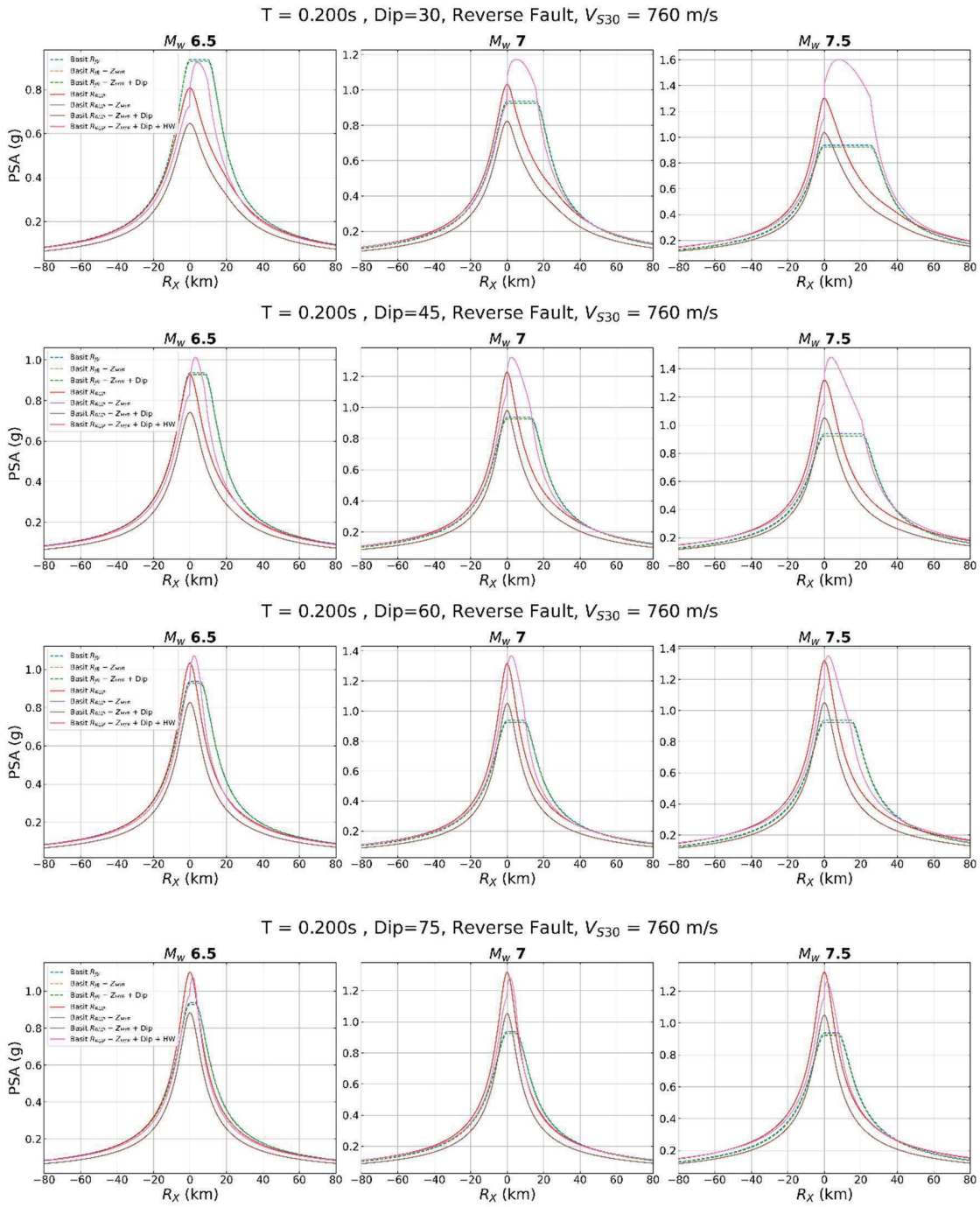

Figure 4.24. Change of spectral acceleration values (T = 0.2 s) for different magnitude values (M_W 6.5, 7.0 and 7.5) dependent on distance (V_{S30} = 760 m/s; reverse fault): dipping angle 30° (1st row), 45° (2nd row), 60° (3rd row), 75° (4th row).

5. CONCLUSIONS AND SUGGESTIONS

5.1. Conclusions

Two databases are compiled in the context of this study, as regional (Turkey) and global (NGA-West2; Ancheta et al., 2014). With taking into account two databases separately, evaluations of the functional forms of the ground-motion prediction equations and the extended-source distance-metrics (R_{JB} and R_{RUP}) as one of the main prediction parameters of these functional forms have been investigated. Evaluations of functional forms have been made on representation abilities of basic and complex forms that have been ranked according to the number of prediction parameters (focal depth, dipping angle, distance between fault fracture and surface, etc.). Choice of distance-metric has been discussed over derived equations, and the impact on epistemic uncertainty and spectral predictions as well.

The results of the regressions for the Turkish database show that there is a clear discrepancy between median predictions of equations that are developed using R_{JB} and R_{RUP} distance-metrics, especially in close distances. This difference may be seen more apparent in faulting types which dipping angle is lower than 90° (normal and reverse faults). Although an improvement has been seen in the residual distributions of the ground-motion prediction equations with the addition of hypocentral depth term to the functional forms, the difference in spectral estimations have been preserved. In this context, it is possible to speak of an epistemic uncertainty over Turkish database, because spectral estimation values that are generated with the developed GMPEs (R_{JB} and R_{RUP}) shows discrepancies especially in close distances on hanging wall sides. However, limitations such as inadequate number of recordings and earthquake parameters are restraining GMPE developers to investigate hanging wall effects on Turkish Strong-Motion database. To speak of an epistemic uncertainty over random variabilities is not so feasible, while standard deviations of these equations are

quite close. Although, standard deviations of R_{JB} equation is slightly lower than R_{RUP} ones.

Global database has been used to evaluate the apparent differences, especially in close distances. It's been thought that uncertainties will be lesser in this database, because number of close distance records and number of prediction parameters are more than the Turkish database. Firstly, the basic functional form has been considered in this database and later a smooth transform has been made to complex functional form with addition of different prediction parameters. Equations have been derived for considered functional form in every stage. Parameters that have been added to function have enhanced the residual distributions and as a result, lowered the standard deviations of the equations. When estimations of R_{RUP} equation in basic functional form have been evaluated, it's been seen that they are quite insufficient especially on hanging wall side. In this context, it is not a convenient approach to use R_{RUP} distance-metric without an additional hanging wall effects model.

As parallel to the previous paragraph, the biggest difference observed between equations that are developed using R_{JB} and R_{RUP} distance-metrics is on sites that are on hanging wall side of the reverse fault. R_{JB} based equation can consider the hanging wall effects on average without an extra definition because of the definition of Joyner-Boore distance. Alongside with this, R_{RUP} based equation requires an additional term to model hanging wall effects. In this context, after adding hypocentral depth and dipping angle terms to the equations, hanging wall function has been added to R_{RUP} equation and turned into complex functional form. In this stage, differences are also observed in median spectral predictions of R_{JB} and R_{RUP} based equations. As an addition to this observation, it is determined that R_{RUP} equation in complex functional form has a similar capacity as R_{JB} based equation. These observations are based on classical residual analyses and standard deviation comparisons. In this context, it is possible to say choosing R_{JB} equation, which uses a simpler functional form, is more reasonable depending on the observations made, regardless of the earthquake database.

Rather than the difference of hanging wall term for R_{JB} and R_{RUP} equations, a resemblance have been spotted between them, which can be explained as the necessity of hypocentral depth term. After evaluating the residual distributions, standard deviation comparisons and the median estimations for both of the databases; a difference has become evident between basic form equations and the hypocentral depth term added equations. The trend became better, total standard deviations got lower and median estimations became lower (especially for close distances) with the addition of hypocentral depth term. Although this term has a positive effect on both equations, this effect is lower on R_{JB} equation. The difference of the positive effect can be observed in the lesser trend in residual distributions of R_{JB} equation and smaller difference between the two functional forms (basic and hypocentral depth term added) of R_{JB} equation. To observe this difference more clearly, regression coefficients that are controlling the hypocentral depth term have been compared for both databases. As a result, it's been seen that contribution of hypocentral depth term on R_{JB} equation is lower than the R_{RUP} one, in both Turkish and global databases.

5.2. Suggestions

Global database has been dominated by reverse style-of-faulting, while Turkish database has been dominated by strike-slip and normal faults. Although, hanging wall model of Campbell and Bozorgnia (2013) considers the hanging wall effects of normal and strike-slip faults as well, it is not suitable to use this model on Turkish data, while this model has been developed for a database which is dominated with reverse faults. Statistical evidence of hanging wall effects is weak due to the lack of data as stated in Campbell and Bozorgnia (2013). Hanging wall effects in normal faults show only a mild difference in spectral values in the simulations done by Collins et al. (2006). However, a difference between median estimations of R_{JB} and R_{RUP} GMPEs that are developed for Turkish database shows the existence of an epistemic uncertainty. In this context, this study can be extended with developing a new hanging wall model with using empirical recordings from a database dominated with normal and strike-slip faults and simulation-based recordings to cover the epistemic uncertainty between R_{JB} and R_{RUP} GMPEs. Evaluations made for Turkish Strong-Motion database have to be repeated with the addition of this new hanging wall term.

R_{JB} and R_{RUP} distance-metrics are the most used distance-metrics in current studies. Although, the clear epistemic uncertainty and functional form complexities between them, push GMPE developers to search new type of distance metrics, such as the Mean Rupture Distance (Thompson and Baltay, 2018) which offers a simpler functional form. In the scope of distance-metrics, this study can be extended with adding new type of distance-metrics, which will offer much simpler functional forms in GMPE applications, to Turkish and global databases. Those two suggestions for future studies cannot be done within the context of this study because of the limitations of time and computational effort.

6. REFERENCES

Abrahamson, N.A., Silva, W.J., “Summary of the Abrahamson & Silva NGA Ground-Motion Relations”, Earthquake Spectra, 24, 67-97, **2008**.

Abrahamson N, Silva W, Kamai R., “Summary of the ASK14 Ground-Motion Relation for Active Crustal Regions”, Earthquake Spectra, 30, 1025-1055, **2014**.

Abrahamson, N. A., Youngs R. R., “A stable algorithm for regression analyses using the random effects model”, Bulletin of the Seismological Society of America, 82, 505-510, **1992**.

Akkar, S., Çağnan, Z., “A local ground-motion predictive model for Turkey and its comparison with other regional and global ground-motion models”, Bulletin of the Seismological Society of America, 100(6), 2978–2995, **2010**.

Akkar, S., Çağnan, Z., Yenier, E., Erdoğan, Ö., Sandıkkaya, M. A., Gülkan, P., "The recently compiled Turkish strong motion database: Preliminary investigation for seismological parameters”, Journal of Seismology, 14, 457–479, **2010**.

Akkar, S., Sandıkkaya, M.A., Bommer, J.J., “Empirical Ground-Motion Models for Point- and Extended-Source Crustal Earthquake Scenarios in Europe and the Middle East”, Bulletin of Earthquake Engineering, 12, 359-387, **2014**.

Akkar, S., Sandıkkaya, M.A., Senyurt, M., Azari, S.A., Ay, B.Ö., “Reference database for seismic ground-motion in Europe (RESORCE)”, Bulletin of Earthquake Engineering, 12, 311-339, **2014b**.

Ancheta, T. D., Darragh, R. B., Stewart, J. P., Seyhan, E., Silva, W. J., Chiou, B.S.J., Wooddell, K.E., Graves, R.W., Kottke, A.R., Boore, D.M., Kishida, T. Donahue J.L., “NGA-West 2 Database”, Earthquake Spectra, 30(3), 989-1005, **2014**.

Bates, D.M.; Maechler, M.; Bolker, B. Lme4: Linear Mixed-Effects Models Using S4 Classes, R Manual, **2013**.

Bindi, D., Massa, M., Luzi, L., Ameri, G., Pacor, F., Puglia, R., Augliera, P., "Pan-European ground-motion prediction equations for the average horizontal component of PGA, PGV, and 5%-damped PSA at spectral periods up to 3.0 s using the RESORCE dataset", Bulletin of Earthquake Engineering, 12, 391-430, **2014**.

Bindi, D., Pacor, F., Luzi, L., Puglia, R., Massa, M., Ameri, G., Paolucci, R., "Ground-motion prediction equations derived from the Italian strong motion database", Bulletin of Earthquake Engineering, 9, 1899–1920, **2011**.

Bommer, J. J., "Challenges of Building Logic Trees for Probabilistic Seismic Hazard Analysis", Earthquake Spectra, 28, 1723–1735, **2012**.

Bommer, J.J., Akkar, S., "Consistent Source-to-Site Distance Metrics in Ground-Motion Prediction Equations and Seismic Source Models for PSHA", Earthquake Spectra, 28, 1–15, **2012**.

Bommer, J. J., Douglas, J., Scherbaum, F., Cotton, F., Bungum, H., Fäh, D., "On the Selection of Ground-Motion Prediction Equations for Seismic Hazard Analysis", Seismological Research Letters, 81, 783-793, **2010**.

Boore, D.M., Atkinson, G., "Ground-Motion Prediction Equations for the Average Horizontal Component of PGA, PGV, and 5%-Damped PSA at Spectral Periods between 0.01 s and 10.0 s", Earthquake Spectra, 24(1), 99-138, **2008**.

Boore, D.M., Stewart, J.P., Seyhan, E., Atkinson, G.M., "NGA-West 2 Equations for Predicting PGA, PGV, and 5%-Damped PSA for Shallow Crustal Earthquakes", Earthquake Spectr, 30, 1057-1085, **2014**.

Budnitz, R. J., Apostolakis, G., Boore, D. M., Cluff, L. S., Coppersmith, K. J., Cornell, C. A. Morris, P. A., "Recommendations for probabilistic seismic hazard analysis: Guidance on uncertainty and use of experts", NUREG/CR-6372, U.S. Nuclear Regulatory Commission, Washington, D.C., **1997**.

Campbell, K. W., "Comprehensive Comparison among the Campbell–Bozorgnia NGA-West2 GMPE and Three GMPEs from Europe and the Middle East", Bulletin of the Seismological Society of America, 106, 2081-2103, **2016**.

Campbell, K., Bozorgnia, Y., “NGA Ground Motion Model for the Geometric Mean Horizontal Component of PGA, PGV, PGD and 5% Damped Linear Elastic Response Spectra for Periods Ranging from 0.01 to 10 s”, Earthquake Spectra, 24(1), 139-171, **2008**.

Campbell K.W., Bozorgnia Y., “NGA-West2 Campbell-Bozorgnia Ground Motion Model for the Horizontal Components of PGA, PGV, and 5%-Damped Elastic Pseudo-Acceleration Response Spectra for Periods Ranging from 0.01 to 10 sec”, PEER Report No. 2013/06, Pacific Earthquake Engineering Research Center, University of California, Berkeley, CA, 238 pp, **2013**.

Campbell K.W., Bozorgnia Y., “NGA-West2 Ground Motion Model for the Average Horizontal Components of PGA, PGV, and 5%-Damped Linear Acceleration Response Spectra”, Earthquake Spectra, 30, 1087-1115, **2014**.

Cauzzi, C., Faccioli, E., Vanini, M., Bianchini, A., “Updated predictive equations for broadband (0.01–10 s) horizontal response spectra and peak ground motions, based on a global dataset of digital acceleration records”, Bulletin of Earthquake Engineering, 13, 1587–1612, **2015**.

Chiou, B., Youngs, R., “An NGA Model for the Average Horizontal Component of Peak Ground Motion and Response Spectra. Earthquake Spectra”, 24, 173-215, **2008**.

Chiou, B.S.J., Youngs, R.R., “Update of the Chiou and Youngs NGA Model for the Average Horizontal Component of Peak Ground Motion and Response Spectra”, Earthquake Spectra, 30, 1117-1153, **2014**.

Collins N., Graves. R.W., Ichinose G., Somerville P., “Ground motion attenuation relations for the Intermountain West, Final report prepared for the U.S. Geological Survey”, Award No. 05HQGR0031, URS Corporation, Pasadena, CA, **2006**.

Derras, B., Bard, P.Y., Cotton, F., “Towards fully data driven ground-motion prediction models for Europe”, Bulletin of Earthquake Engineering, 12, 495–516, **2014**.

Donahue, J.L., Abrahamson, N.A., “Simulation-based hanging wall effects”, Earthquake Spectra, 30, 1269-1284, **2014**.

Erdoğan, Ö., “Main Seismological Features of Recently Compiled Turkish Strong Motion Database”, Yüksek Lisans Tezi, Orta Doğu Teknik Üniversitesi, Ankara, **2008**.

Joyner, W. B., Boore, D. M., “Peak horizontal acceleration and velocity from strong-motion records including records from the 1979 Imperial Valley, California, earthquake”, Bulletin of the Seismological Society of America, 71, 2011-2038, **1981**.

Joyner, W. B., Boore, D. M., “Methods for regression analysis of strong-motion data”, Bulletin of the Seismological Society of America, 83, 469-487, **1993**.

Kaklamanos, J., Baise, L.G., Boore, D.M., “Estimating unknown input parameters when implementing the NGA ground-motion prediction equations in engineering practice”, Earthquake Spectra, 27, 1219–1235, **2011**.

Kale, Ö., Akkar, S., Anooshiravan, A., Hamzehloo, H., “A ground-motion predictive model for Iran and Turkey for horizontal PGA, PGV and 5%-damped response spectrum: Investigation of possible regional effects”, Bulletin of the Seismological Society of America, 105, 963-980, **2015**.

Kale, Ö., Padgett, J., Shafieezadeh, A., “A ground motion prediction equation for novel peak ground fractional order response intensity measures.”, Bulletin of Earthquake Engineering, 15. 10.1007/s10518-017-0122-x, **2017**.

Kalkan, E., Gülkan, P., “Site-Dependent Spectra Derived from Ground Motion Records in Turkey”, Earthquake Spectra, 20, 1111-1138, **2004**.

Kotha, S. R., Bindi, D., Cotton, F., “Partially non-ergodic region specific GMPE for Europe and Middle-East”, Bulletin of Earthquake Engineering, 14, 1245-1263, **2016**.

Kuehn, N., Scherbaum, F., “A partially non-ergodic ground-motion prediction equation for Europe and the Middle East”, Bulletin of Earthquake Engineering, 14, 2629-2642, **2016**.

Sandıkkaya, M.A., Akkar, S., Bard, P.Y., “A Nonlinear Site Amplification Model for the Next Pan-European Ground-Motion Prediction Equations”, Bulletin of the Seismological Society of America, 103, 19-32, **2013**.

Thompson, E., Baltay, A., “The Case for Mean Rupture Distance in Ground-Motion Estimation.” Bulletin of the Seismological Society of America. 108. 10.1785/0120170306, **2018**.

Wells D.L., Coppersmith, J., “New empirical relationships among magnitude, rupture length, rupture width, rupture area, and surface displacement”, Bulletin of the Seismological Society of America, 84, 974-1002, **1994**.

Zhao, J.X., Zhang, J., Asano, A., Ohno, Y., Oouchi, T., Takahashi, T., Ogawa, H., Irikura, K. Thio, H.K., Somerville, P.G., Fukushima, Y., “Attenuation relations of strong ground motion in Japan using site classification based on predominant period”, Bulletin of the Seismological Society of America, 96(3), 898–913, **2006**.